AEDC-TR-76-25

cy. 2

PERFORMANCE CHARACTERISTICS OF A HUELS-TYPE ARC HEATER OPERATING ON HYDROGEN, HELIUM, OR AIR

McDONNELL DOUGLAS RESEARCH LABORATORIES
ST. LOUIS, MISSOURI 63166

March 1976

Final Report for Period 15 April 1974 — 17 June 1975

Prepared for

DIRECTORATE OF TECHNOLOGY (DY)
ARNOLD ENGINEERING DEVELOPMENT CENTER
AIR FORCE SYSTEMS COMMAND
ARNOLD AIR FORCE STATION, TENNESSEE 37389

This final report was submitted by McDonnell Douglas Research Laboratories, St. Louis, Missouri 63166, under contract F40600-74-C-0010, with Arnold Engineering Development Center, Arnold Air Force Station, Tennessee 37389. Major U. L. Barnwell was the AEDC Technical Representative.

This report has been reviewed by the Information Office (OI) and is releasable to the National Technical Information Service (NTIS). At NTIS, it will be available to the general public, includint foreign nations.
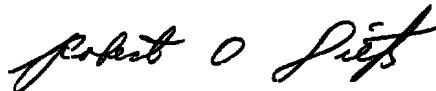
APPROVAL STATEMENT

This technical report has been reviewed and is approved for publication.

FOR THE COMMANDER

MELVIN L. GUIOU
Captain, USAF
Research & Development
  Division
Directorate of Technology

ROBERT O. DIETZ
Director of Technology

REPORT DOCUMENTATION PAGE		READ INSTRUCTIONS BEFORE COMPLETING FORM
1 REPORT NUMBER AEDC-TR-76-25	2. GOVT ACCESSION NO.	3. RECIPIENT'S CATALOG NUMBER
4. TITLE (and Subtitle) PERFORMANCE CHARACTERISTICS OF A HUELS-TYPE ARC HEATER OPERATING ON HYDROGEN, HELIUM, OR AIR		5 TYPE OF REPORT & PERIOD COVERED Final Report for the Period 15 April 1974 – 17 June 1975
		6. PERFORMING ORG. REPORT NUMBER
7. AUTHOR(s) J. H. Painter and J. F. Shaeffer		8. CONTRACT OR GRANT NUMBER(s) F40600-74-C-0010
9 PERFORMING ORGANIZATION NAME AND ADDRESS McDonnell Douglas Research Laboratories McDonnell Douglas Corporation St. Louis, Missouri 63166		10. PROGRAM ELEMENT, PROJECT, TASK AREA & WORK UNIT NUMBERS Program Element 65802F
11. CONTROLLING OFFICE NAME AND ADDRESS Arnold Engineering Development Center (DYFS) Air Force Systems Command Arnold Air Force Station, Tennessee 37389		12. REPORT DATE March 1976
		13. NUMBER OF PAGES 137
14. MONITORING AGENCY NAME & ADDRESS(if different from Controlling Office)		15. SECURITY CLASS. (of this report) UNCLASSIFIED
		15a. DECLASSIFICATION/DOWNGRADING SCHEDULE N/A

16 DISTRIBUTION STATEMENT (of this Report)

Approved for public release; distribution unlimited.

17. DISTRIBUTION STATEMENT (of the abstract entered in Block 20, if different from Report)

18. SUPPLEMENTARY NOTES

Available in DDC

19. KEY WORDS (Continue on reverse side if necessary and identify by block number)

Arc heaters	Dust erosion	Arc radiation
Hydrogen	Wind tunnels	Electric arcs
Helium	Test facilities	Electrode phenomena
Scaling		

20. ABSTRACT (Continue on reverse side if necessary and identify by block number)

The performance characteristics of a scale 0.5 Huels-type arc heater were determined operating on hydrogen, helium, or air. Data were acquired on hydrogen at pressures from 10 to 50 atm, on helium from 25 to 100 atm, and on air from 10 to 100 atm. All three gases were tested at three arc current levels (240, 320, and 400 A) using the same basic arc heater. The hydrogen enthalpies were five to seven times those of air, and the helium enthalpies were 41% to 69% higher than air. Prediction codes for

DD FORM 1473 1 JAN 73   EDITION OF 1 NOV 65 IS OBSOLETE

20. ABSTRACT (Continued)

scaling hydrogen and helium arc heaters to larger scale were developed from a similar code for air which was shown to accurately predict the performance of the present AEDC Dust Erosion Tunnel (N = 1. 73) arc heater.   The hydrogen (HYARC) and helium (HEARC) codes incorporated Huels-type geometry and were correlated to the N-250 performance.   They were then used to predict the performance of the Dust Erosion Tunnel heater on these higher enthalpy gases.   These codes are for high pressure, high flow rate arc heaters and are based on a rod-arc model with radiation losses and convective turbulent heating of the operating gas and include an optional nozzle sonic flow relation for mass flow rate determination.

PREFACE

The work reported herein was conducted by the McDonnell Douglas Research Laboratories (MDRL), McDonnell Douglas Corporation (MDC), St. Louis, Missouri, for the Arnold Engineering Development Center (AEDC), Air Force Systems Command (AFSC), under contract F40600-74-C-0010, from 15 April 1974 to 17 June 1975. The AEDC Technical Representative was Major U. L. Barnwell. The Program Element Number is 65802F.

The authors wish to acknowledge the contributions and assistance of the following persons whose help was instrumental in performing the work reported herein: Mr. Richard Smith, ARO, Inc.; Major U. L. Barnwell, AEDC; Mr. Robert Binz, Mr. Harold Springston, Mr. John Bomar, Mr. John Ziemer, Mr. Edward Schuette, Mr. Ronald Williamson, and Mr. Walter Rinehart, MDRL.

This technical report has been reviewed by Dr. R. J. Hakkinen, Manager-Flight Sciences, MDRL and Dr. D. P. Ames, Director, MDRL.

The reproducibles used in the reproduction of this report were supplied by the authors.

CONTENTS

CONTENTS

LIST OF ILLUSTRATIONS

LIST OF ILLUSTRATIONS

LIST OF ILLUSTRATIONS

LIST OF TABLES

LIST OF TABLES

1. INTRODUCTION

The AEDC Dust Erosion Tunnel (DET) is currently using a Huels-type, high voltage arc air heater to accelerate the test section dust cloud for determination of the surface-recession characteristics of reentry vehicle (RV) materials in an abrasive environment. The maximum attainable particle velocity is presently less than 7000 ft/s. The use of hydrogen or helium instead of air as the driving gas has the potential of higher gas enthalpies thus increasing this upper velocity limit. However, no data were available in the open literature on the performance characteristics of the Huels-type arc heater operating on hydrogen or helium to confirm the higher gas enthalpies.

The objective of this work was to map the performance of a Huels-type arc heater using gaseous hydrogen at pressures of 10, 15, 25 and 50 atm and helium at pressures of 25, 50, 75 and 100 atm with arc currents of 250, 320 and 400 A. A supersonic nozzle having a 0.162 in. diam throat was used to constrict the flow, and measurements of the stagnation enthalpy, stagnation pressure, and arc power were made. These performance data were compared with data using air and with computer coded correlations derived to permit scaling of the arc heater. Electrode erosion was documented during these performance tests. Minor modifications to the basic arc heater were made to achieve stable operation over the full test matrix with optimum performance as a goal.

Use of a Linde N-250 arc heater satisfied all test requirements. This heater was less than one-third the size of the AEDC DET heater. MDRL had previously conducted more than 700 tests on air using a Linde N-250 arc heater with nozzle throat diameters ranging from 0.142 to 0.250 in. Unrestricted flow tests with a 0.375 in. diam front electrode had also been run. One scale factor of significance with high voltage arc heaters is the ratio of the nozzle throat area to the front electrode gas flow area. In order to maintain the ratio present in the DET arc heater, the N-250 required a 0.162 in. diam throat. Since the heater had been operated on air with throats near that size, inspection of those data and the heater specifications indicated that operating on air at pressures from 5 to 50 atm and arc currents from 200 to 400 A was feasible.

The AEDC DET scale N = 1.73 high voltage arc heater has a nozzle throat diameter of 0.5625 in. Operation of this scale heater was satisfactory for air as the working gas, but there was serious doubt about this configuration being optimal for use with hydrogen. The scaling relations for air used by Linde had proven to be erroneous,[1] so it was doubtful that they could accurately be applied to hydrogen. Thus, selection of the optimum scale heater for hydrogen required scaling studies as well as performance measurements.

A minimum-energy-addition, arc-model-scaling computer code had been used successfully by MDRL on air arc heaters. The addition of the proper thermodynamic and transport properties for helium and hydrogen plus an improved model for the Huels-type arc heater was a major part of this program. Scaled performance calculations were then made with the improved codes.

2. TEST APPARATUS

The arc heater used in these tests was a nominal 250 kW Huels-type, high-voltage unit. It was mounted and tested in the McDonnell Douglas Research Laboratories (MDRL) High Impact Pressure (HIP) facility.[3] The HIP subsystems, controls, and data acquisition system were used along with special gas controls. The instrumentation used was a combination of standard and special equipment selected for specific test requirements. Data reduction routines were written to convert the raw signals into printed engineering units using the HIP computerized data acquisition system.

2.1 THE N-250 ARC HEATER

Figure 1 shows the N-250 arc heater used in these tests. Two tandem cylindrical electrodes were separated by a central gas-injection chamber and insulated from each other by a threaded Delrin cylindrical insulator. The 5.6 in. long rear electrode (anode) had an inside diameter of 0.625 in. The front electrode (cathode) had an inside diameter of 0.375 in. The cathode length was 5 in. in most tests and 8 in. in a few tests, designated as N-250-5 or N-250-8. Both electrodes and the center chamber were water cooled. Four tubular gas injectors were used. The gas was injected tangentially to the heater walls in a counter-clockwise direction looking downstream. The resultant radial pressure gradient stabilized the arc on the heater centerline. The injection pressure ratio (inector-pressure/arc-chamber pressure) was varied from 1.1 to 2.2 in these tests.

A magnetic field coil was used on the rear electrode to rotate the arc termination and prevent arc transfer to the rear plug.

A nozzle module was bolted to the downstream end of the heater to constrict the flow. The nozzle throat diameter was 0.162 in. for all tests designated by N-250-5-0.162 or N-250-8-0.162. The nozzle design is discussed in Section 2.2.

Figure 2 shows the N-250 arc heater mounted in the MDRL HIP test cell. Each component was individually water cooled and monitored for energy losses. The differential temperature sensors and turbine flowmeters can be seen beneath the arc heater test stand. The test set-up allowed rapid disassembly for weighing and cleaning the electrodes post-test. Much of the gas flow instrumentation was fastened to the rear panel on the test stand, so that the entire basic system was portable.
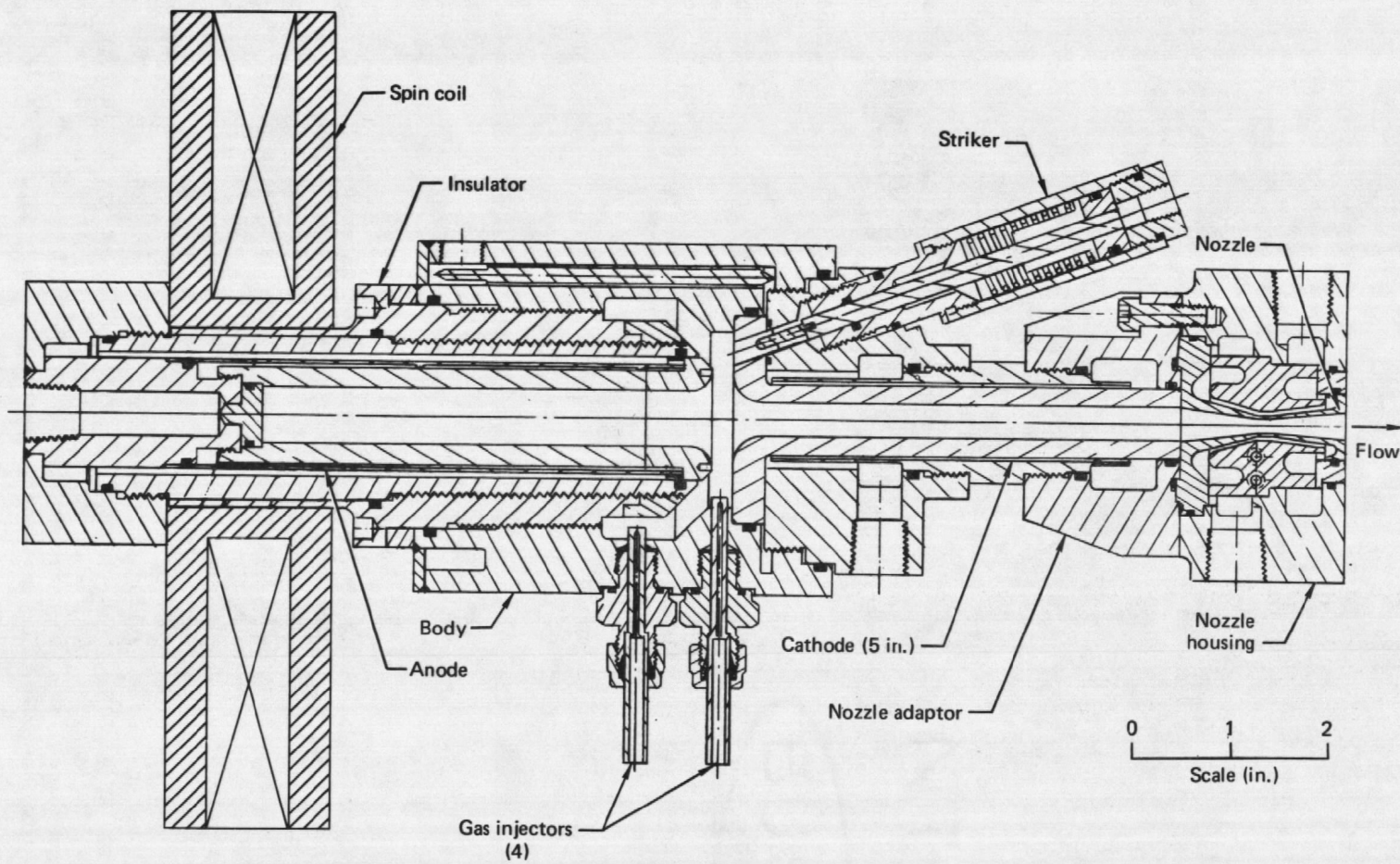
Figure 1 N-250 arc heater
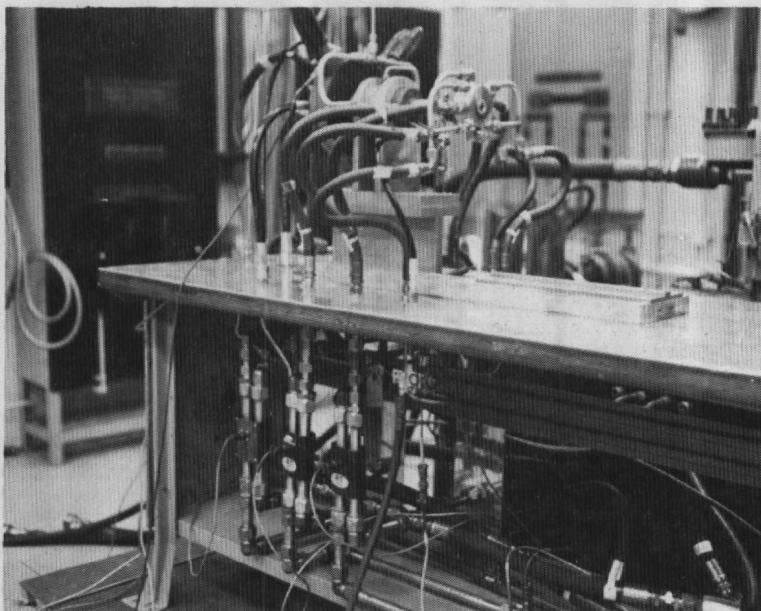
Figure 2 N-250 arc heater mounted in the HIP facility

2.2 ARC HEATER NOZZLE

The nozzles used in these tests (Figure 1) were scaled to duplicate the AEDC DET arc heater throat-to-electrode area ratio.

$$\left(\frac{A*}{A_c}\right)_{N-250} = \left(\frac{A*}{A_c}\right)_{DET} \tag{1}$$

$$\left(\frac{d*}{0.375}\right)^2_{N-250} = \left(\frac{0.5625}{1.300}\right)^2_{DET} \tag{2}$$

$$d* = 0.162 \text{ in.} \tag{3}$$

The nozzle inlet diameter matched the electrode diameter (0.375 in.), and the exit diameter was sized for proper expansion from 25 atm, 30,000 Btu/lb reservoir conditions to atmospheric pressure. This yielded a 0.296 in. diam, Mach 2.75 test stream. The convergence and divergence of the nozzle were conical for ease of machining; a short cylindrical throat was incorporated for erosion protection and improved source flow.

The nozzle throat cooling was designed to withstand 6000 Btu/ft^{2}s heat flux without nucleate boiling with a coolant flow rate of 30 gpm. The coolant flow velocity at the throat exceeded 170 ft/s, which was sufficient to sweep vapor bubbles away at the higher heating rates. The first and second nozzles experienced local heating rates to approximately 9800 Btu/ft^{2}s before failure, and the third nozzle liner experienced heating rates to 6700 Btu/ft^{2}s without

failure. The calculated combined thermal and mechanical stress at the throat was 20,000 psi at the design heat flux. The nozzle throat wall thickness was initially 0.0315 in. All of the hydrogen testing was completed with two such nozzles. A third nozzle was built with a 0.047 in. throat wall thickness for the high-pressure air and helium tests.

2.3 INSTRUMENTATION AND DATA ACQUISITION

The arc heater was instrumented to determine the following parameters.

o Arc current   o Anode power loss
o Arc voltage   o Cathode-body power loss
o Arc chamber pressure   o Nozzle power loss
o Gas flow rate   o Injector pressure

These parameters were scanned at 100 scans/s on hydrogen and 10 scans/s on helium and air. These data were averaged and the arc power, energy balance enthalpy, thermal efficiency, and sonic flow enthalpy were calculated and printed out approximately once each second of the test.

Table 1 lists the primary instruments and their accuracy. The considerable electrical noise encountered when operating on hydrogen required thorough shielding of all instruments, increased sampling rates and averaging larger sampled batches in order to acquire acceptable data. No noise problems were encountered on helium or air. The sampling rates and batches were reduced without increasing the data scatter significantly.

The arc voltage on hydrogen oscillated significantly and caused strong random fluctuations in the printed data. Several attempts to reduce these oscillations were made by changing the sampling rate and the averaging batch size; however, voltage spikes persisted. A satisfactory technique was derived by filtering the signal with a digital voltmeter isolation amplification network. This was not necessary for the helium or air tests.

The arc chamber pressure was measured on the side wall of the center body. Previous tests have shown that this value may be higher than the stagnation pressure at the nozzle entrance. This may partially explain some of the deviations found between the sonic flow and energy balance enthalpies.

The anode and nozzle had individual coolant differential temperature sensors and water flowmeters for measuring the power losses to these components. The cathode and body coolant were supplied through the same port, and since the body power losses are minimal it was decided to combine them with those of the cathode.

The hydrogen flow rates were measured using a sonic nozzle flowmeter with a 0.055 in. diam throat. The flowmeter was calibrated by the MCAIR Bureau of Standards at air flow rates from 0.004 to 0.123 lb/s. The orifice coefficient on air was derived from 28 data points and was accurate within $\pm$ 1.5% with a confidence level of 99.5%. Conversion of the air calibration to hydrogen was accomplished using the techniques given in References 6 and 7. Godt[7] found for critical nozzle flowmeters having throat diameters from 0.0308 to 0.0707 in. that the relative values of the nozzle discharge coefficients demonstrate that a flowmeter calibrated on one gas can be used to measure flow rates of the other gases within $\pm$ 0.1%.

The helium flow rates were measured using a 0.070 in. diam sonic nozzle flowmeter for arc pressures to 75 atm. Because of gas supply limitations with conventional storage bottles, the 100 atm test flow rates were based on a calibration of the four 0.0625 in. diam injectors. The injectors were calibrated on helium in series with the 0.070 in. diam sonic nozzle. The subsonic mass flow rate followed the general equation for subcritical real gas flow through a thin-plate orifice within $\pm$ 0.56%.

$$\dot{m} = CA_i \, P_i \left(\frac{g}{RT_i} \frac{2\gamma}{\gamma-1} \left[\left(\frac{P_o}{P_i} \right)^{2/\gamma} - \left(\frac{P_o}{P_i} \right)^{\frac{\gamma+1}{\gamma}} \right] \right)^{1/2} . \tag{4}$$

The air flow rates were measured using the 0.055 in. diam sonic nozzle for arc pressures from 50 to 100 atm and 0.043 in. diam sonic nozzle for arc pressures from 10 to 25 atm.

Tests were made on all flow systems to determine if the flowmeters were choked. Corrections were necessary on some of the high current hydrogen tests where the injector pressure exceeded 73% of the flowmeter pressure.

All primary instrumentation signals were recorded on discs in the Research Data Acquisition System (RDAS). Data for the hydrogen tests were scanned at 100 scans/s; data for the air and helium tests were scanned at 10 scans/s. The disc-recorded information was transferred to tape post-test, processed into engineering units, and printed in the format discussed in Appendix A.

2.4 ARC HEATER SUBSYSTEMS

The arc heater was tested in the MDRL HIP facility. The water, power, and air subsystems were more than sufficient for this scale heater. The standard HIP arc heater (MDC-300) is four times the size of the N-250.[2]

A 13 Ω ballast resistor was necessary for this program. The resistor consisted of 60 water-cooled stainless steel 0.25 in. diam tubes with 0.020 in. wall thickness; each tube was 10 ft long. The tubes were manifolded in two banks of 30, and each bank was separately cooled. Connections of 0.9, 1.8, 3.5, 7 and 13 Ω were possible. The maximum current capability was in excess of 400 A. This ballast resistor provided the immediate voltage reserve required by an arc excursion without the inherent time delay of the power supply. The 7 Ω ballast connection was used on all reported hydrogen, helium and air tests.

Cooling water was supplied by a three-stage centrifugal pump capable of 1200 gpm at 600 psi. The normal flow rates were 23 gpm to the nozzle, 34 gpm to the cathode-body and 20 gpm to the anode. The ballast resistor required 120 gpm and the spin coil, 2 gpm.

Power was supplied by two, three-phase, full-wave rectifier modules with saturable reactor current controls. The units were connected in series for an open circuit voltage of 10.2 kV. The maximum power capability of these two units was 5 MW for 6 min. Additional identical power units were connected in series without activation to utilize the inductance of their large smoothing reactors (8 mH). The number of additional units varied from 1 to 3. Six power units were available.

The hydrogen and helium gas supplies consisted of multiple type-1A cylinders manifolded as shown in Figure 3. The gas flowed through an on-off solenoid valve, a check valve, and a dome-loaded regulator to the primary flowmeter, then through a second check valve to the arc heater injectors. Argon or nitrogen was used to start the heater during the hydrogen tests, and the dome regulator load gas was either argon or nitrogen. The normal number of hydrogen cylinders was eight. As many as 20 helium cylinders were manifolded for the high pressure tests.
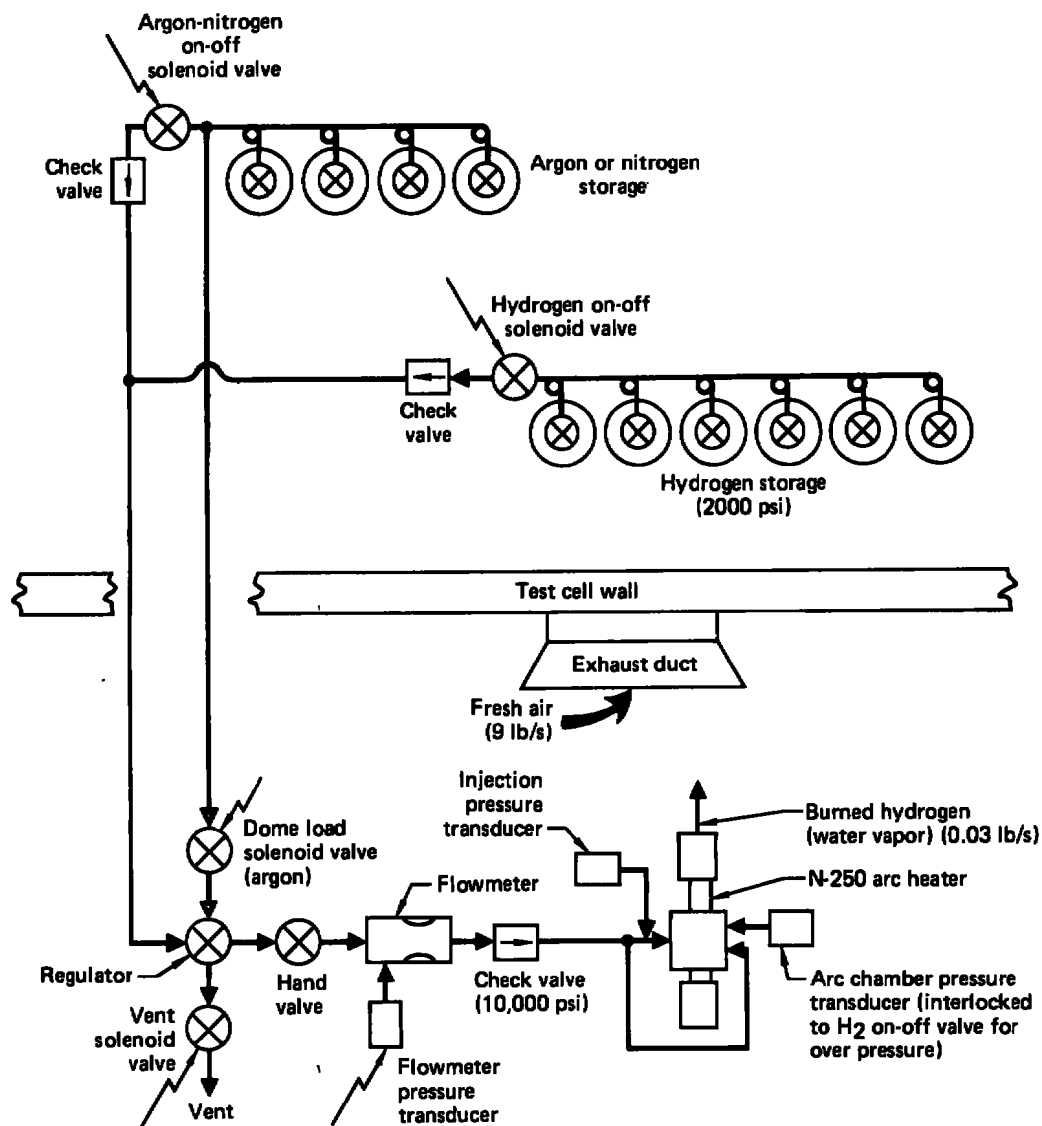
Figure 3 Gas flow system for arc heater operation on hydrogen

17

Air was supplied from the HIP system which is capable of 6000 psi supply pressure and flow rates in excess of 4 lb/s. The air was routed to the same regulator and flowmeter system used for hydrogen and helium.

The HIP Research Data Acquisition System (RDAS), used for all tests, consists of a Varian model 620/f-100 computer with 32,000 (16-bit) words of core memory, a disc memory with a capacity of 2.34 million (16-bit) words, a 7-track magnetic tape unit with 556 bpi, an electrostatic printer/plotter, a card reader and a teletype. The system currently has 48 data channels and is expandable to 256. The RDAS has a maximum sequential scanning capability of 50,000 channels/s with a 100 μs software overhead between records. It can also be programmed to scan selected channels on an individual basis at a maximum rate of 33,000 channels/s with a 60 μs software overhead between records. This mode of scanning can be used for the acquisition of temperature-time data to calculate heat flux incident on a model subjected to the high-temperature plasma environment.

Binary information including sign and parity checks is the primary output. The format is suitable for digital editing, sorting, computing, and plotting by electronic computers. The data are packed in IBM format, on 7-channel, magnetic tape at a packing density of 556 bits/in.

The overall system accuracy, from the signal input to the digital tape output, is approximately ± 0.10%. This accuracy takes into account all items including the multiplexing unit.

The digital readout is available for the display of any given input channel for signal conditioning set-up and check-out, as well as viewing any channel during an arc heater test. This readout was used to monitor the arc pressure for these tests.

3. TEST TECHNIQUE AND MATRIX

The techniques used to operate the arc heater in this program were basically those developed for the HIP facility over the past decade, plus special safety procedures for hydrogen operation. The test matrix included operation at three arc currents at pressures from 10 to 50 atm on hydrogen, 25 to 100 atm on helium, and 10 to 100 atm on air.

3.1 ARC HEATER OPERATION

Preparation of the arc heater for testing included careful assembly and mounting followed by a full-flow water check, static gas-pressure check, and an insulator resistance check. The procedures outlined in Reference 8 were followed where applicable.

The normal arc heater starting procedure for a hydrogen test was as follows:

1. Observe the hydrogen detector alarm to ensure a safe test cell hydrogen level.

2. Turn on low-speed exhaust fan in the HIP test cell.

3. Visually check the gas flow system and arc heater.

4. Open the argon or nitrogen gas supply bottles (hydrogen bottles closed).

5. Check the functioning of all flow system components to ensure proper control and operation using argon.

6. Follow applicable HIP facility operating procedures in preparation for the test.

7. When all subsystems including the data acquisition system are ready for the test, turn on the high-speed test-cell exhaust fan. Check to see that all interlocks are satisfied.

8. Close the argon, nitrogen and hydrogen on-off valves.

9. Manually open the hydrogen bottle valves and check the supply pressure in the bottles.

10. Observe the flowmeter pressure with the main solenoid valve closed to ensure no leakage through the system.

11. Open the argon-nitrogen on-off valve and adjust the regulator to the desired starting flow rate.

12. Turn on the power supplies. (For nitrogen starts, engage striker.)

13. Stabilize the arc heater on argon or nitrogen, then open the hydrogen on-off valve and close the argon-nitrogen on-off valve.

14. Stabilize the arc heater on hydrogen and acquire the desired data by regulating the hydrogen gas flow rate and arc current. Hold each point for 30 s minimum.

15. Turn off the power supplies. (Loss of current automatically switches back to argon or nitrogen.)

16. Allow the high-speed fan to continue blowing while the hydrogen bottles are closed manually and the system is purged with argon or nitrogen.

17. Observe the hydrogen-detector alarm to ensure a safe test cell hydrogen level prior to entering.

18. Secure all systems and reduce data.

Rigid safety precautions and procedures were followed for hydrogen arc heater operation.

All gaseous hydrogen was stored in an eight-bottle rack along the outside of the building. Bottled hydrogen was acquired from the pan stock crib on an as-needed basis. No more than eight full bottles were allowed on the premises at one time. No smoking was allowed in the vicinity of the HIP test cell or hydrogen storage.

All personnel were familiar with the industrial safety procedures for handling hydrogen and adhered to them at all times.

The hydrogen supply system was constructed using valves, fittings, and pipe made of materials that were compatible with hydrogen. Connections were minimized to avoid leaks.

The complete hydrogen supply system was pressure checked at least weekly using 2500 psi helium. The system was pressurized for at least 10 min, and the pressure decay had to be less than 1 psi/min. Leaks greater than this rate were located, corrected, and rechecked prior to operation.

All hydrogen bottles were closed manually, and the system was purged with inert gas when the next test was to be more than one-hour later and/or when the testing was complete for the day.

The hydrogen bottles were returned to the pan stock crib when further testing was not scheduled within a one week period.

Arc heater operation on helium did not require any special precautions. The arc was started on helium by turning on the power supply with a low flow rate (0.005 lb/s). The desired arc pressure and arc current were then set and held for at least 30 s. Usually three arc current levels were tested at a fixed pressure during a single test.

Operation on air required an argon start. As the arc current was initiated the main air valve opened. When the air supply pressure exceeded the argon supply pressure, a check valve closed off the argon. The test procedure after starting was the same as for helium.

Following most of the tests, the electrodes were removed, weighed, inspected, cleaned, reweighed, and re-installed or replaced. Section 4 discusses the resultant contamination measurements. The nozzle throat diameter was measured, and the nozzle was cleaned for the next test.

3.2 DATA ACQUISITION

The experimental data were acquired using the instrumentation and subsystems described in Sections 2.3 and 2.4. The procedure consisted of the following steps:

1. Load acquisition system into the computer via the boot-strap loader.

2. Enter by teletype the date, run number, number of channels (21) scanned, and scan interval (0.01 s for hydrogen and 0.1 s for helium and air).

3. Start the system acquisition and verify that it is functioning during the test.

4. Stop the system acquisition post-test and load the vortex system into the computer.

5. Transfer disc data to magnetic tape.

6. Call the engineering data process program and print out data.

7. Pack as many tests as possible on a single magnetic tape when time permits.

In addition to the primary data acquisiton system, it was also the practice to record the arc voltage, arc current, system pressures, system water flow rates, and arc heater description on a separate data sheet. Electrode weights, arc track locations, and other pertinent data were also recorded.

A complete list of instruments and their calibrations was maintained and updated as changes were made (Table 1).

21

TABLE 1 INSTRUMENTATION

Parameter	Instruments		Calibrated range	Overall system accuracy (%)	Test no.
	Mfg	Model			
Arc voltage	G.E.	JTG-1	0 - 3000 V	0.6	35 - 109
Arc current	G.E.	JDC-1	0 - 900 A	1.5	35 - 109
Arc pressure	CEC	326-1	0 - 1500 psia	0.6	35 - 64
	CEC	326-1	0 - 1500 psia	0.6	65 - 86
	CEC	326-12	0 - 1500 psia	0.3	87 - 109
Flowmeter pressure	Statham	PG285TC	0 - 5000 psig	1.0	35 - 86
	CEC	326-8	0 - 3500 psia	0.2	87 - 109
Injector pressure	CEC	313-1	0 - 5000 psig	0.6	35 - 86
	CEC	326-12	0 - 2500 psia	0.3	87 - 109
Gas temperature	MDC	I/C	0 - 500°F	0.8	35 - 109
	HY-CAL	RTS 4135	0 - 125°F	0.5	35 - 86
	HY-CAL	RTS 4135	0 - 125°F	0.5	87 - 109
Water temperature	MDC	C/A	0 - 600°F	0.7	35 - 109
Anode ΔT	DELTA-T	100	0 - 100°F	1.0	35 - 109
Cathode-body ΔT	DELTA-T	100	0 - 100°F	1.0	35 - 109
Nozzle ΔT	DELTA-T	100	0 - 100°F	1.0	35 - 109
Anode w	Brooks	HP-16M	0 - 50 gpm	1.5	35 - 109
Cathode-body w	Brooks	HP-16M	0 - 50 gpm	1.5	35 - 109
Nozzle w	Brooks	HP-16M	0 - 50 gpm	1.5	35 - 109
Body w	Brooks	HP-8M	0 - 6 gpm	1.5	35 - 109

3.3 TEST MATRIX

Table 2 shows the test matrix for this program and lists the test
numbers for each condition. Each test condition was repeated except the
240 and 400 A points at 75 and 100 atm on air. The arc current levels were
established by stability limitations and the specification of a minimum
increment of 25%. These currents correspond to scaled (I/N) DET arc heater
currents of 800, 1100 and 1400 A which are moderate to high for that heater.
The enthalpies are thus representative of the peak values attainable with a
Huels-type heater such as the one used in the DET.

Numerous additional tests were made on all three gases, and some of
these data are included in the analysis section of this report. The tests
shown in Table 2 represent the best data acquired at the primary conditions
of interest.

Several tests were made in the early part of the program on nitrogen.
Specifically, tests 3 to 54 included stabilization on nitrogen and then a
switch to hydrogen. The nitrogen data were not of primary interest and thus
were not fully reduced nor analyzed.

The striker start on nitrogen was initially thought to be necessary to
minimize the transient from the starting gas to hydrogen. This procedure
was later proven unnecessary when argon starts were successful.

**TABLE 2 ARC HEATER OPERATION ON HYDROGEN, HELIUM OR AIR:
MATRIX TEST NUMBER/s**

	Arc current (A)	Arc pressure (atm)					
		10	15	25	50	75	100
Hydrogen	240	37,38	59,60	56,57	—	—	—
	310	37,38	59,60	56,57	64,74	—	—
	400	37,38	59,60	56,57	—	—	—
Air	240	77,79	75,76	78,84	92,107	93,———	108,———
	320	77,80	75,76	78,83	92,107	93,94	108,109
	400	77,80	75,76	78,84	92,107	93,———	108,———
Helium	240	—	—	95,106	98,99	100,104	103,105
	320	—	—	95,106	98,99	100,104	103,105
	400	—	—	95,106	98,99	100,104	103,105

---

4. ARC HEATER PERFORMANCE CHARACTERISTICS

The absolute and relative performance of a Huels-type arc heater operating on hydrogen, helium or air is discussed in this section. The same basic arc heater with only minor changes was operated on all three gases at the same arc currents and overlapping arc pressures. The primary performance parameters discussed herein include the gas stagnation enthalpy and pressure, the arc voltage, the energy losses, the electrode erosion, the resultant test stream contamination, and the inferred arc length required for scaling purposes.

The performance on each gas is discussed separately in the same format; comparisons are made at the end of this section.

4.1 HYDROGEN ARC CHARACTERISTICS

The arc heater was operated on hydrogen at arc currents of 240, 310 and 400 A at pressures of 10, 15 and 25 atm and at 310 A and 50 atm. The arc parameter values were significantly different from those operating on air or helium; yet the general trends were similar. The arc fluctuations were quite strong on hydrogen requiring additional ballast and inductance in the power circuit. The hydrogen enthalpies were as much as seven times those of air and four times those on helium, while the hydrogen arc voltages were a factor of two higher than those for the other two gases.

Figure 4 shows the arc heater firing on hydrogen. At 240 A current and 25 atm pressure the exhaust jet was a deep blue at the nozzle exit changing to white with a light green border in the subsonic portion of the plume when the hydrogen was burning. The supersonic portion of the exhaust jet appeared more stable than the arc current-voltage oscillations indicated.

A prolonged test condition could not be achieved without the use of approximately 16 mH additional inductance and 7 Ω ballast resistance in series with the arc. The arc current oscillations without these stabilizing circuit components were significantly stronger, and in some cases the arc was totally unstable. At 10 atm and 240 A, the arc current oscillation (as recorded on an oscillograph) was reduced from ± 23% to ± 13% with the addition of the ballast resistor. No major instabilities were encountered using the added inductance and ballast resistance.

Table A-1 in Appendix A presents a summary of the hydrogen data acquired. The tabulated values were extracted from the printed data sheets. Each point represents a stable test condition where sufficient time was allowed for equilibration of the major parameters, especially the differential temperature sensors.

The nozzle throat became coated with a thin layer of copper melt flow during a test; the thickness of this layer was dependent on run time, arc pressure and the arc current level. As the throat size decreased, the arc voltage decreased and reductions were necessary in the hydrogen flow rate to maintain a fixed arc pressure. In one test (64) the nozzle throat diameter decreased from 0.162 in. to 0.144 in. Normally the diameter reduction was less than 3%.
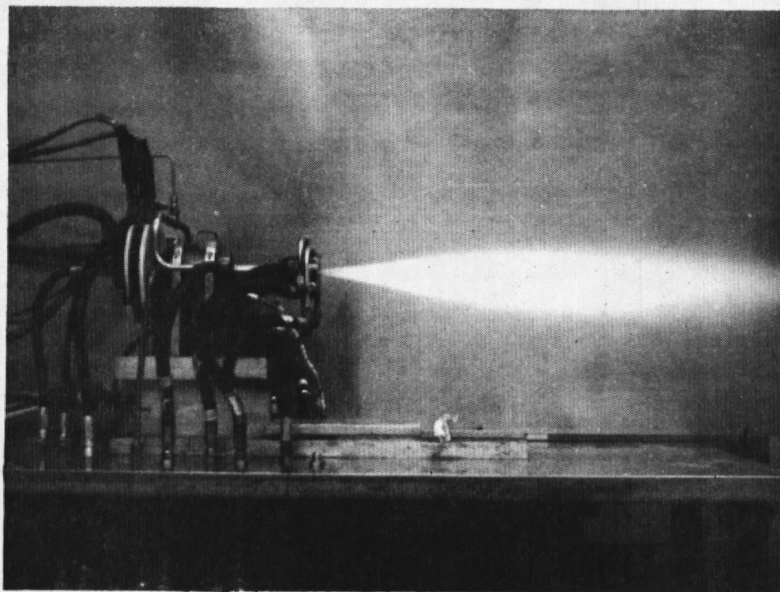
Figure 4 Arc heater operating on hydrogen (25 atm; 240 A)

4.1.1 Hydrogen Enthalpy

The enthalpy levels achieved on hydrogen are shown in Figure 5 as a function of arc current and pressure. Also shown are the enthalpy levels predicted by the hydrogen scaling algorithm (HYARC) described in Section 5. The experimental enthalpy was determined from an energy balance on the arc heater combined with the measured hydrogen flow rate.

The enthalpy varied from 27,700 to 41,600 Btu/lb over the range tested. In general, the enthalpy characteristics were as predicted except at the low pressure and highest arc current. For these conditions, a problem was experienced where the erosion of the entrance to the front electrode was quite severe and the gas vortex was disrupted, resulting in a shorter arc length and lower arc voltage than predicted. The gradual decay of enthalpy as the pressure is increased at a fixed arc current is normal for a Huels-type arc heater. The increase in arc voltage as pressure increases does not compensate for the higher gas flow rate and energy losses, and thus the enthalpy drops gradually.

The repeatability of the energy balance enthalpy improved with increased pressure. The enthalpy at 10 atm was repeated within approximately $\pm$ 11% of the average value, and at 15 atm it was repeated within approximately $\pm$ 7%. At 25 atm, the repeatability improved with increased arc current. At 240 A and 25 atm, the enthalpy was repeated within $\pm$ 6% of the average value, whereas at 400 A it was the same within measurement error in both tests. At 50 atm the enthalpy was repeated within $\pm$ 4% of the average value.

25
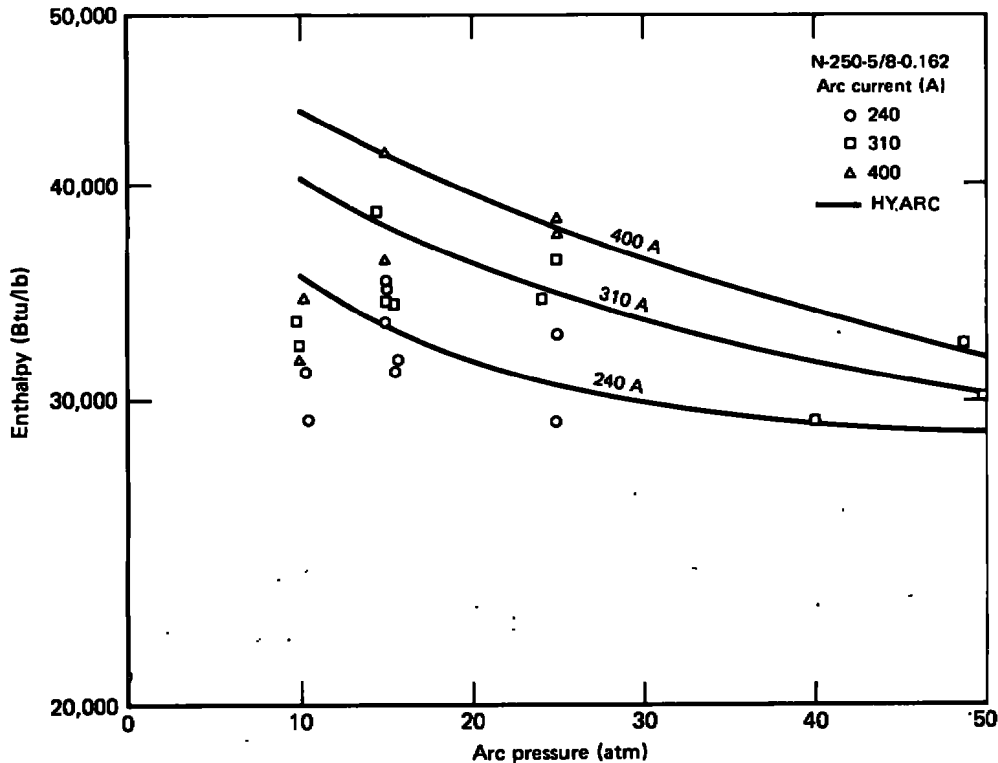
Figure 5 Hydrogen enthalpy performance of the N-250 arc heater

The sonic flow enthalpy was computed for each data point. The enthalpy is useful provided the radial variation of gas properties is not significant through the nozzle throat and the throat size remains fixed. The relation used was derived from the basic sonic flow equation and equilibrium thermodynamic properties of hydrogen. These properties were incorporated in a subroutine to the data reduction program. The sonic flow ratio ($\dot{m}/A* P_o$) was calculated for equilibrium hydrogen at pressures from 5 to 50 atm and temperatures from 5000 to 10,000°R. These values were then curve-fitted to within ± 5% resulting in the following equation.

$$T_o = 2.4 \left(\frac{A* P_o}{\dot{m}} \right)^{1.23} \qquad (5)$$

This equation used the experimental flow rate, pressure, and original throat size to compute the stagnation temperature which in turn yielded the sonic flow enthalpy from a subroutine.

Comparisons between the energy balance enthalpies and sonic flow enthalpies are shown in Figures 6 through 8. At the low-current level, the agreement is fair, but as the arc current is increased and test time elapses, the two values diverge significantly. This discrepancy was a strong indica-

tion that the nozzle throat area was being reduced by resolidified electrode melt. Post-test inspection of the nozzles verified the throat area reduction. Since the calculated sonic flow temperature varied as the nozzle throat diameter to the 2.46 power, a diameter reduction from 0.162 in. to 0.144 in. results in a 34% increase in calculated sonic gas temperature and a typical increase from 30,000 Btu/lb to 70,000 Btu/lb in the calculated sonic flow enthalpy. Thus a factor of 2.33 increase in calculated sonic flow enthalpy could result from a 0.009 in. thick layer of melt flow in the nozzle throat.
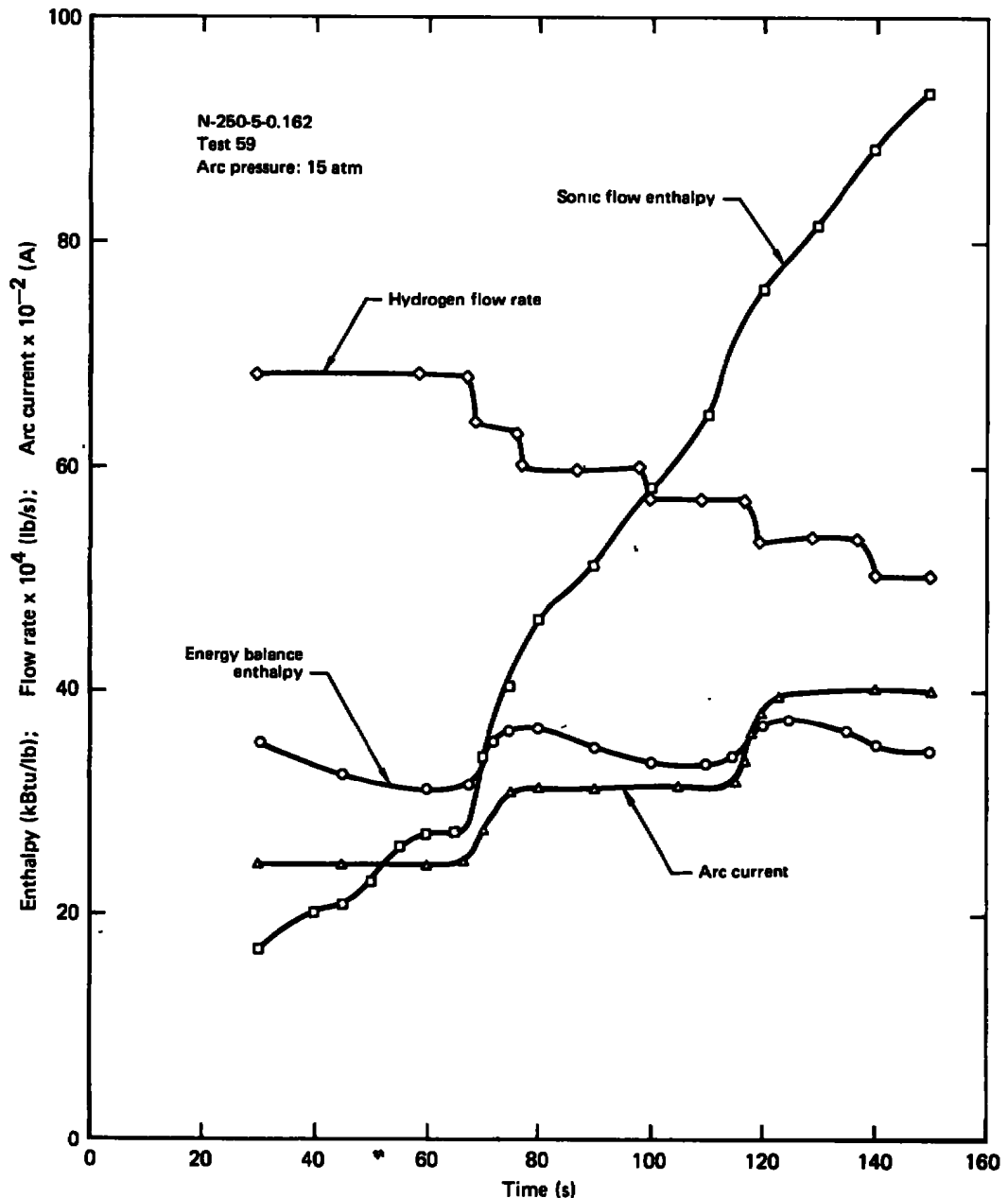
Figure 6 Typical hydrogen test characteristics (P_o = 15 atm)
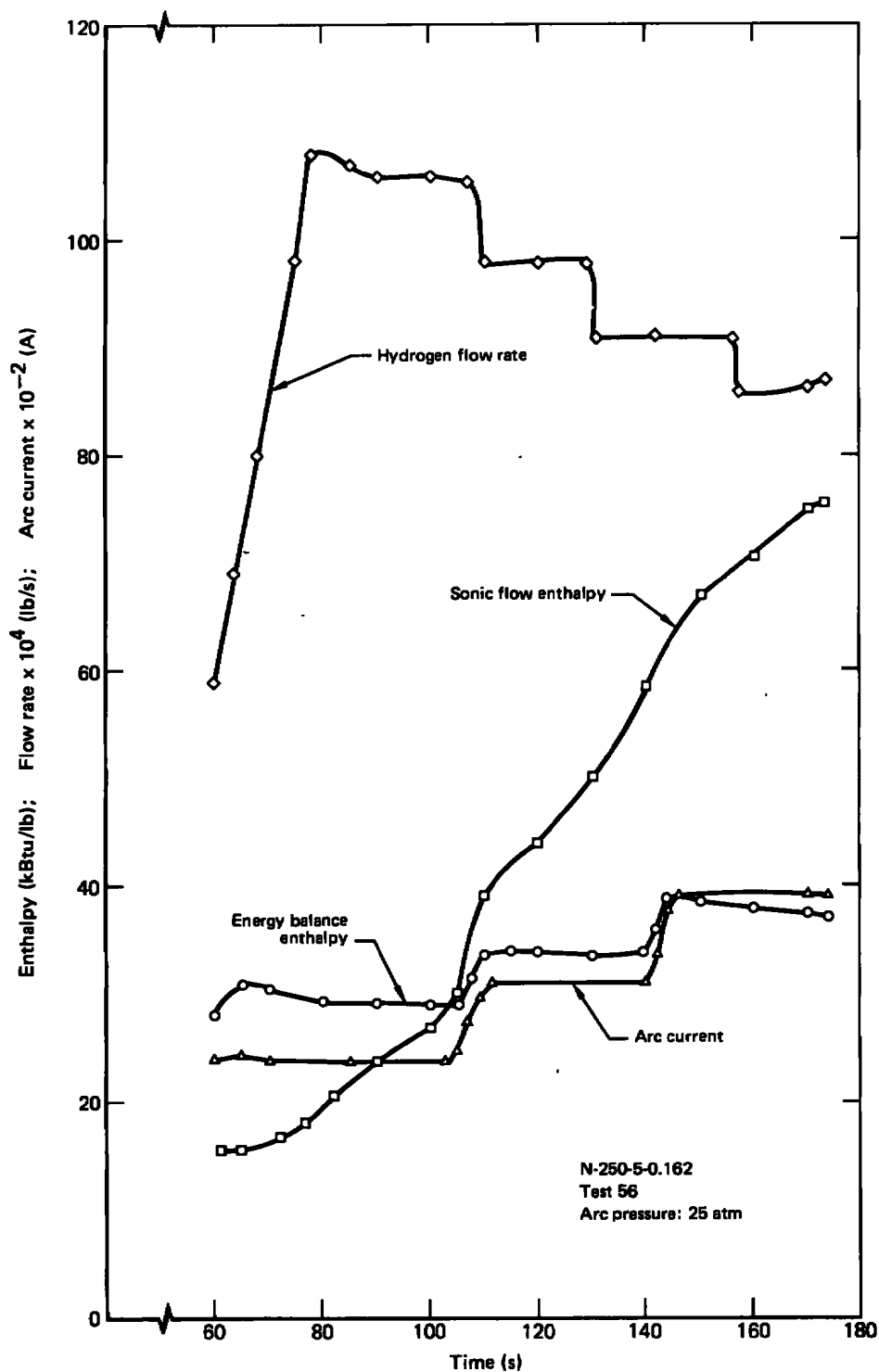
Figure 7   Typical hydrogen test characteristics (P_o = 25 atm)
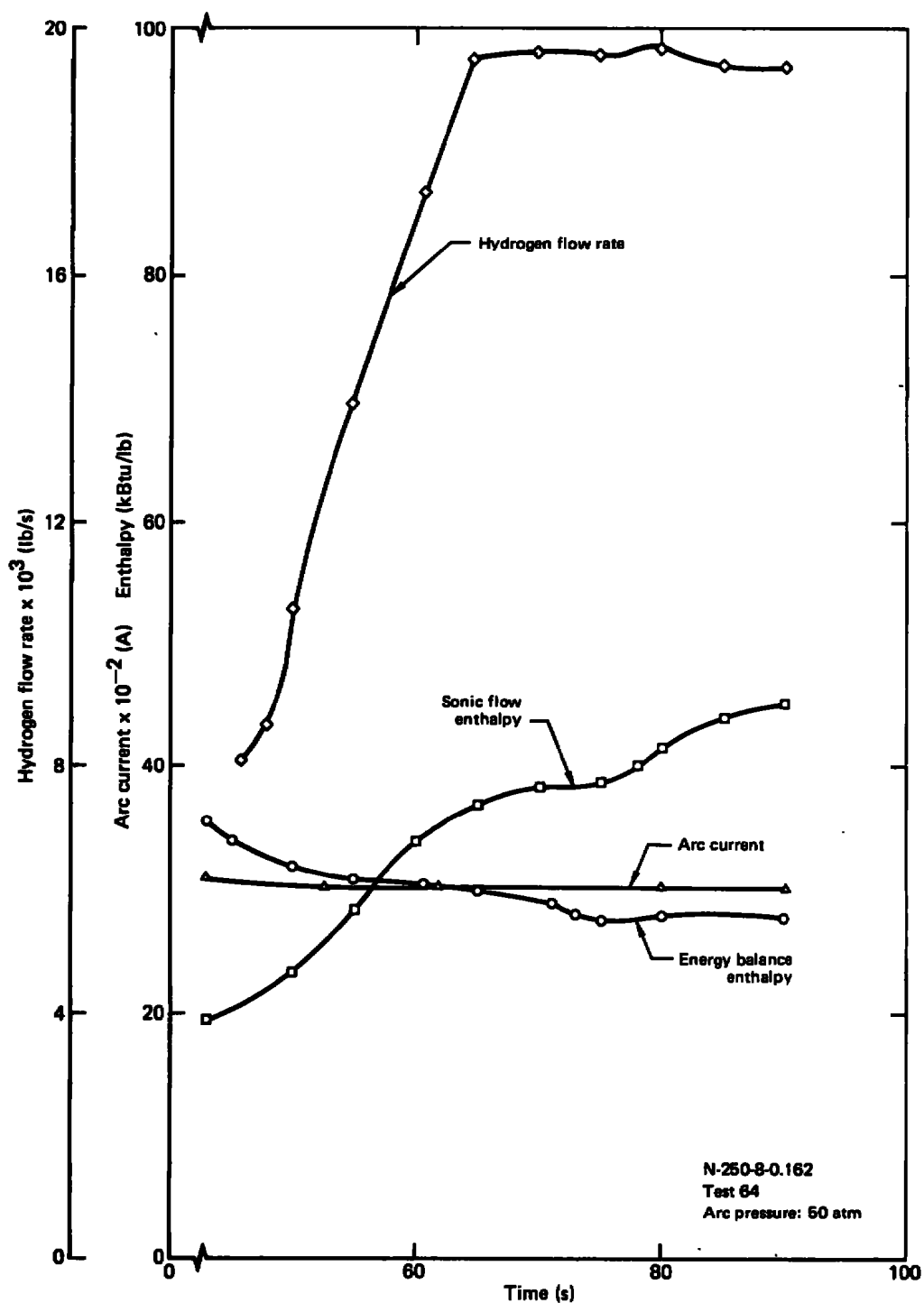
Figure 8 Typical hydrogen test characteristics (P_o = 50 atm)

In test 61, a steady arc current of 240 A and a pressure of 25 atm was held for nearly 3 min. In this test, the energy balance enthalpy was 32,000 Btu/lb at the beginning and 30,000 Btu/lb at the end. The sonic flow enthalpy rose from 22,000 Btu/lb to 85,000 Btu/lb. This change was indicative of a final throat diameter of 0.132 in. which is somewhat less than the 0.144 in. minimum measured.

4.1.2 Hydrogen Arc Voltage

The arc voltage operating on hydrogen was nearly a linear function of the hydrogen flow rate (Figure 9) and nearly an inverse square root function of the arc current (Figure 10). The arc voltage increased from 550 to 3600 V as the hydrogen flow rate increased from 0.004 to 0.02 lb/s. The increased flow rate caused an increased arc pressure. The arc voltage increased linearly with pressure as shown in Figure 11 where the correlation equation was found to be:

$$V = 67.2 \, P_o + 140 \qquad (I = 300 \text{ A}). \qquad (6)$$

This equation along with the arc current dependence in Figure 10 was used in the basic HYARC program to establish an arc length correlation. The results of that correlation are shown in Figure 12 where the arc voltages from the complete test matrix, including peak values during each test, are compared with the improved HYARC output. This comparison is discussed in Section 5.
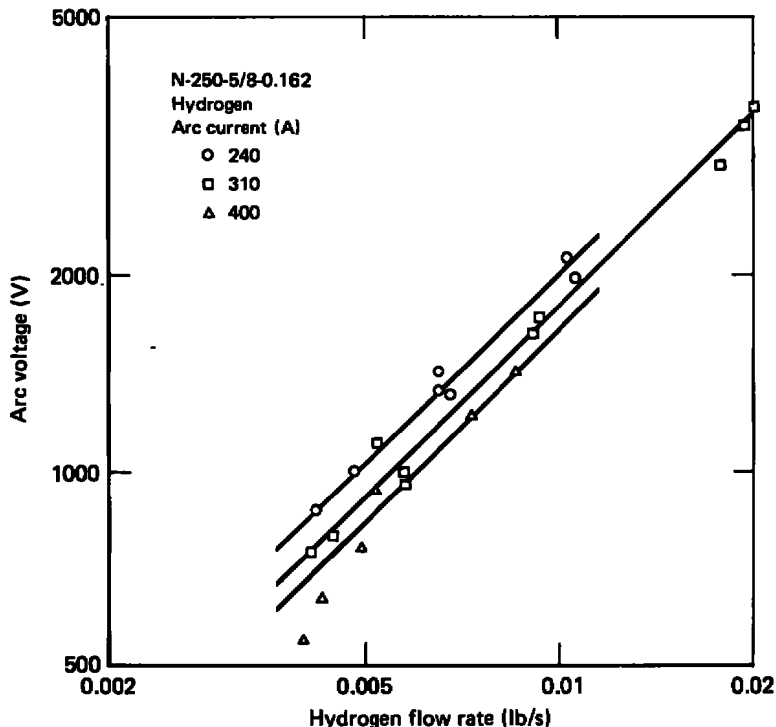
Figure 9   Effect of hydrogen flow rate on arc voltage
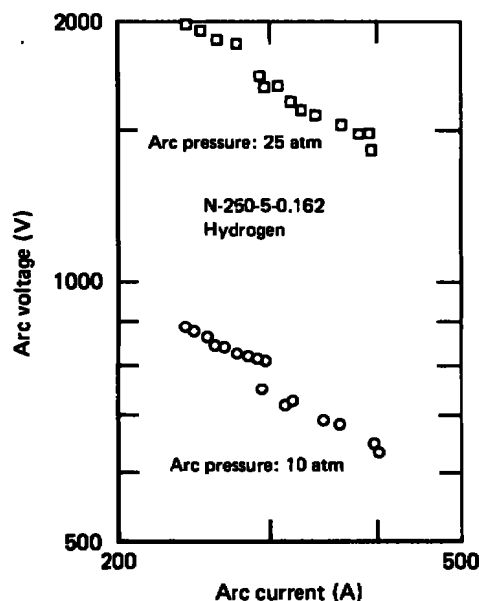
Figure 10 Effect of arc current on hydrogen arc voltage

The arc voltage decreased during a test for several reasons. The nozzle throat area reduction was accompanied by a hydrogen flow rate reduction (to maintain a fixed pressure) which in turn reduced the arc extension forces and the arc column cooling, resulting in lower arc voltage. In addition the roughened electrodes in the restrike region created high electric field points that retained the arc terminations longer, thus lowering the average arc length and voltage. Finally, the roughened entrance region disturbed the gas vortex resulting in more rapid column spreading which caused early restrike and short, low-voltage arcs.

Oscillations in the arc voltage were analyzed early in the testing to eliminate noise on the data record. A storage oscilloscope was used, and noise frequencies of 150 kHz with a modulation of 2.5 kHz were identified. The signal-to-noise ratio was as low as 0.5. An isolation amplifier was subsequently used to eliminate the noise from the data record. The oscillograph traces of the arc voltage indicate oscillations in excess of $\pm$ 12% of the average value at 50 atm and 300 A.

Inspection of the oscillograph traces at high speed revealed a sawtooth arc voltage resulting from the arc rotation and downstream extension followed by abrupt shunting upstream. This is typical of Huels-type arc heater voltage behavior.[7]

31
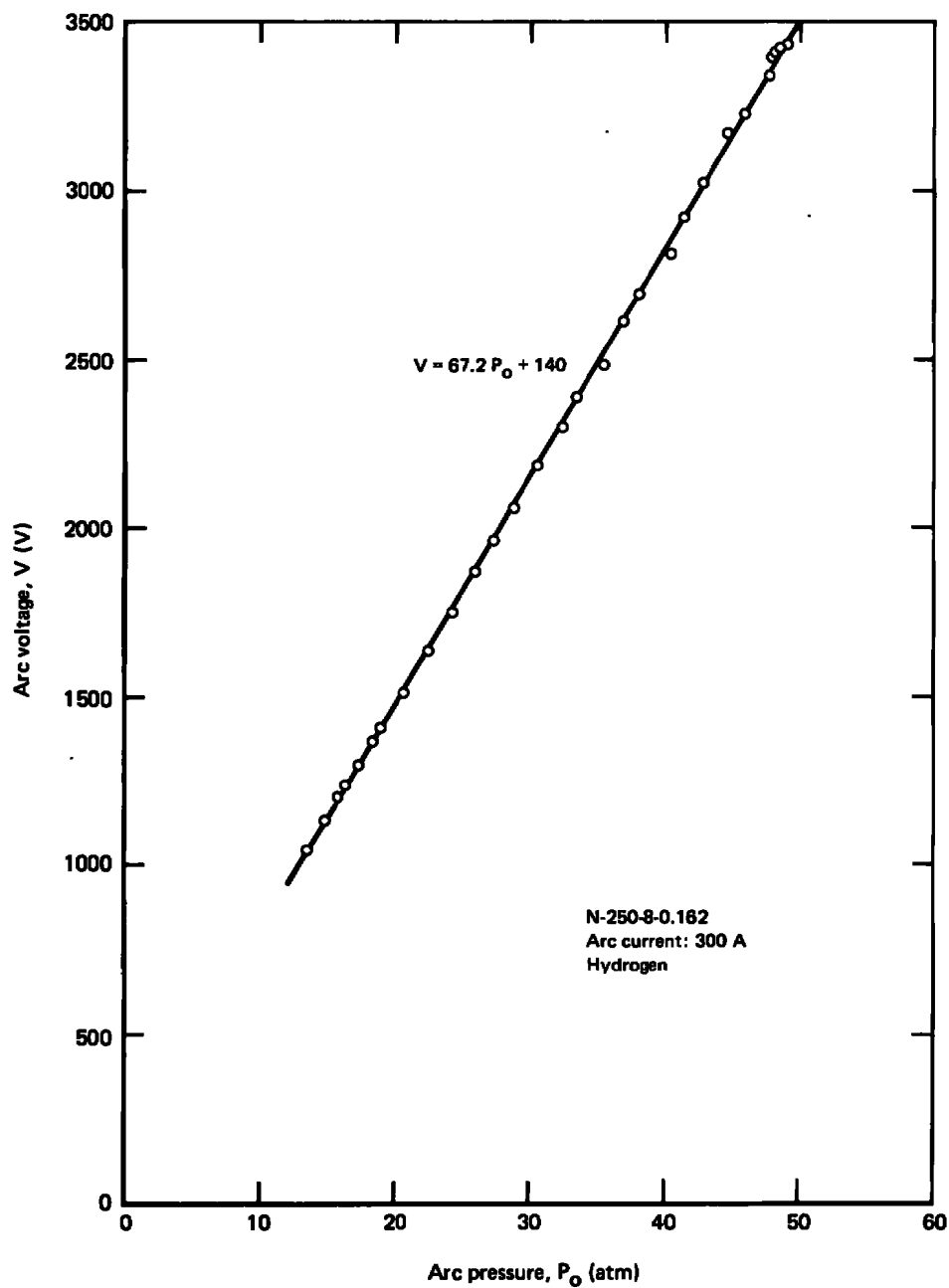
Figure 11   Correlation of hydrogen arc voltage
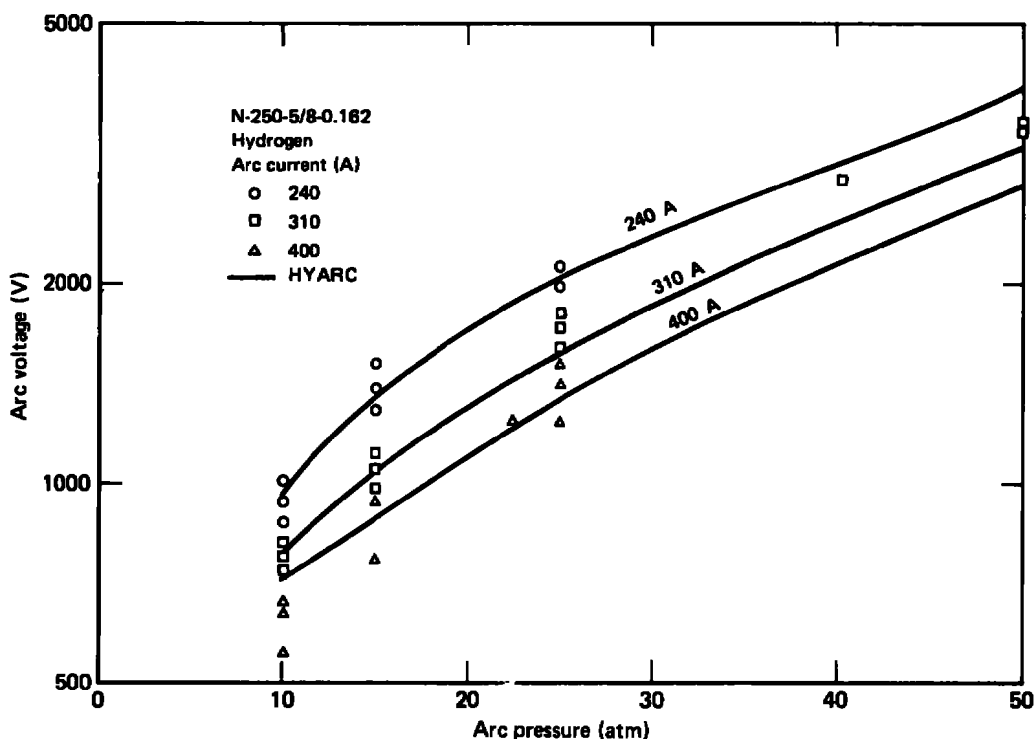
Figure 12 Hydrogen arc voltages

4.1.3 Energy Losses on Hydrogen

The energy losses to the anode, cathode—body, and nozzle operating on
hydrogen are given in Table A-1. Anode (rear electrode) losses varied from
11.7% to 23.6% of the total loss over the full matrix of test conditions.
The magnitude of the anode losses increased with arc current and pressure as
shown in Figure 13. The anode percent of the total losses increased with
arc current at 10 atm pressure but decreased at 15 and 25 atm. The anode
percent of the total losses increased with pressure from 12.7% to 18.9% at
the 310 A level. As the gas flow rate increased (higher pressure), the rear
arc termination moved further back exposing a larger area to arc radiation.
Since there was cold reverse flow along the rear electrode wall, the losses
were predominantly by radiation. The location of the rear arc tracks combined
with the anode losses indicate radiative heating rates from 845 to 1945
Btu/ft^2s at 400 A - 10 atm and 310 A - 50 atm respectively. These values
were correlated with the HYARC radiation flux calculation as discussed in
Section 5.

The energy losses to the cathode—body varied from 53.5% to 71.5% of the
total losses. The absolute cathode—body losses increased with arc current
and pressure as shown in Figure 13. Above 15 atm pressure the percent loss
attributable to the cahtode increased with arc current and pressure. The
predictions shown by HYARC are discussed in Section 5. In general, the data
correlate well.

33
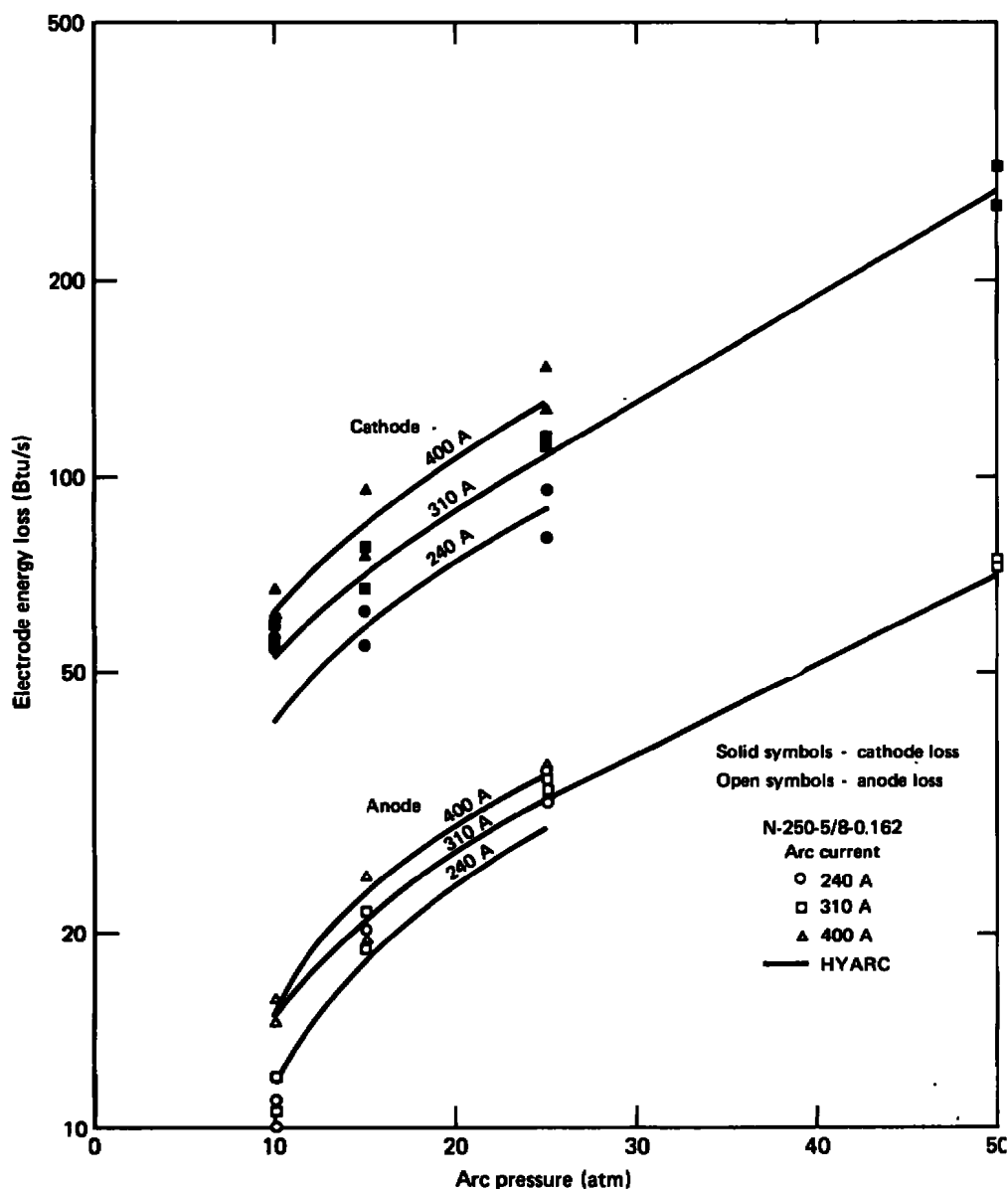
Figure 13 Electrode energy losses on hydrogen

Separate body loss measurements were not made but a reasonable estimate is that they comprise 6% to 7% of the total losses when considering that the body coolant flow includes the entrance corner and upstream cathode flange losses plus the body losses.

An estimate of the experimental convective heating was obtained by comparing cathode-body losses using an 8 in. long cathode and a 5 in. long cathode for the same arc current and pressure. Thus, the losses in the last

3 in. of the longer cathode are primarily convective since the arc attachment is contained within the first 5 in. The experimental heat flux to the last 3 in. of the cathode was 940 Btu/ft^{2}s at 25 atm and 240 A. The HYARC predicted convective heat flux was 1150 Btu/ft^{2}s. The comparative fluxes at 15 atm and 240 A were 920 Btu/ft^{2}s measured and 837 Btu/ft^{2}s predicted. A discussion of the convective correlation used is given in Reference 7.

The nozzle (Section 2.2) energy losses varied from 13.8% to 25% of the total energy loss. In contrast to the anode and cathode-body, the nozzle losses remained relatively constant with increased arc current at pressures $\geq$ 15 atm. The nozzle losses increased with hydrogen flow rate to the 0.8 power. They correlated within $\pm$ 20% using the equation shown in Figure 14 as a function of flow rate and enthalpy difference between the bulk gas and the nozzle wall. This equation was used in the HYARC computer code. An
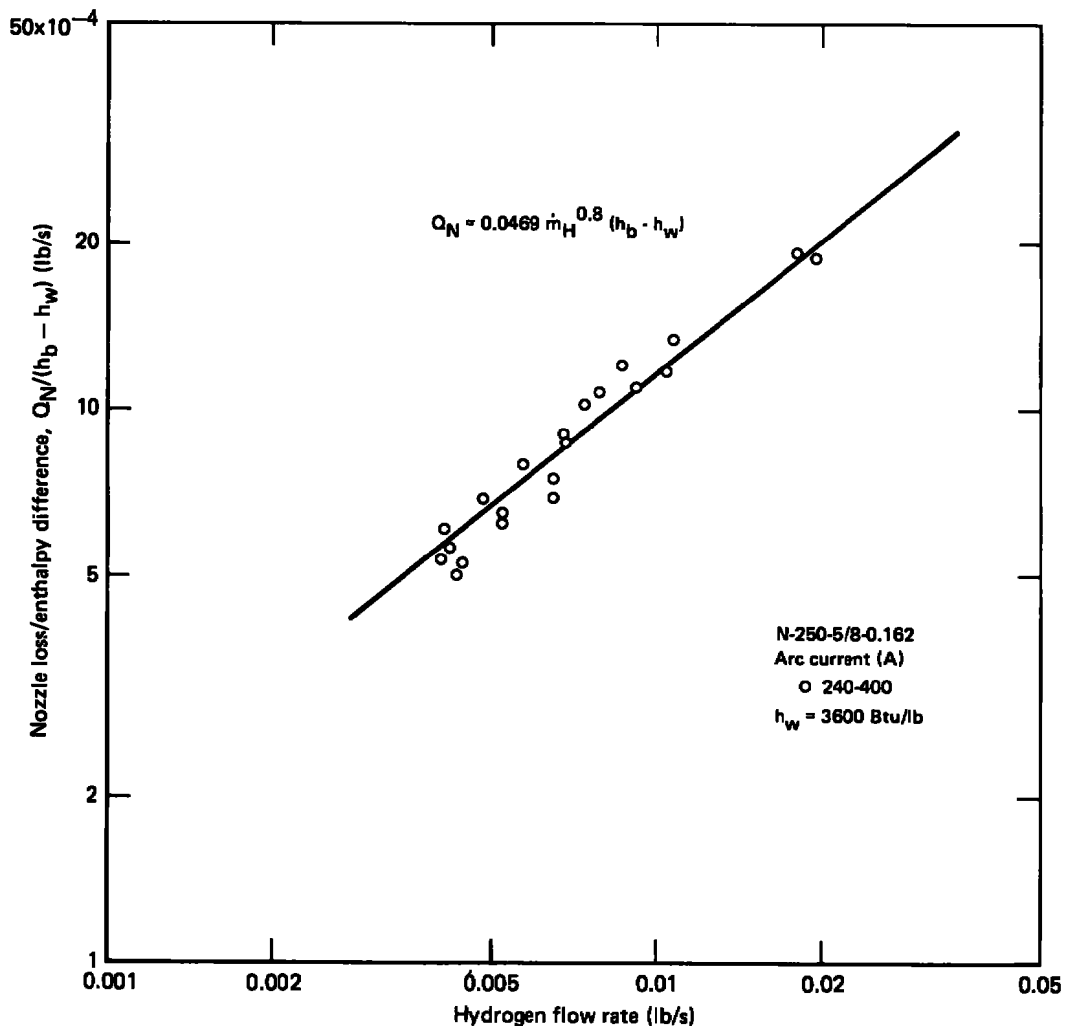
Figure 14   Correlation of nozzle heat transfer on hydrogen

35

estimate was made of the peak throat heat flux encountered. A Bartz[10] heat flux distribution was assumed throughout the nozzle and integrated over the surface area. The experimental nozzle loss was then divided by the integrated heat-flux-ratio/area product to determine the nozzle throat flux. The estimated peak flux of 9800 Btu/ft^{2}s occurred at 50 atm and 310 A. One 30 s test was completed (64) with this heat flux, but the nozzle throat failed in the second (71) and third (74) tests. The duration of the third test was sufficient to obtain repeatability data.

Figure 15 shows the nozzle after test 57 at 25 atm pressure. There was some indication of nucleate boiling despite the fact the estimated throat flux was less than 6000 Btu/ft^{2}s for this test. The white area on the hot backwall of the entrance region to the nozzle was caused by precipitation of water impurities in a poorly cooled region. The two nozzle failures in later tests occurred at the juncture of the straight throat section and the divergent section where the peak heat flux and a stress concentration were combined. A dark ring can be seen in Figure 15 at this point.
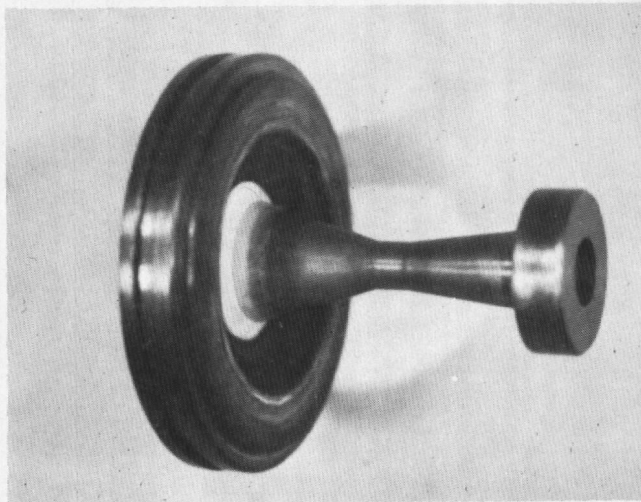
Figure 15   Arc heater nozzle after 25 atm hydrogen tests

4.1.4   Electrode Erosion and Test Stream Contamination

The electrode weight losses were divided by the total hydrogen mass flow between weighings to determine the test stream contamination. Several tests were made at the 240 A level at pressures from 10 to 25 atm, and contamination was determined for a single current level. However, many of the tests were made at three arc current levels, and thus the contamination was representative of that occurring at a median arc current. Figure 16 shows the test stream contamination on hydrogen. At 240 A the contamination level is much lower at low pressure than the higher current. The trend shows considerably less difference at the higher pressure levels.
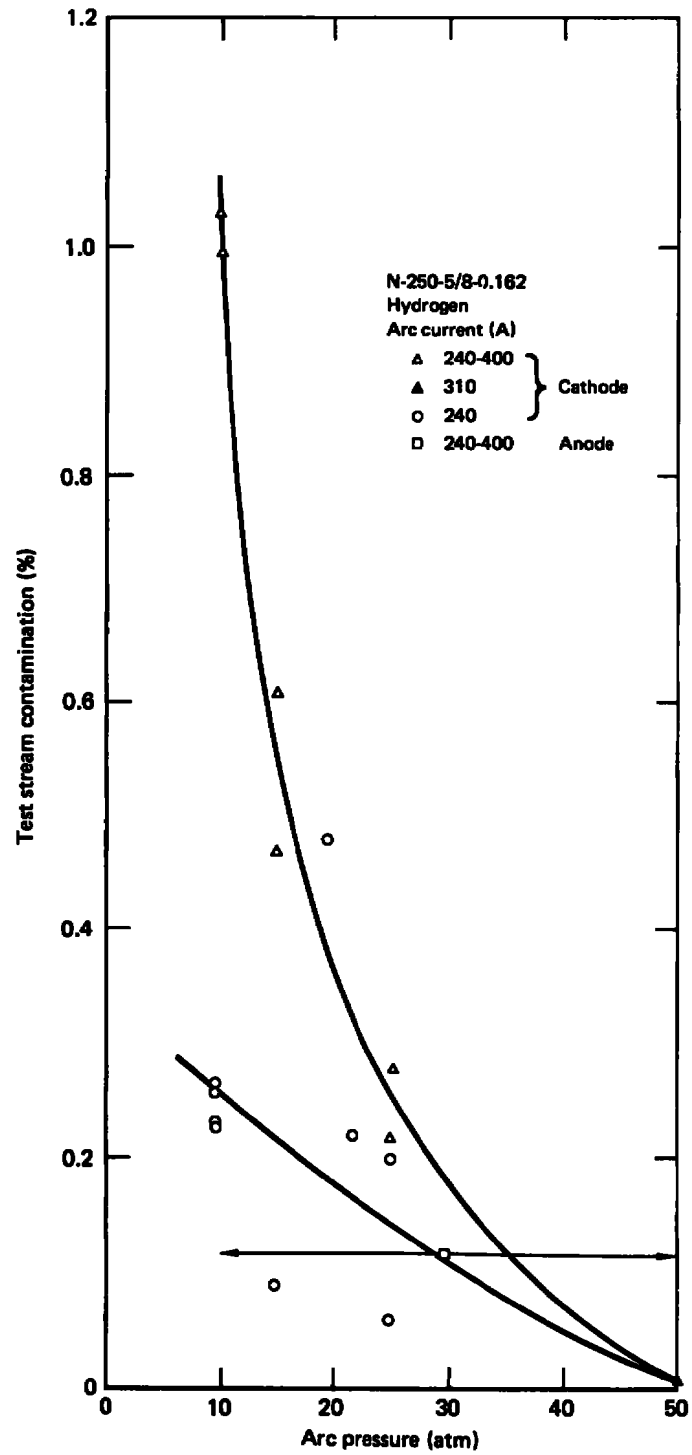
Figure 16 Test stream contamination on hydrogen

Figure 17 shows the post-test entrance region of two typical front electrodes (cathodes) for pressures of 15 and 25 atm and arc currents of 250 – 400 A. At 15 atm, evidence of short arcing and entrance radius erosion is visible, whereas at 25 atm, the primary erosion is further inside the cathode barrel. The electrode used in the 50 atm test did not experience the entrance damage. Arc tracks were visible from the entrance to 5.5 in. inside the barrel with only minor erosion.
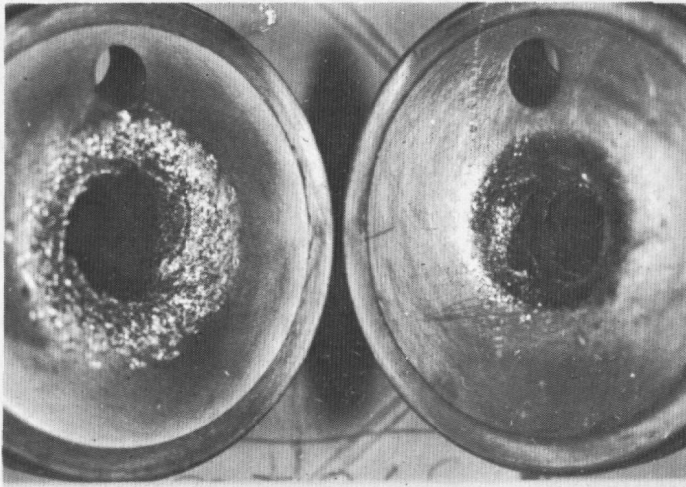
Pressure: 15 atm   OFHC copper   Pressure: 25 atm
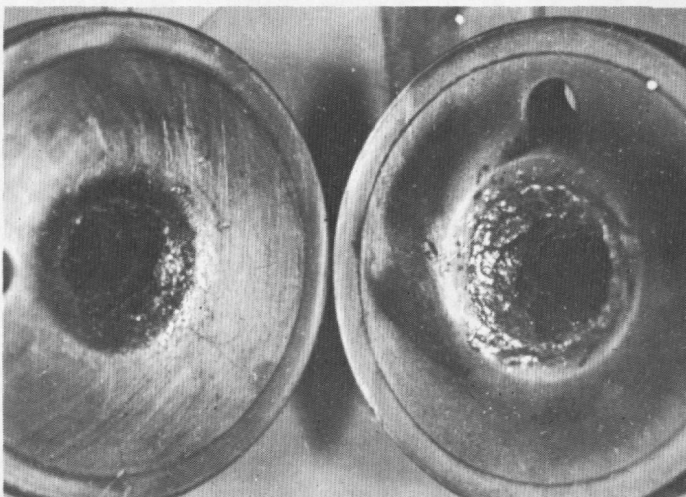
OFHC copper   Pressure: 25 atm   Silver-copper
                    Current: 240-400 A

Figure 17   N-250-5-0.162 front electrodes (cathodes) after operation on hydrogen

Tests were made at 25 atm and 240 - 400 A using an 80% silver, 20% copper cathode. Figure 17 compares the entrance region of that electrode to the previously tested OFHC copper. The erosion was more severe, but the test stream contamination (defined as the electrode mass loss as a percent of the total gas flow rate) was reduced from 0.28% to 0.22%. The reason for the reduced contamination was increased melt solidification. The nozzle and downstream cathode regions were heavily coated with silver-copper melt.

Figure 18 shows the rear electrode (anode) erosion characteristics. This anode was used for tests 1 through 34 at 10 to 15 atm pressure and 240 to 400 A. The anode used for tests 35 through 74 looked very similar with less entrance corner damage. It was subjected to pressures from 10 to 50 atm and arc currents from 240 to 400 A. The anode average test stream contamination for the complete test matrix (tests 36 to 74) was 0.12%. The anode exhibited erosion and melt flow over the first 1.38 in. inside the barrel; beyond that point there were circular surface patterns to 3.00 in. inside the barrel with essentially no erosion.
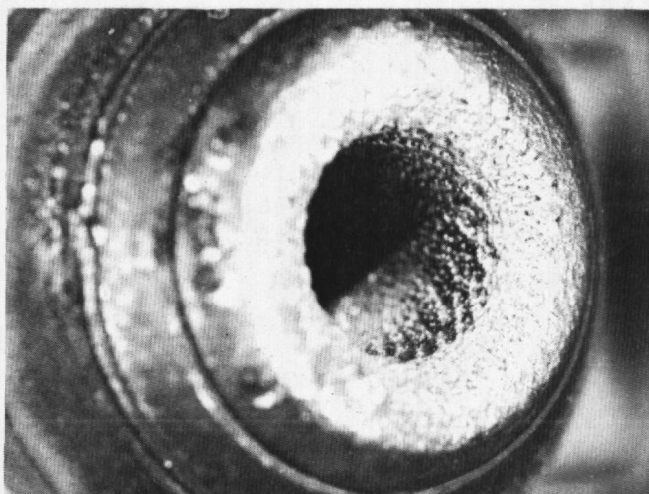
Post tests: 1-34   Current: 240-400 A
Pressure: 10-15 atm   OFHC copper

Figure 18   N-250-5.0.162 rear electrode (anode) after operation on hydrogen

4.1.5 Hydrogen Arc Length

Determination of the hydrogen arc length received considerable attention in order to derive a correlation equation for the HYARC scaling program. Careful measurements of the arc track locations were made throughout the testing. However, for economical reasons it was not feasible to change electrodes for each new condition nor to test each arc current separately. Thus, arc tracks accumulated over a wide band in each electrode making it difficult to distinguish the new tracks from the old, especially midway down the 0.375 in. diam cathode.

Figure 19 presents the arc length data as a function of arc current and pressure. The lengths shown are the combined depths in the anode and cathode plus the 0.25 in. gap between electrodes. The 240 A points shown are primarily from single current tests as are the 310 A points. The 400 A points represent estimated lengths based on the brightest tracks from multi-current tests. The HYARC lengths shown are discussed in Section 5.
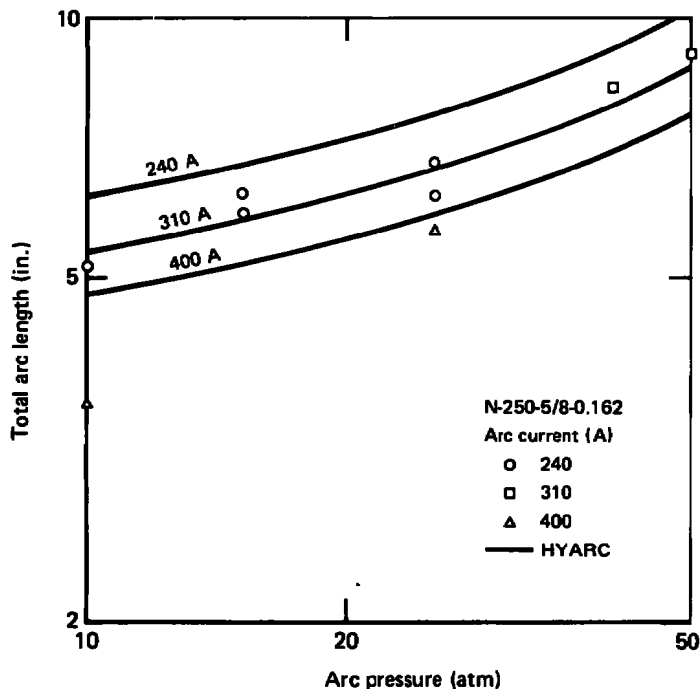
Figure 19   Hydrogen arc lengths

4.2   HELIUM ARC CHARACTERISTICS

The arc heater was operated on helium at nominal arc currents of 240, 320 and 400 A at nominal pressures of 25, 50, 75 and 100 atm with a few intermediate levels. The operating characteristics were similar to those on air with better stability, significantly less electrode erosion and higher gas enthalpies.

Table A-2 in the appendix summarizes the complete helium test matrix including duplicate points. The tabulated values were extracted from the printed data sheets. Each point represents a stable test condition where sufficient time was allowed for equilibration. No nozzle throat-area reduction problems were encountered on helium. The throat diameter remained constant at 0.162 in.

All helium tests were made using one pair of electrodes and one nozzle. The higher pressure tests utilized four 0.062 in. diam gas injectors (tests 103 through 106). The latter test (106) was a duplicate test at 25 atm. All

other tests utilized four 0.052 injectors. The larger injectors reduced the supply pressure requirements to a readily available level (2600 psi). The injection pressure ratio for the small injectors (0.052 in.) ranged from 1.18 to 1.37; the lower value was 25 atm and 400 A and the higher value was 75 atm and 240 A. In general, the higher the gas enthalpy at a fixed arc pressure, the lower the injection pressure ratio. The injection-pressure ratio with the larger injectors (0.062) ranged from 1.15 to 1.28. For a given test condition, the ratio was lowered approximately 6% using these injectors.

In order to complete test 105 at 100 atm and three arc current levels each for 30 s, it was necessary to manifold 20 helium bottles. The initial attempt at 100 atm (test 101) fell short (90 atm) because of supply depletion. The second attempt (test 103) using the larger injectors reached and held the 95 atm level with 12 supply bottles. The third attempt (test 105) using 20 bottles was successful (100 atm).

4.2.1 Helium Enthalpy

The energy balance enthalpies achieved on helium are shown in Figure 20 as a function of arc pressure and current. The helium enthalpies were a factor of four lower than the hydrogen enthalpies. The helium flow rates were a factor of two higher than those on hydrogen, and the helium arc voltages were more than a factor of two lower than the hydrogen arc voltages. Thus, for similar thermal efficiencies, the factor of four difference in the enthalpies was reasonable.

The peak helium enthalpy was 9700 Btu/lb at 25 atm and the minimum was 4700 Btu/lb at 100 atm. At the 400 A level, the factor-of-four increase in arc pressure caused only a 24% drop in the energy balance enthalpy; at the 200 A level, the drop was more severe, 38%.
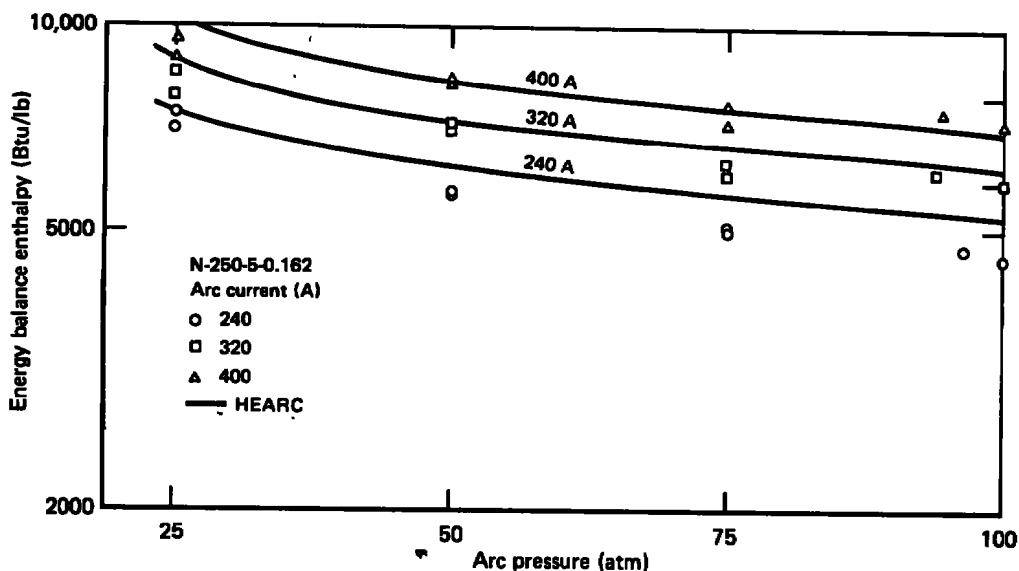
Figure 20 Helium enthalpy performance

41

The predicted enthalpies using the HEARC computer code are also shown in Figure 20. This code is discussed in Section 5.

Agreement between energy balance enthalpy and sonic flow enthalpy was better on helium than on hydrogen primarily because of a constant throat area. General agreement of $\pm$ 5% was found using the sonic nozzle mass flowmeter and small injectors. When using the larger injectors and a subsonic mass flow calibration, the enthalpies differed by 8% to 21% with the sonic flow values consistantly higher. The sonic flow enthalpy on helium is:

$$h_{sf} = 11.87 \left(\frac{P_o A^*}{\dot{m}_{He}} \right)^2 \qquad (7)$$

A comparison of tests 95 to 106 and 100 to 104 from Table A-2, indicated that the suspicious parameter was the mass flow rate. Both comparisons were at fixed pressure and throat area, and both indicated better agreement in the enthalpies when the sonic mass flowmeter was used. However, checks of the subsonic injector flow calibrations did not reveal any significant errors.

4.2.2 Helium Arc Voltage

The helium arc voltages were lower by a factor of two and less sensitive to gas flow rate than the hydrogen arc voltages. Figure 21 shows the helium arc voltages as a function of flow rate and arc current for the full test matrix from 25 to 100 atm. Above 50 atm (0.04 lb/s), the voltage was very insensitive to arc current and depended primarily on the mass flow rate. The helium data shown were correlated using the following equation:

$$V = 1.5 \times 10^4 \, \dot{m}_{He}^{0.72} \qquad (8)$$

The worst discrepancies were less than 8% over the full range of the data. Most of the data were correlated much closer using Equation (8).

Figure 22 compares the correlated arc voltage from HEARC with the experimental values. The arc length used in HEARC was based on post-test arc track locations and experimental arc voltages. Considering this fact, agreement is quite good. These comparisons are discussed further in Section 5. The pressure dependence was approximately the 0.736 power, whereas the current dependence at constant pressure varied from the 0.20 power at 100 atm to the 0.36 power at 25 atm. Note that this arc current effect was largely absorbed by the mass flow correlation, which is typical for a Huels-type arc heater.[2]

The arc voltage did not vary with time at a given pressure and current. The low electrode erosion and constant throat area maintained a very steady arc voltage. The voltage oscillations were mild. The variation in the point average over a 0.85 s period varied less than 6% for a steady current and pressure.
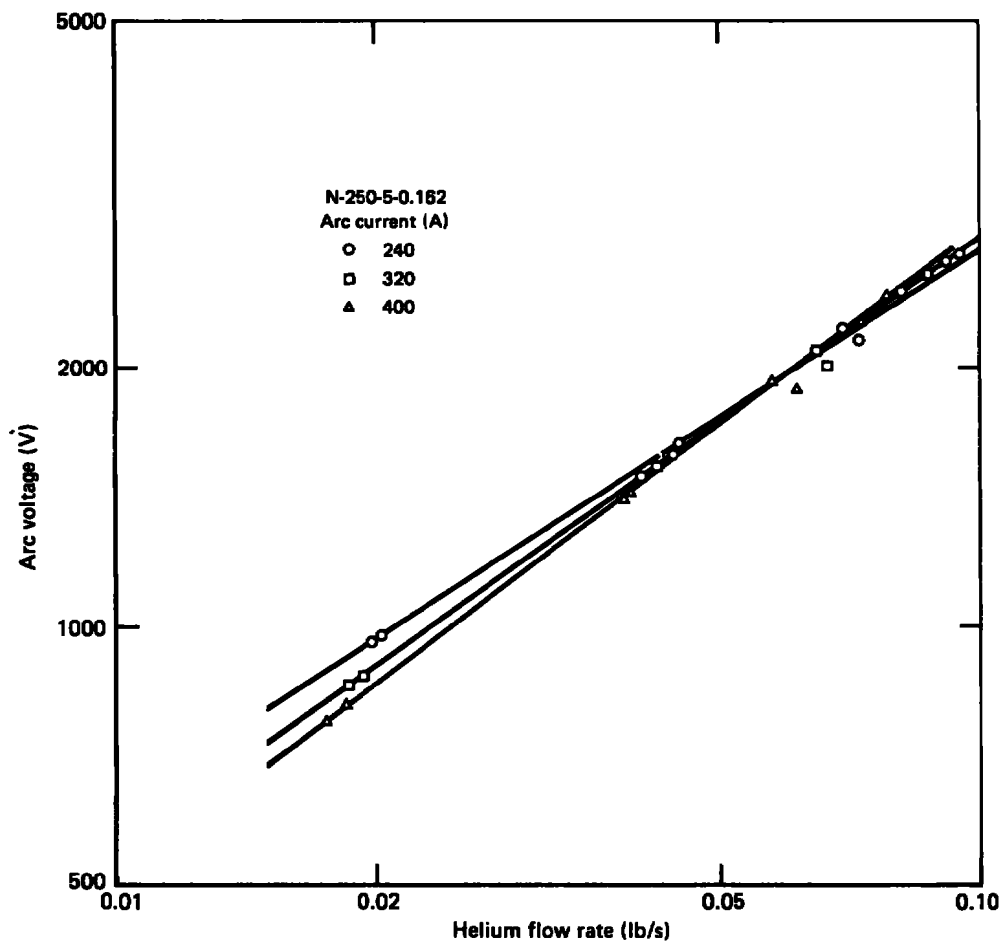
Figure 21 Helium arc voltage characteristics
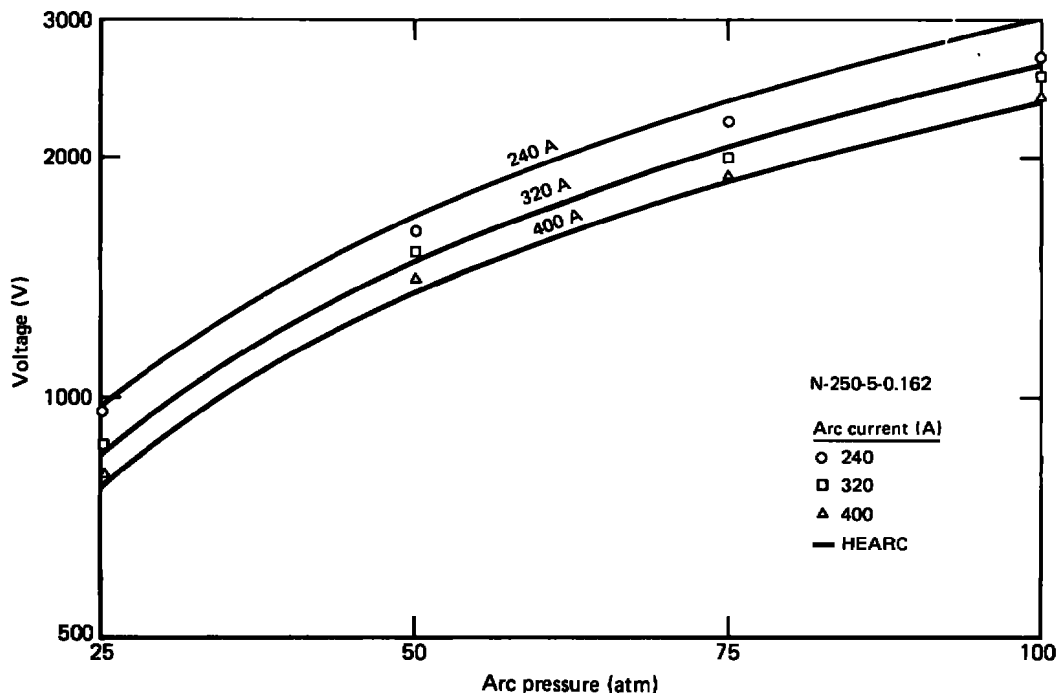
Figure 22 Comparison of measured and predicted helium arc voltages

4.2.3 Energy Losses on Helium

The energy losses to the anode, cathode-body, and nozzle operating on helium are given in Table A-2. Anode losses varied from 18% to 32% of the total losses over the full matrix of the test conditions. The variation of these losses with current and pressure is shown in Figure 23. The magnitude of the anode losses consistently increased with arc current and arc pressure, as did the percent of the total losses. The anode loss dependence on current was approximately the 1.2 power, and the dependence on pressure was nearly linear. As the anode termination moved rearward with increased mass flow (and pressure), it encountered a stronger radial magnetic field from the spin coil. The anode area exposed to radiation thus was not linear with flow rate; hence, the total anode loss became less pressure dependent as shown in Figure 23.

The front electrode (cathode) losses varied from 56% to 70% of the total losses over the full test matrix. The magnitude of the cathode losses increased with arc current and pressure as shown in Figure 24. The cathode percent of the total losses decreased with increased pressure and was relatively insensitive to increased pressure and to arc current. The predicted cathode losses from HEARC also are shown in Figure 24. Good agreement was achieved at the middle pressure range as discussed in Section 5. In contrast to the hydrogen data, these data do not indicate a significant body loss.

The nozzle energy losses on helium varied from 12% to 16% of the total losses. The magnitude of the nozzle losses increased with arc current and pressure, whereas their percentage of the total loss was relatively insensitive to both parameters.
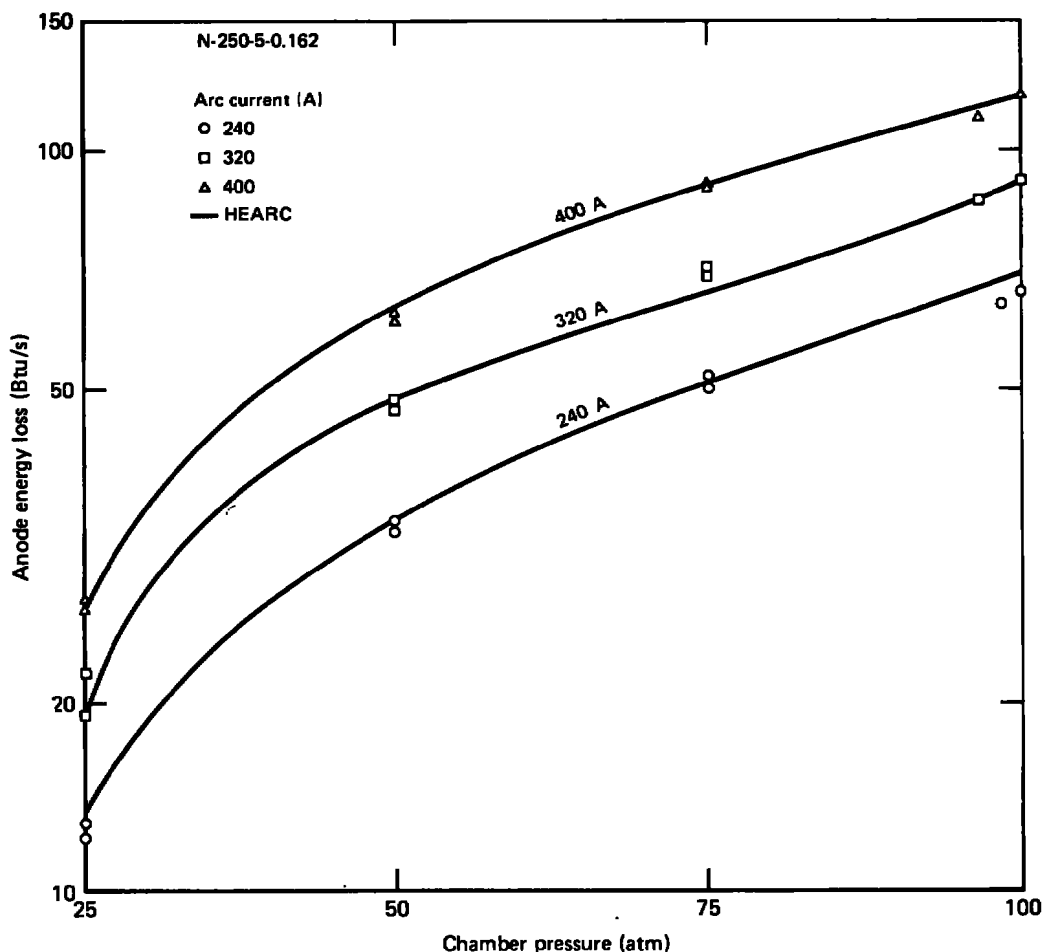
Figure 23 Comparison of measured and predicted anode energy losses on helium

The nozzle energy losses were correlated as a function of the gas flow rate and energy balance enthalpy as shown in Figure 25. A wall temperature of 600°F was used in the correlation. No attempt was made to vary the wall temperature with heat flux. All of the data except test 95 correlated within ± 5% using the following equation:

$$Q_N = 0.04 \, \dot{m}_{He}^{0.7} \, (h_b - h_w) . \tag{9}$$

Equation (9) closely follows typical turbulent convective heat transfer correlations. The weaker dependence on mass flow rate (0.7 power rather than the usual 0.8 power) was somewhat arbitrary. Inclusion of the data from test 95 results in a closer correlation with $\dot{m}^{0.8}$, but the accuracy is reduced to ± 15%.

45

The peak nozzle loss occurred at 100 atm and 400 A. That loss was converted to a peak throat heat flux of 6700 Btu/ft^{2}s using a Bartz[8] heat flux distribution integrated over the nozzle surface area. No damage to the nozzle was encountered in the helium tests.
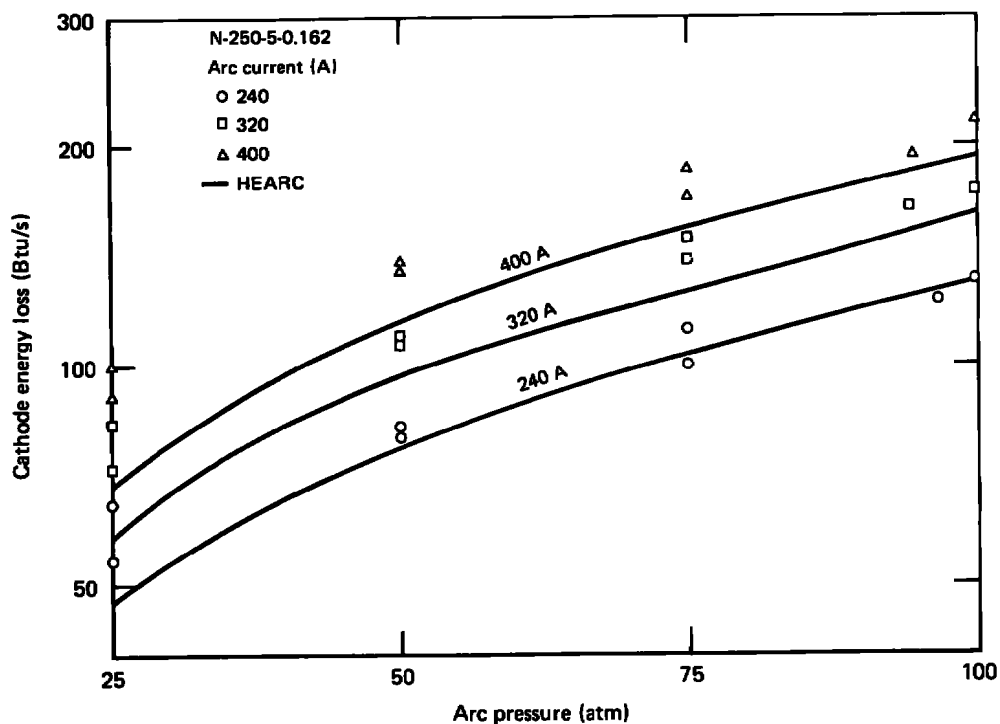
Figure 24 Comparison of measured and predicted cathode
energy losses on helium
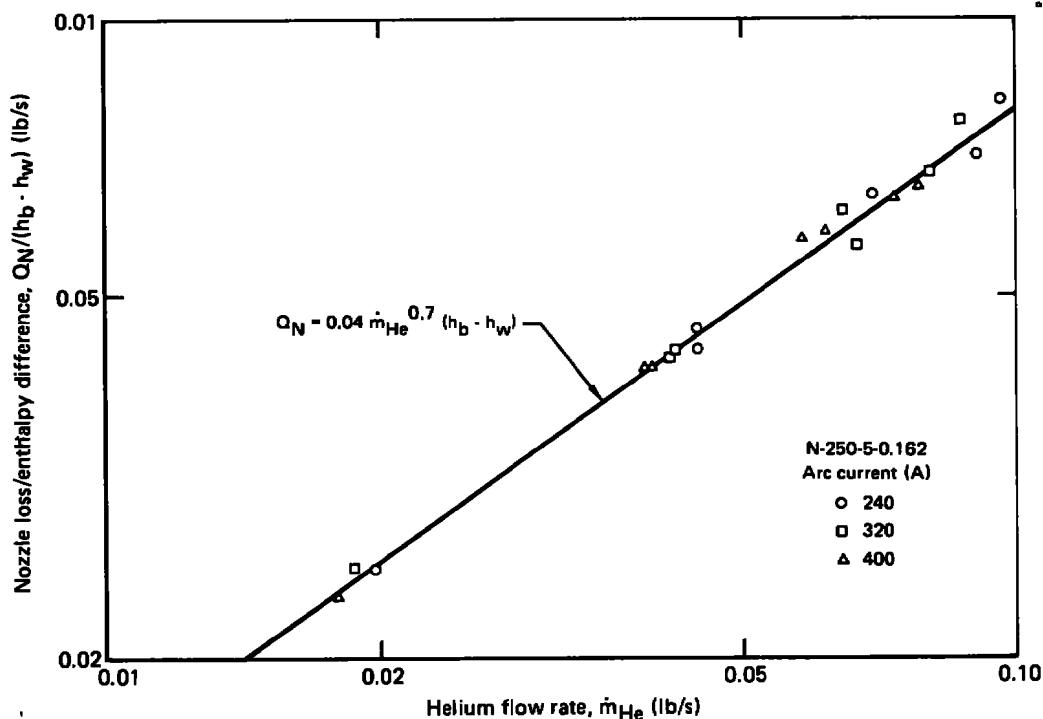
Figure 25 Correlation of arc heater nozzle heat transfer on helium

4.2.4 Electrode Erosion and Test Stream Contamination

At the beginning of the helium testing, the cathode weight was 510.4 g and the anode weight was 510.3 g. After 15 tests on helium at pressures to 100 atm and currents to 400 A, the cathode weight was 503.8 g, a loss of 6.6 g, and the anode weight was 510.2 g, a loss of 0.1 g. The total helium used in these tests was approximately 67.2 lb. Thus the average test stream contamination (electrode mass loss) for all tests was 0.02% of the total gas flow rate. Figure 26 shows the variation of the helium test stream contamination with arc pressure. The higher mass flow rate at higher pressures moves the arc termination more rapidly, reducing electrode material loss and melt flow.

The anode surface was virtually undamaged in the helium test matrix. The surface condition varied slightly with the arc pressure and current. The cathode surface was roughened but did not lose significant material. The entrance corner and downstream barrel were undamaged.

47
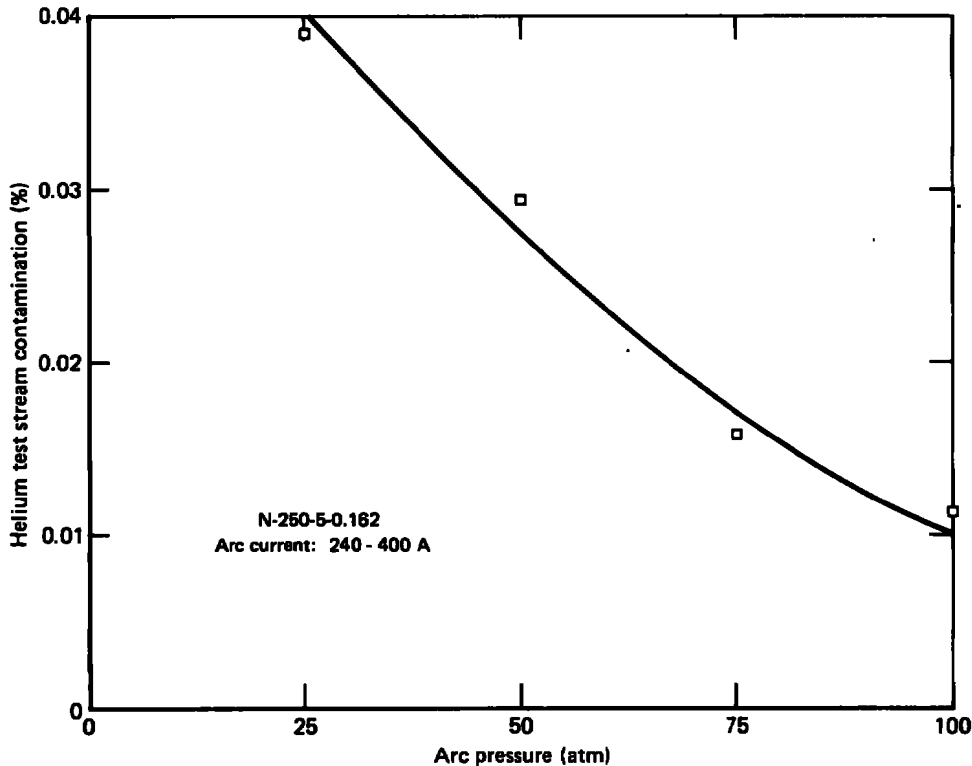
Figure 26   Helium test stream contamination

4.2.5   Helium Arc Length

Figure 27 shows the arc track locations in the anode as a function of helium arc pressure. Since the arc current was varied during a given test, its positioning effect was not documented. However, the surface roughness is normally more severe at high arc current, which was found to be nearest the downstream end of the anode. It is characteristic of Huels-type arc heaters that arc shunting is enhanced by both higher arc current and higher arc potential gradients.[7] Extension phenomena include gas forces from the reverse flow and Lorentz forces from the centering field coil rear of the arc termination. The data indicate that the extension forces predominate to 60 atm at which point the shunting and restrike phenomena begin to reduce the arc length in the anode barrel.

Typical cathode arc tracks are shown in Figure 28. The maximum arc extension was linear with pressure (flow rate) ranging from 1.50 to 4.25 in. downstream of the cathode barrel entrance. The cathode was 5 in. long in all these tests. The minimum restrike position is also shown in Figure 28. Arc column shunting (restrike) occurs near the entrance (0.75 to 1.5 in.). Except for the 100 atm tests, the restrike tracks were in essentially the same position. The arc attachment region was divided into two zones: the rough zone probably characterizes the 400 A arc erosion, and the spiral track zone probably represents the 240 A arc extension tracks.
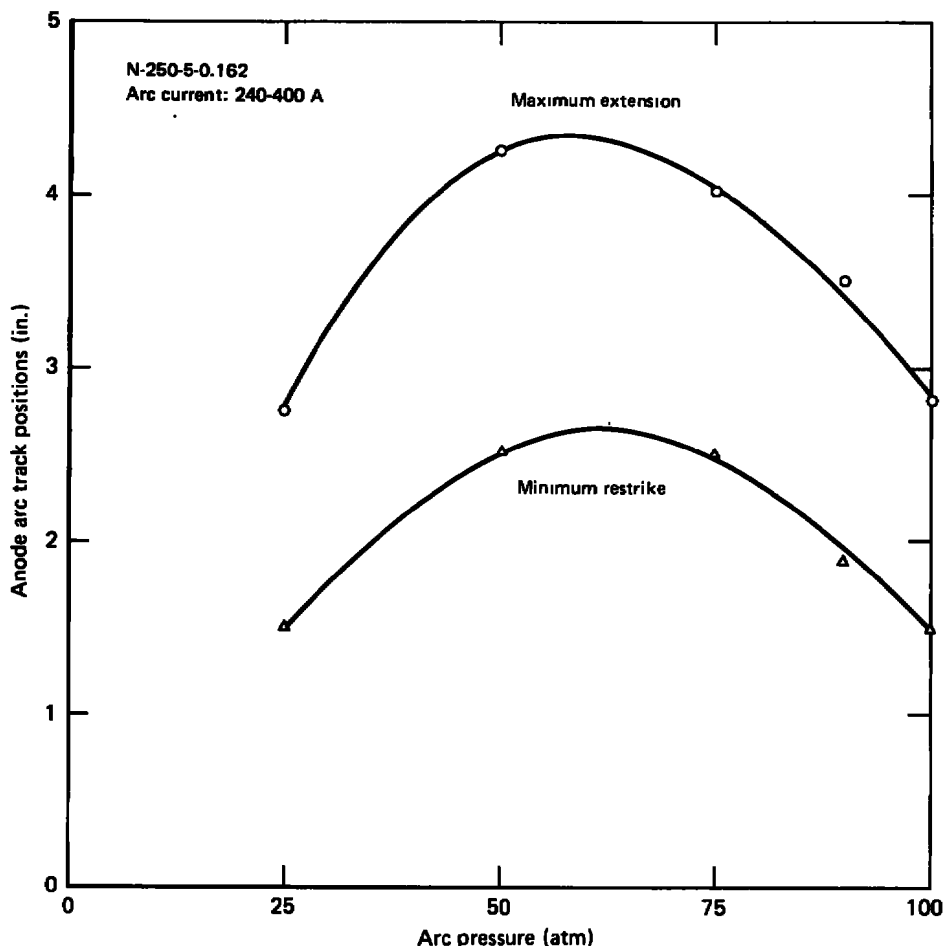
Figure 27   Helium arc anode positions

An accurate definition of the total arc length was not feasible, but approximations could be inferred from the arc track locations. Figure 29 shows the range of possible arc lengths from the arc tracks. The maximum possible length is the sum of the maximum anode plus cathode positions plus the electrode gap (0.25 in.). The minimum possible length is the sum of the shortest positions and the gap. The possible arc length range is quite wide (± 2 in.). The most probable arc length combined the minimum anode track depth with the maximum cathode track depth and vice versa. That narrowed the range as shown in Figure 29. The average arc length was relatively constant above 50 atm with the possible arc length span increasing with pressure.

The arc length required for an arc voltage match using HEARC is also shown. There was reasonable agreement between the most probable arc lengths and required arc lengths at the higher pressures. The inferred arc lengths do not include any arc twisting which has been reported in the past. Future studies should include arc visualization for a better definition of the arc characteristics.
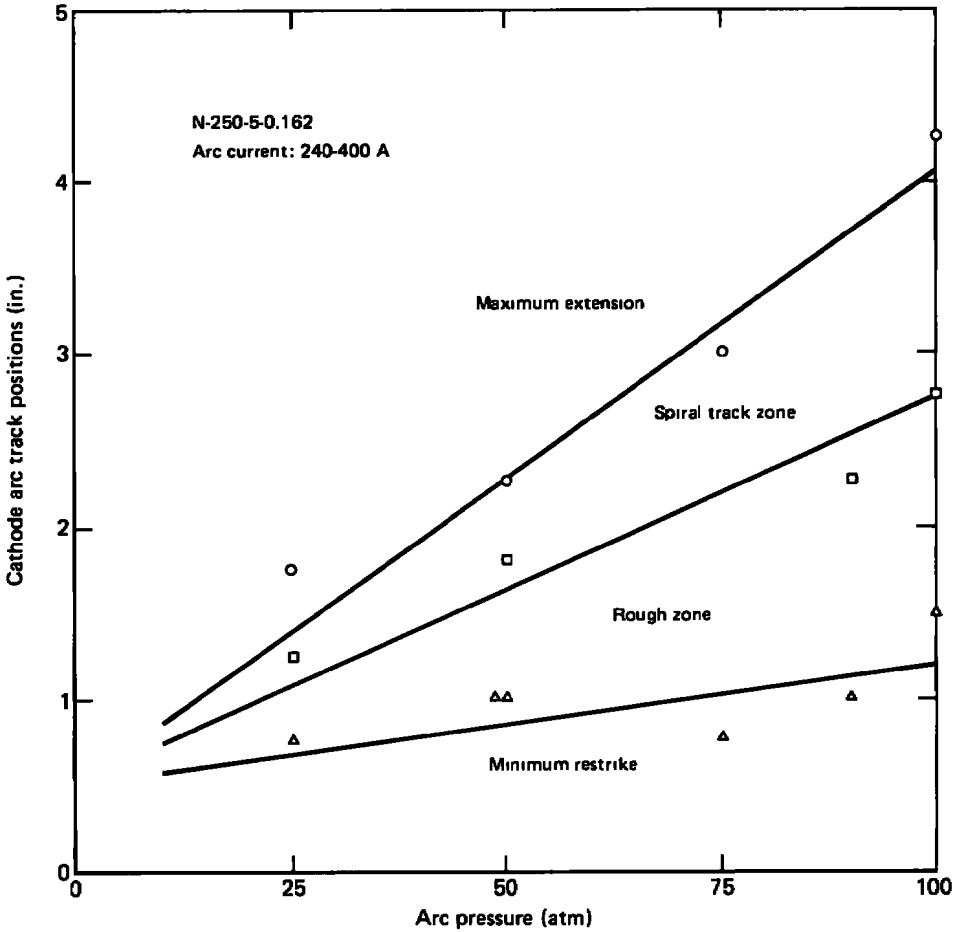
Figure 28 Helium arc cathode positions
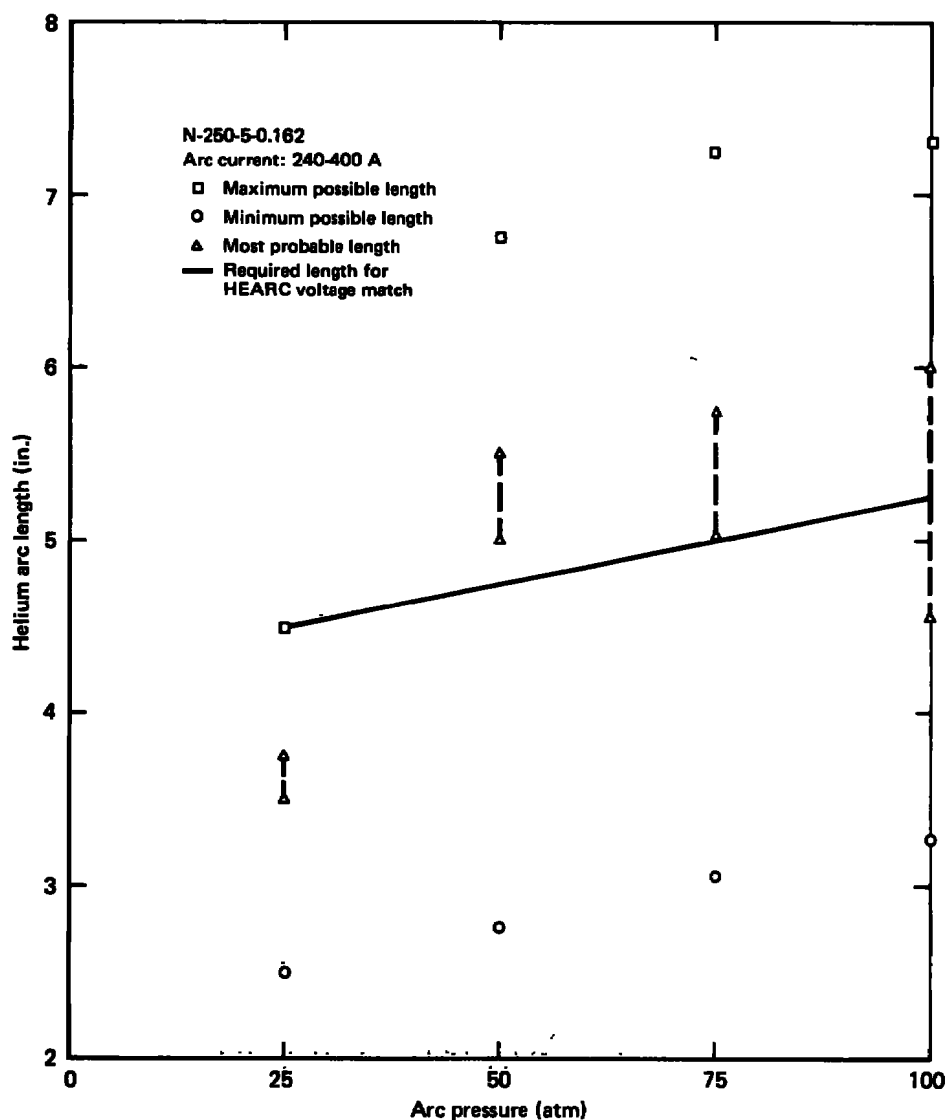
Figure 29 Helium arc lengths

4.3 AIR ARC CHARACTERISTICS

The arc heater was operated on air at nominal arc currents of 240, 320 and 400 A at nominal arc pressures of 10, 15, 25, 50, 75 and 100 atm.

Table A-3 summarizes the complete air test matrix, including duplicate points. The tabulated values were extracted from the printed data sheets, and each point represents a stable test condition where sufficient time was allowed for equilibration.

The 7 Ω ballast resistance and the additional line inductance were used for all air tests. Early tests on nitrogen indicated that some of the lower pressure conditions could have been run without these additional circuit components, but they did add to the stability and allowed direct stability comparisons to be made over the full test range of the other gases.

Tests 75 through 78 were made using four 0.032 in. diam gas injectors. The injection pressure ratio varied from 1.10 to 1.34. Tests 79 through 84 were made using four 0.025 in. diam gas injectors. The injection pressure ratio for these tests varied from 1.79 to 2.13. Some performance improvement was seen at the 10 atm level using the smaller injectors, but there was no significant difference at the 25 atm level. Tests 92 through 94 and 107 through 109 were made using four larger injectors (0.036 in. diam) to reduce the gas system pressure level. The injection pressure ratio varied from 1.24 to 1.40.

All of the air tests in Table A-3 were made using the 5 in. long cathode and the 0.162 in. diam nozzle throat. The eroded electrode material coated the nozzle throat resulting in reduced gas flow rates for a fixed pressure and discrepancies between energy balance and sonic flow enthalpies. Normally the post-test throat diameter was approximately 0.158 in., but after tests 76 and 78, it was less than 0.140 in. The throat was cleaned after each test.

4.3.1 Air Enthalpy

The energy balance enthalpies achieved on air are shown in Figure 30 as a function of arc pressure and current. The air enthalpies were a factor of 5 to 7 lower than those on hydrogen and 41% to 69% lower than those on helium for the same arc current and pressure.
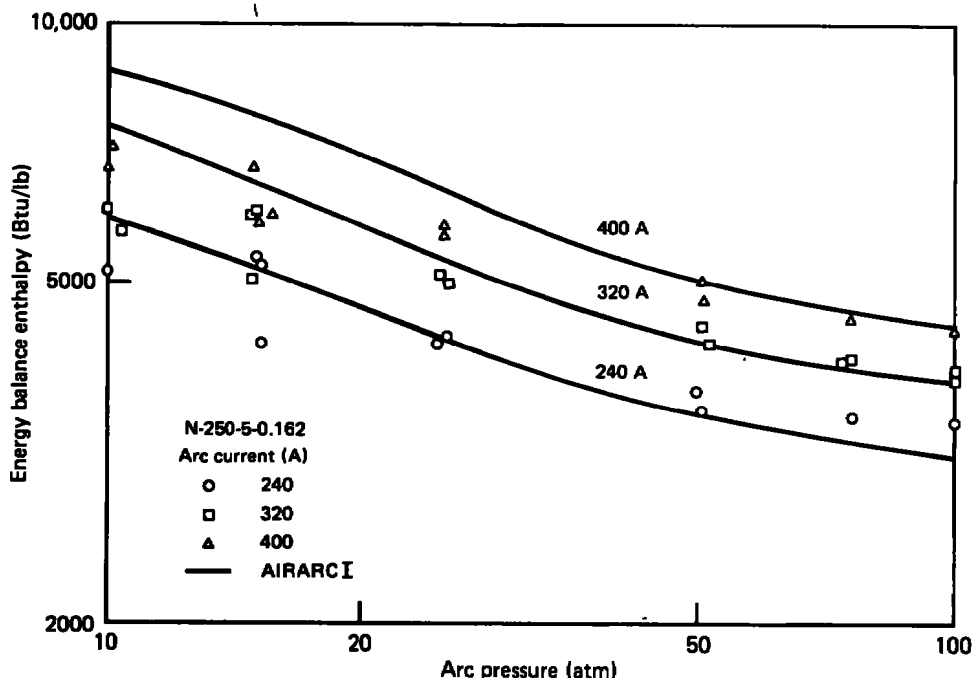
Figure 30 Air enthalpy performance

The peak air enthalpy was 7200 Btu/lb at 10 atm, and the minimum was 3400 Btu/lb at an order of magnitude higher pressure. At a given arc current, a factor of ten increase in pressure decreased the enthalpy by as little as 33% and at most 44%.

The predicted enthalpy values from AIRARC I are also shown in Figure 30. These predictions were based on arc lengths derived from the experimental arc tracks. The actual air flow rates were used instead of the sonic flow relation to avoid throat-area change problems. The nozzle energy loss correlation developed in Section 4.3.3 was added to the calculated arc region losses to determine convective losses downstream of the arc. Agreement is good at the higher pressures, with the worst agreement occurring at the high arc current and low pressure. The factors involved in this comparison are further discussed in this section and Section 5.

Agreement between energy balance enthalpy and sonic flow enthalpy in certain tests below 25 atm was reasonably good. These tests did not result in significant throat-area reduction. In a majority of the tests on air, particularly above 25 atm, the sonic flow enthalpy was consistently higher by 25% or more. A coated nozzle throat diameter of 0.155 in. would have caused this enthalpy difference. Normally the post-test throat diameter was 0.158 in. after the high-pressure tests.

4.3.2 Air Arc Voltages

The air arc voltages varied from 400 to 3000 V as the pressure was increased from 10 to 100 atm. Figure 31 shows the experimental values as a function of arc current and pressure. As expected, the arc voltages were higher at the lower arc currents. The sensitivity to arc current decreased from 10 to 25 atm, then increased again as the pressure was increased to 100 atm.

The arc voltage and current were very stable over the full range of test conditions. The 10-scan average (0.85 s elapsed time) voltage at 240 A and 100 atm varied less than $\pm$ 1%. Above 15 atm, the arc voltage repeatability was remarkable compared with other Huels-type heaters. At 50, 75 and 100 atm, the repeat test voltages were identical within the accuracy of the measurements.

The predicted arc voltages shown in Figure 31 were based on arc lengths inferred from the arc tracks post-test. These lengths are discussed in Section 4.3.5. The predicted arc voltages could possibly have been matched closer by using a technique similar to that used in HYARC, but the agreement shown in Figure 31 was judged sufficiently accurate. This technique was also a better test of the scaling accuracy of AIRARC.
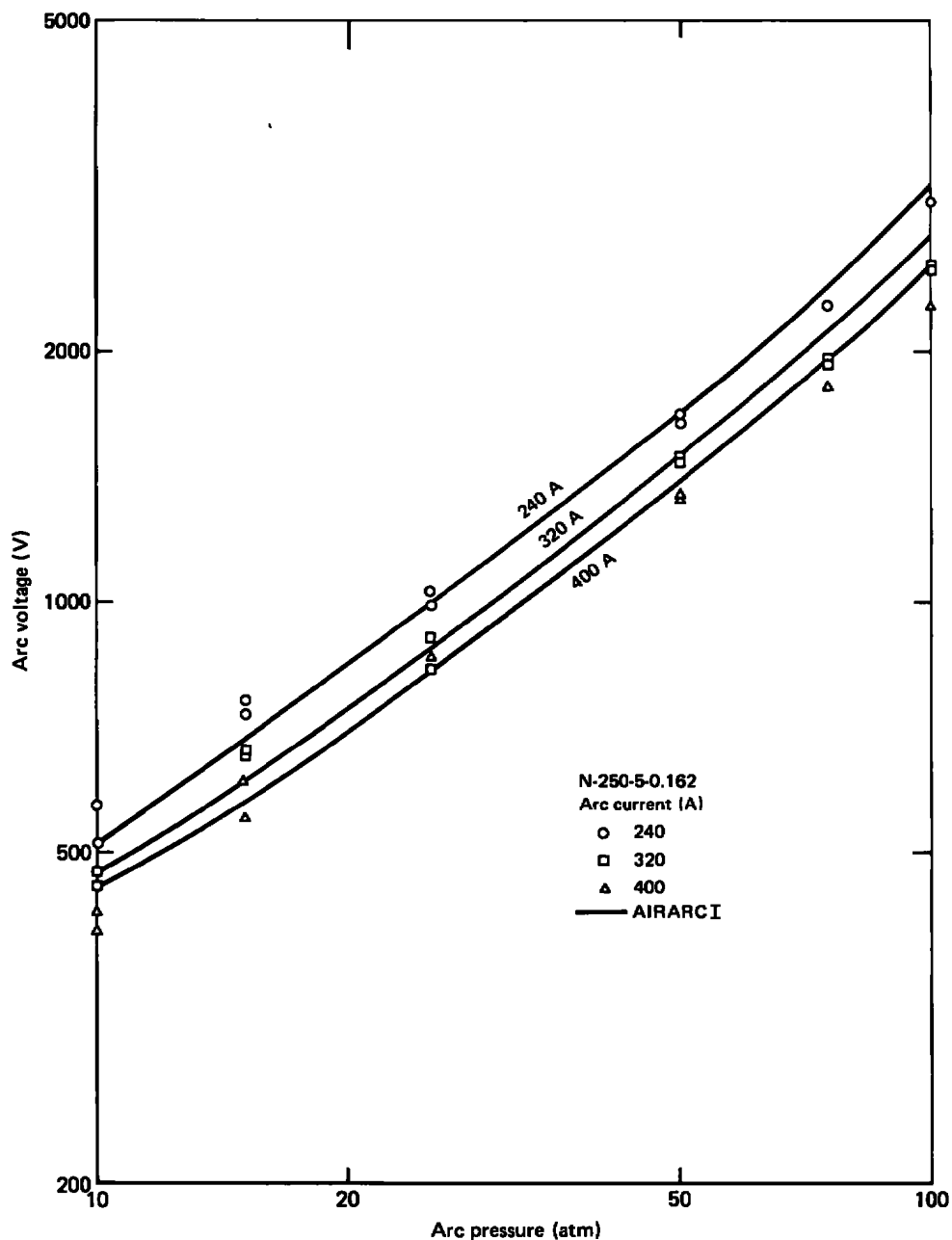
Figure 31 Air arc voltages

4.3.3 Energy Losses on Air

The energy losses to the anode, cathode-body, and nozzle are given in Table A-3 for the complete air test matrix. The anode losses varied from 14% to 26% of the total losses and consistently increased with arc current and pressure. The cathode-body losses varied from 58% to 74%, and the nozzle losses varied from 11% to 21% of the total energy losses.

Figure 32 shows the combined electrode losses (excluding the nozzle) as a function of arc current and pressure on air. The data can be correlated using the following equation:

$$Q = Q_A + Q_C = 0.044 \ I \ P_o^{0.58} \qquad (10)$$
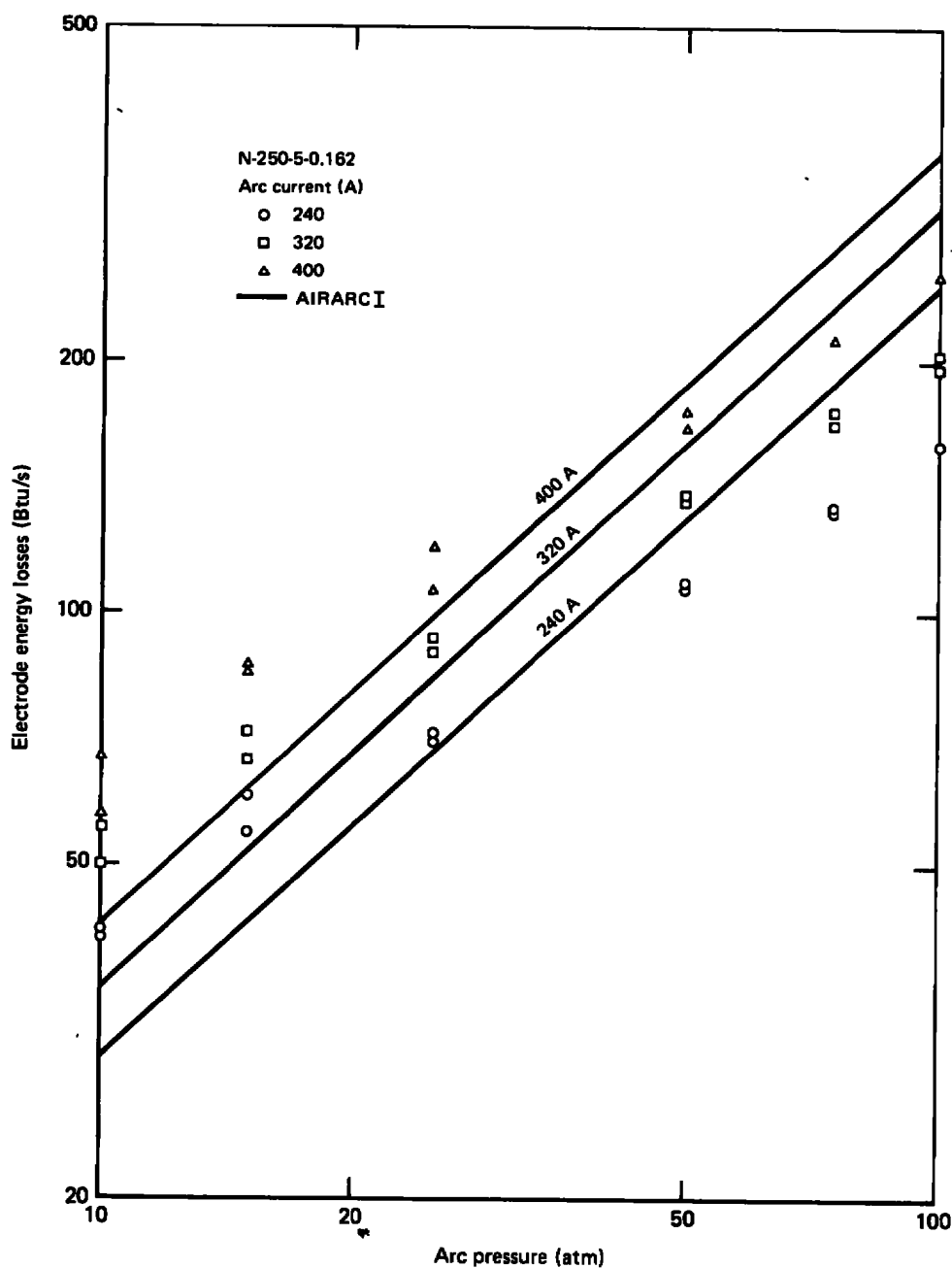
Figure 32 Electrode energy losses on air

The predictions shown in Figure 32 were made using AIRARC I which combines volumetric radiation (optically thin) and a standard convective correlation. Although the absolute magnitudes of the predictions are not significantly in error, particularly in the middle pressure range, the functional dependence on pressure appears high (0.92 power). The data were quite repeatable and consistent. A much closer correlation of the data was achieved using AIRARC II as discussed in Section 5.

The air nozzle energy losses (Figure 33) were correlated using the same equation as for the hydrogen nozzle losses:

$$Q_N = 0.0469 \ \dot{m}_a^{0.8} \ (h_b - h_w) \ . \tag{11}$$

Equation (11) has the same general turbulent convection form as the helium nozzle loss equation and standard pipe correlations. The coefficient and mass flow rate exponent are slightly different.

The peak nozzle loss occurred at 100 atm and 400 A. That loss was converted to a peak throat heat flux of 5900 Btu/ft^{2}s using a Bartz[8] heat flux distribution integrated over the nozzle surface area. No damage was encountered to the nozzle during the air tests.
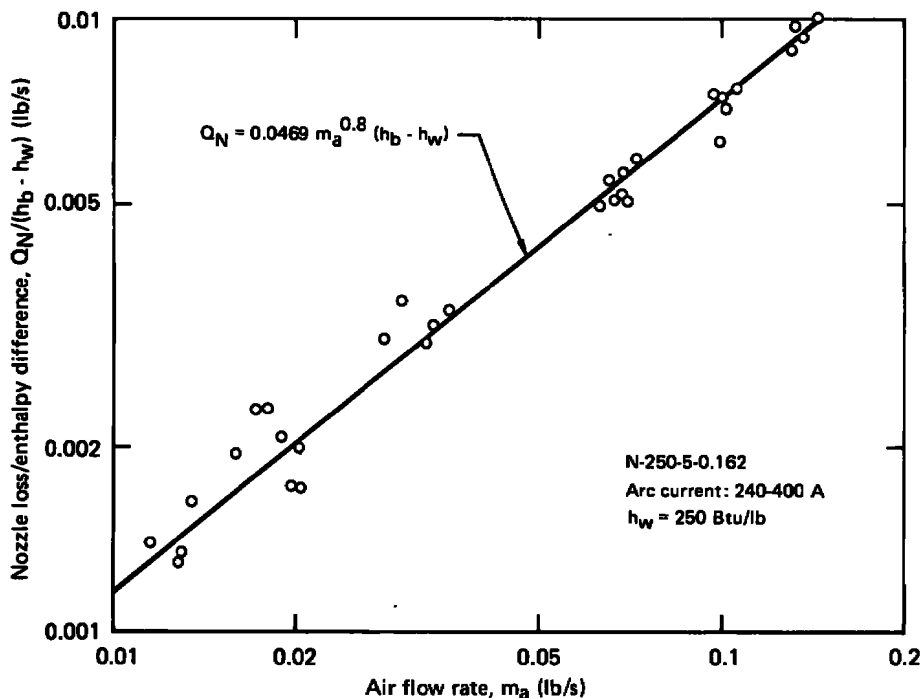
Figure 33 Correlation of the air nozzle energy loss

56

4.3.4 Electrode Erosion and Test-Stream Contamination

The test-stream contamination on air was determined for a wide range of conditions using pre- and post-test electrode weights. Figure 34 depicts the results as a function of arc pressure. The level was generally between 0.16% and 0.27%. This was of the same order as that on hydrogen at 25 atm but considerably lower than that on hydrogen at 10 atm and much higher at 50 atm. The air contamination was an order of magnitude higher than that on helium.

All reported tests at pressures of 25 atm and below were made using an 80% silver, 20% copper anode. From Figure 34 there appears to be a significant reduction in test-stream contamination at the lower pressures using the silver alloy. This agrees with past experience with the Huels-type arc heater. [9]

N-250-5-0.162
Arc current: 240 - 400 A
Test gas: Air
   O OFHC cathode - OFHC anode
   ● OFHC cathode - 80% Ag 20% Cu anode
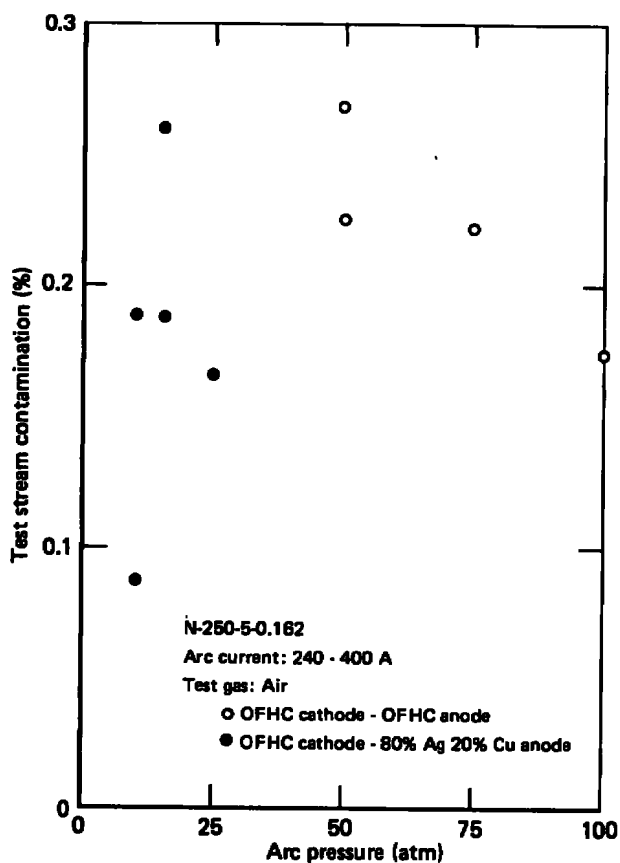
Figure 34   Test stream contamination on air

4.3.5 Air Arc Length

The arc length in the N-250 operating on air was required as an input to the AIRARC scaling program. Measurements of the arc track locations were made when discernable. The heavy oxide buildup and melt flow caused considerable ambiguity in these measurements. Figure 35 shows the best arc length estimates made from the arc track locations. There was a general trend for the arc to lengthen as the gas flow rate (pressure) was increased. The most probable arc length range shown pairs the anode restrike position with the cathode extension position and vice versa.

The arc lengths required by AIRARC for a good match of the experimental voltages are also shown in Figure 35. For pressures from 15 to 100 atm, these lengths fall within the span of the most probable arc lengths.

The 6 in. arc length selected prior to testing was based on previous scaling studies discussed in Section 5. As can be seen in Figure 35, the 6 in. length was a fair approximation over the higher pressure range (> 25 atm).

It should be reiterated that the use of the arc tracks for an inferred arc length does not include consideration of any twisting which has been reported in the past.[10]
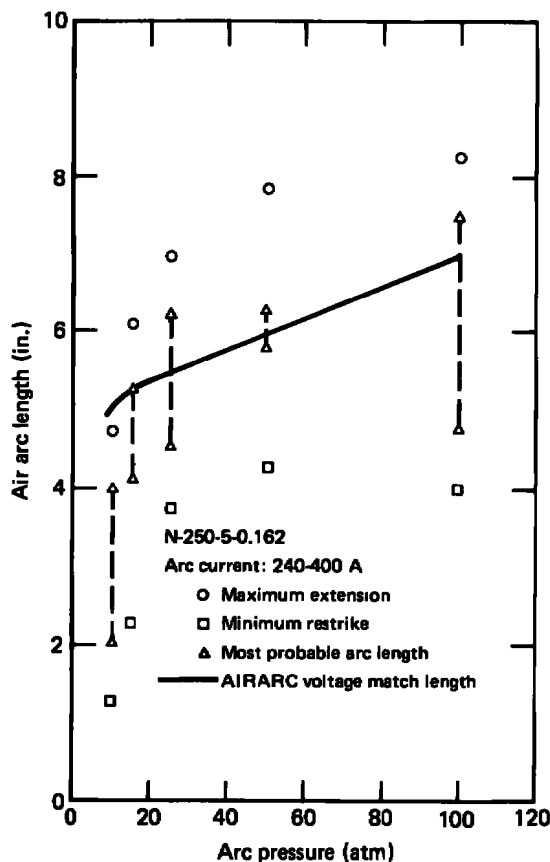
Figure 35 Arc length operating on air

4.4 COMPARISON OF HYDROGEN, HELIUM AND AIR ARC CHARACTERISTICS

The performance characteristics of the N-250 arc heater on hydrogen, helium or air have been described in the preceding sections and some comparisons have been made. This section provides a convenient, compact comparison of the major performance parameters.

4.4.1 Enthalpy Comparisons

Table 3 summarizes the energy balance enthalpies measured on the three gases tested over the complete test matrix. Direct comparisons can be made at 25 and 50 atm among all three gases. The hydrogen enthalpies were approximately four times those on helium and five to seven times those on air for the same arc current and pressure. At the high pressures, the helium enthalpies were 41% to 69% higher than air.

TABLE 3 COMPARATIVE N-250-5-0.162 ARC HEATER PERFORMANCE ON H_2, He OR AIR

Arc current (A)	Test gas	Arc pressure (atm)					
		10	15	25	50	75	100
		Average energy balance enthalpy (Btu/lb)					
240	H_2	30,200	33,300	30,900	—	—	—
	He	—	—	7,300	5,800	5,100	4,800
	Air	5,600	4,900	4,300	3,700	3,500	3,400
320	H_2	32,800	35,700	35,000	31,200	—	—
	He	—	—	8,300	7,200	6,200	6,100
	Air	5,900	5,700	5,100	4,400	4,100	3,900
400	H_2	32,900	38,900	37,800	—	—	—
	He	—	—	9,300	8,300	7,600	7,400
	Air	7,000	6,200	5,700	4,900	4,500	4,400

The performance advantage of hydrogen is shown in Figure 36 where the significantly higher enthalpies from Table 3 are compared graphically. Also shown are the performance predictions of the three versions of the minimum energy addition scaling program.
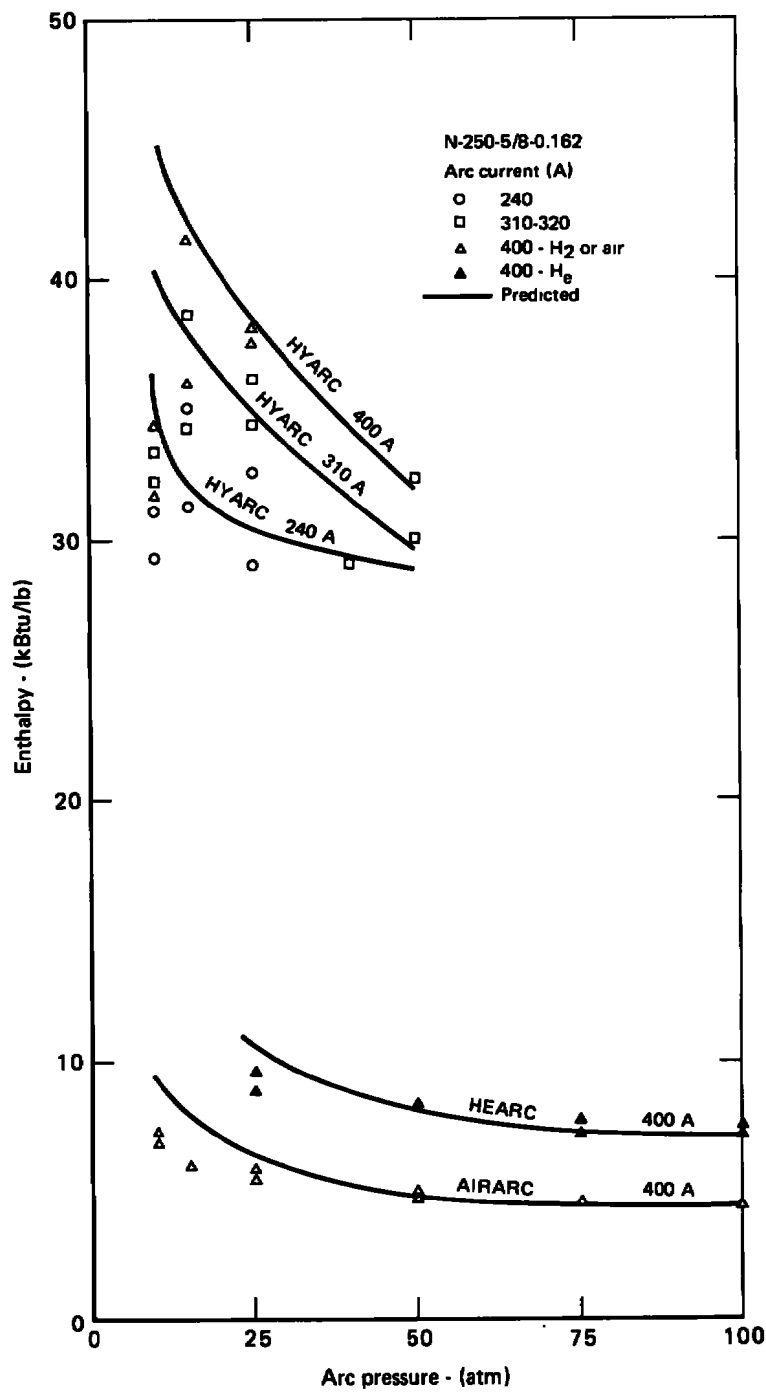
Figure 36 Comparison of enthalpy-pressure performance on H_2, He or air

4.4.2 Arc Voltage Comparisons

Figure 37 compares the arc voltages on hydrogen, helium and air for the same and similar arc currents and pressures. The hydrogen arc voltages were more than a factor of two higher than those on air, and the air voltages were approximately 10% higher than those on helium.

The voltage and current oscillations on hydrogen were more severe than those on air, with the helium arc characteristics being the most stable of the three. Noise frequencies of 150 kHz with a modulation of 2.5 kHz were identified on hydrogen. An isolation amplifier was necessary to obtain an accurate hydrogen arc voltage.

4.4.3 Test-Stream Contamination Comparison

The electrode erosion and resultant test-stream contamination varied significantly with the test gas and, on hydrogen, with the test pressure. Figure 38 compares the total test stream contamination (anode plus cathode mass loss) as a percent of the gas mass flow rate for all three gases.

At low pressure, the arc was relatively short on hydrogen and was not evenly distributed on the electrode surface. The result was severe erosion and high contamination. The low-pressure air tests were made using a silver-copper anode which appears to have helped reduce the total contamination. Contamination on air was more severe than on hydrogen or helium at the higher pressures. Anode erosion at 75 and 100 atm on air was quite severe, whereas the erosion was negligible on helium for the same conditions.
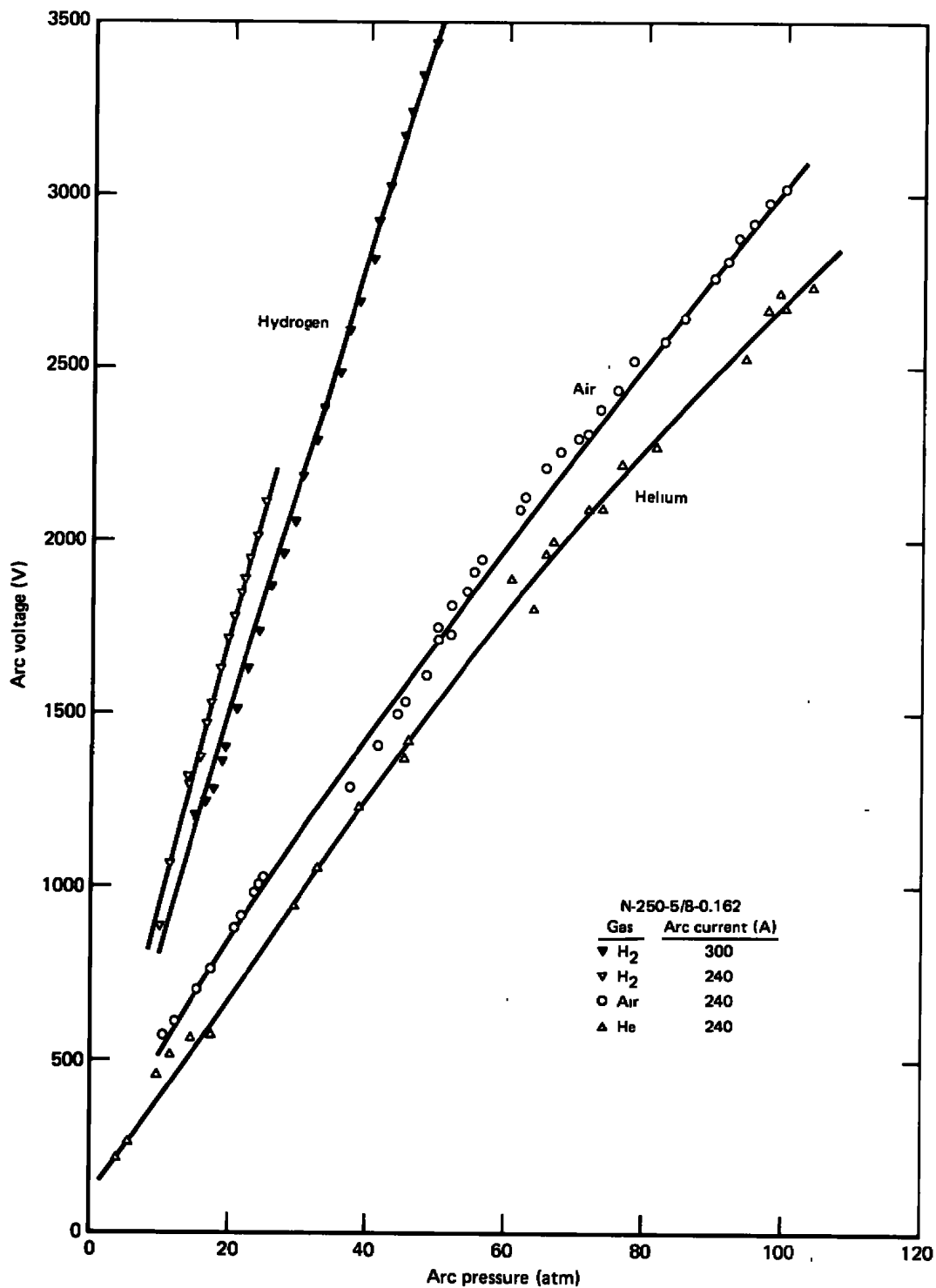
Figure 37   Arc voltage characteristics on H_2, He or air
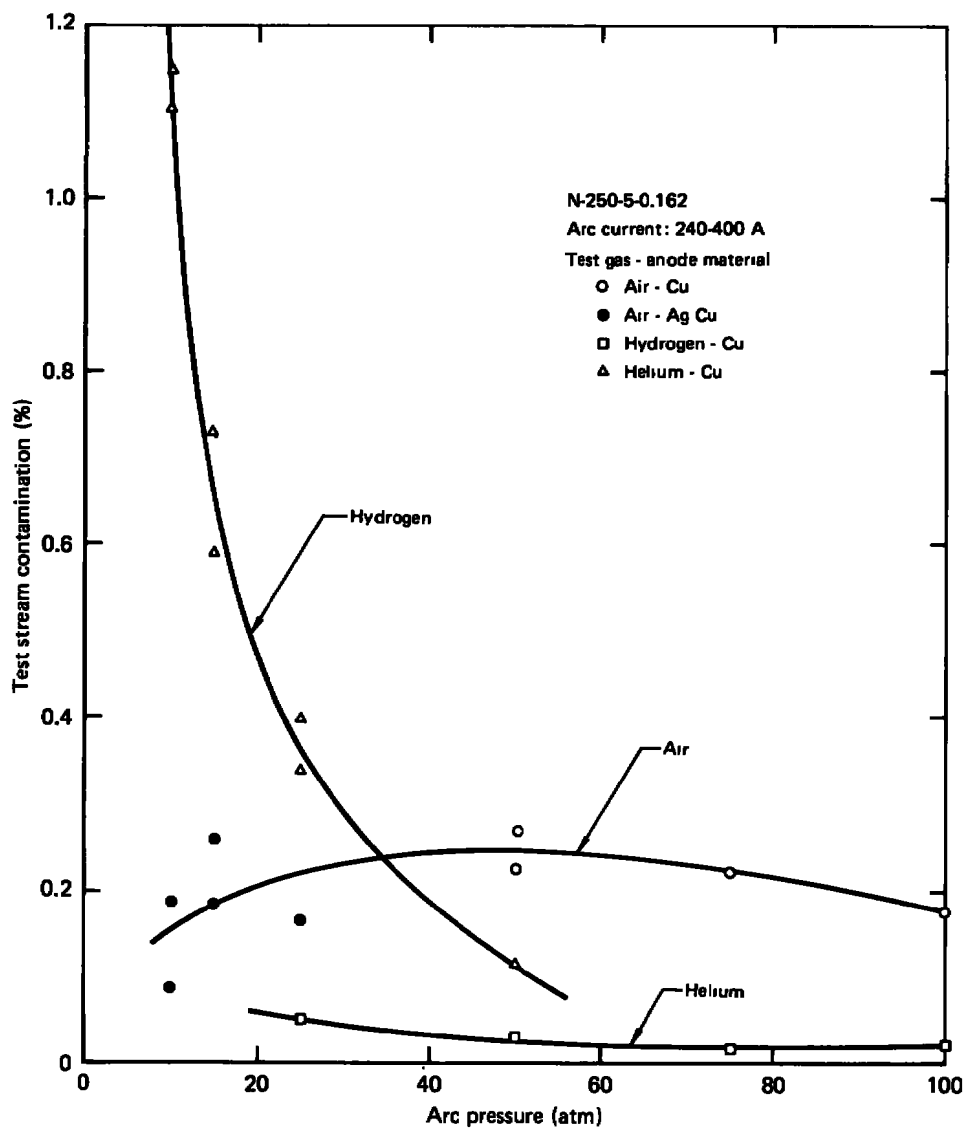
Figure 38 Test stream contamination comparison

5. ARC HEATER SCALING

Scaling of Huels-type arc heaters received considerable attention a decade ago[8,10], and simple rules were derived from data on small arc heaters. The use of these simple scaling rules led to sizable design errors for larger scale heaters.[11] The power capability of the heaters was under-estimated by a factor of four, and the scaled arc voltages were high, leading to predicted enthalpies considerably above those actually achieved.[1]

Later work[12] developed an analytical model for high pressure, high flow rate arc heaters which included radiation from the arc column and turbulent convective heating of the gas. This model, for fixed-length arc heaters, was computer coded and shown to yield reasonable agreement with limited experimental data. A study by MDRL[2] resulted in the addition of the sonic flow relation and wall convection losses, and in improvements of the transport and thermodynamic properties used in the above model.

Comparisons with data from fixed-length arc heaters were favorable in the moderate pressure regime (25 to 125 atm).[13] Comparisons with Huels-type arc heater (MDC-200) data were surprisingly favorable in the higher pressure regime[15] (50 to 250 atm), but perhaps fortuitous since the model did not consider the variable arc position.

In order to assess the accuracy of the modified code for scaling Huels-type arc heaters, comparisons with experimental arc voltages from four different scale heaters were made.[13] These heaters included the N-250 (N = 0.5)[14] used in this study, the Linde N-1000 (N = 1)[14], the MDC-200 (N = 2)[15], the Linde N-4000 (N = 2)[14], and the USAF-AFFDL RENT heater (N = 4).[1] The nozzle throat diameters, throat air flow rates and arc currents were normalized using the arc heater scale to allow direct comparisons. The arc lengths were scaled linearly as $L/N = 12$ in. Figures 39 and 40 illustrate the results of these comparisons for 45 and 11 atm. At 45 atm pressure, the scaled voltages range from 76% to 103% of the measured values. At 11 atm, they range from 84% to 104%. These data cover a wide range of variables and arc heater scale, thus indicating that the arc length can be scaled linearly.

The effect of the individual operating variables is shown in Figure 41 for an N = 1 heater[14] where the arc voltage comparison is presented as a function of scaled arc current, mass flow rate, and nozzle throat diameter. Again the arc length was scaled linearly. The strongest effect is due to mass flow rate where a factor of eight increase causes only a 23% deviation.

Having established that the improved computer code could be used with confidence for scaling, attention was next devoted to further improvements that better modeled the Huels-type heater and accurately matched the air data accumulated in this experimental program. This version of the code was labeled AIRARC.

The gas transport properties, thermodynamic properties and other features of the code were then modified for hydrogen (HYARC) and helium (HEARC). Correlation of the experimental data on these gases using the revised codes plus the confidence in scaling air data implies that reliable estimates can be made for larger scale hydrogen and helium arc heaters. Such estimates have been made and are included in this section.
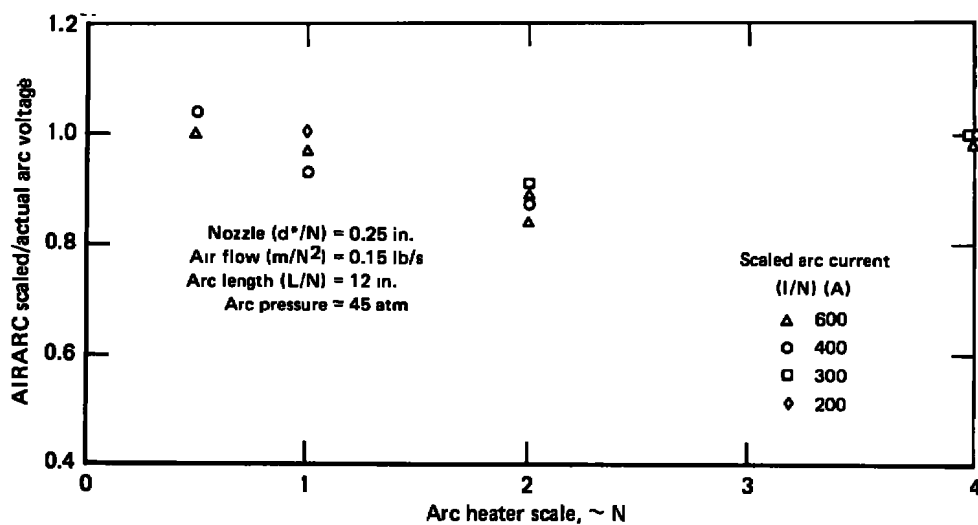
Figure 39   Comparison of scaled and actual voltages in Huels-type arc air heaters
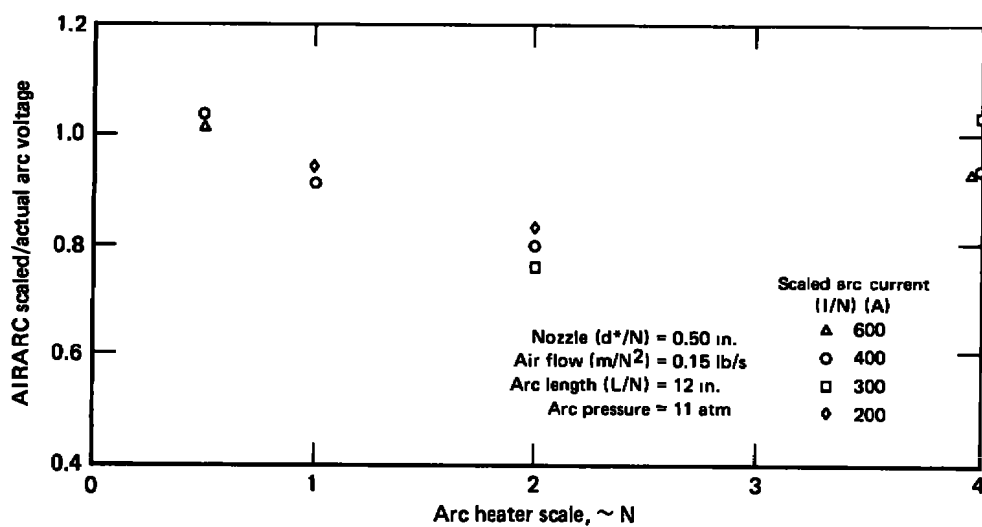
Figure 40   Comparison of scaled and actual voltages in Huels-type arc air heaters
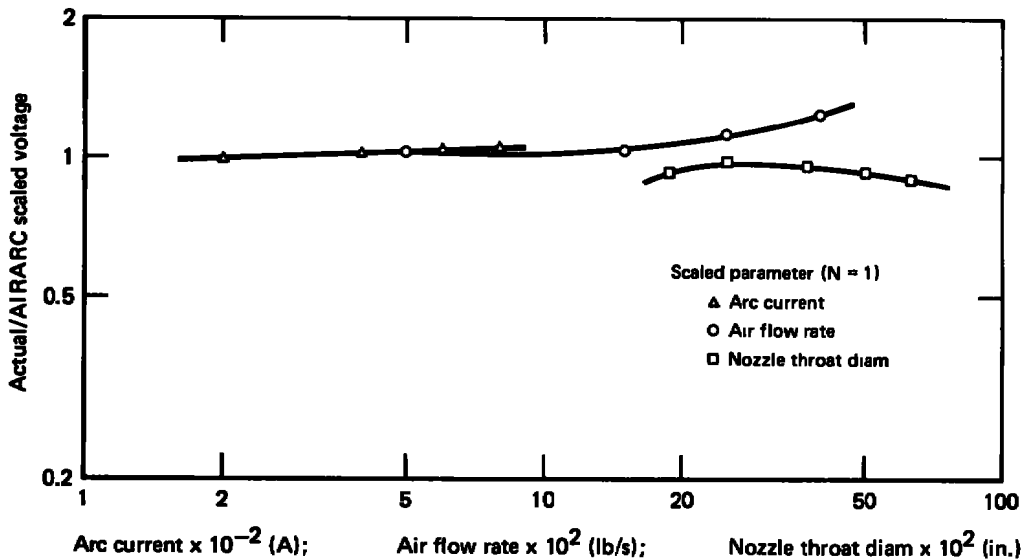
Figure 41 Effect of scaling parameters on AIRARC predicted voltages

5.1 SCALING CODE

The arc heater scaling code is based on a model[12] for high pressure, high flow rate operation. Energy input is by ohmic heating of the arc column and losses include radiation and convection. The bulk gas is heated by turbulent convection from the arc. The solution of the model is based on the principle of energy conservation, minimum energy addition, total gas energy balance, and optional nozzle throat sonic flow. The algorithm is essentially the same for each operating gas, the difference being the use of the appropriate thermodynamic and transport properties.

The input parameters required for the algorithm are:

      o Arc current
      o Chamber pressure
      o Arc heater geometry
              Constrictor diameter
              Front constrictor length
              Nozzle throat diameter
              Arc length.

Based on the above information, the algorithm predicts the following:

o Enthalpy	o Convective heat flux
o Voltage	o Constrictor heat load
o Mass flow rate	o Rear electrode heat load
o Efficiency	o Electrical gradient
o Electrical power input	o Power in the gas
o Stagnation temperature	o Arc temperature
o Radiative heat flux	o Arc diameter

5.1.1 Physical Model

The physical model for high-pressure arc heater operation is based on the analysis of Richter.[12] The justification and rationalization of this approach is presented in Reference 12. The incorporation of total gas energy balance for determining bulk gas temperature and convective losses to the constrictor wall, and of nozzle sonic flow relation for determining mass flow rate are from Painter.[16]

The physical model characterizing a high pressure, high flow rate arc heater is illustrated in Figure 42. The arc column is considered as a central conductive body (wire like) at a uniformly high temperature and is the only source of ohmic heat. The bulk gas in the annulus surrounding the arc is heated by convective turbulent transfer from the arc. In addition to heating the gas, the arc column also loses energy directly to the constrictor wall by volumetric radiation. The arc and bulk gases are considered to be optically thin. The bulk gas loses energy to the constrictor wall by convection.
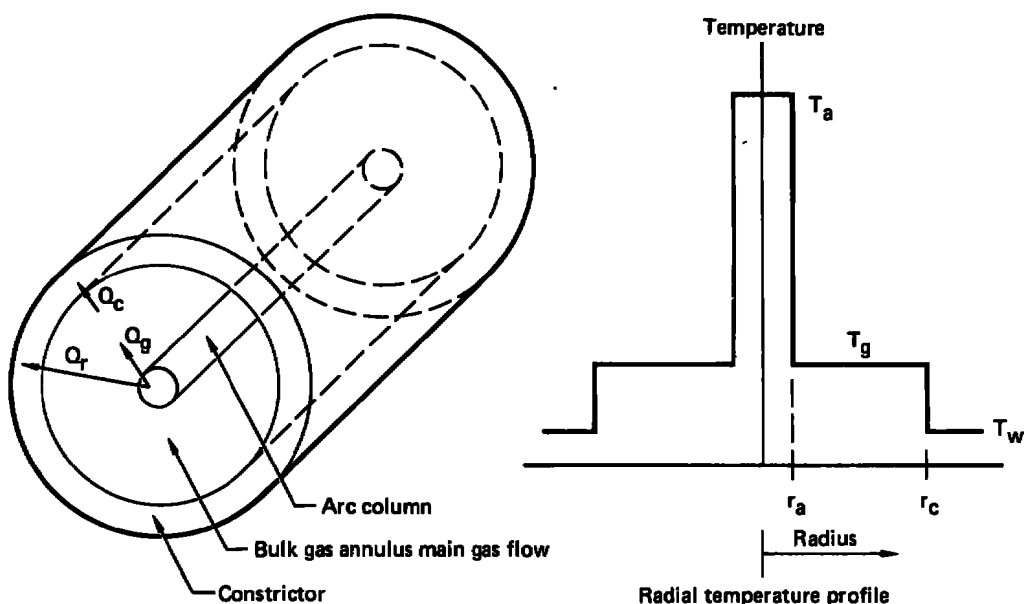
Figure 42   High pressure arc heater model

The algorithm has been adapted to characterize Huels-type configurations, Figure 43, by allowing for the following types of energy losses which are incorporated into the detailed energy balance equations.

1. Rear Electrode – This loss is by radiation from the arc only. Since a portion of the room-temperature inlet gas has reverse flow along the electrode wall, hence shielding it from the hot core gas, there is no convection. The bulk gas is still heated convectively from the arc, but there is no convective loss to the wall of the rear electrode.

2. Front Electrode – These losses are by radiation from the arc only, over the distance that the arc extends into the constrictor. Convection from the hot bulk gas is allowed over the entire constrictor length.

3. Nozzle – Losses to the nozzle are included by using an empirical convection relation based on experimental data.
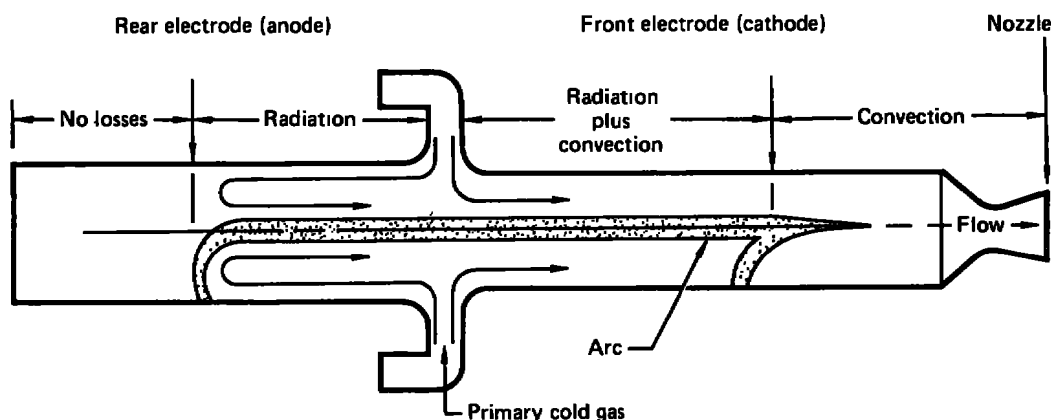
Figure 43 Huels-type arc heater energy loss model

This arrangement recognizes some of the realities of the Huels-type configuration, namely that convective losses to the wall of the front electrode do occur from the hot gas downstream of the arc termination, that the rear electrode has no convective losses resulting from the reverse flow of the cool inlet gas, and that there are losses to the nozzle.

The front and rear arc lengths and the front constrictor lengths were input parameters to the algorithm, so that other arc heater configurations could also be simulated.

The following equations show the development of the model. The first part of the analysis is presented for completeness only; it may also be found in Reference 12.

The power balance on the arc column per unit length is:

$$P_1 = P_r + P_c \; . \tag{12}$$

The electrical power input to the arc per unit length is:

$$P_1 = \frac{I^2}{\sigma \frac{\pi}{4} D_a^2} = \frac{x}{D_a^2} \; . \tag{13}$$

The power radiated per unit length of the arc column (to the constrictor walls) is:

$$P_r = U \frac{\pi}{4} D_a^2 = Y D_a^2 \; . \tag{14}$$

The power convected from the arc to the bulk gas per unit length is:

$$P_c = h(T_a - T_g) \, \pi \, D_a \; . \tag{15}$$

The heat transfer coefficient from the arc to the gas is:

$$h_{ag} = \frac{Nu \; \lambda}{D_c - D_a} \; . \tag{16}$$

The Nusselt number is:

$$Nu = 0.0265 \; (Re)^{0.8} \; (Pr)^{0.3} \; . \tag{17}$$

The Reynolds number is:

$$Re = \frac{4 \, \dot{m}_g}{\pi \, \mu \, (D_c + D_a)} \; . \tag{18}$$

Summarizing, the resultant expression for P_c is:

$$P_c = Z \frac{D_a \, (D_c + D_a)^{0.2}}{D_c^2 - D_a^2} \; , \tag{19}$$

where Z is a parameter independent of arc diameter and is defined as:

$$Z = 0.0265 \left(\frac{4 \, \dot{m}_g}{\pi \, \mu} \right)^{0.8} (Pr)^{0.3} \, \lambda \, \pi \, (T_a - T_g) \; . \tag{20}$$

The arc diameter is obtained by solving the power balance equation, Equation (12), as rewritten in terms of the arc diameter.

$$\frac{X}{D_a{}^2} - \left[Y \, D_a{}^2 + Z \, \frac{D_a \, (D_c + D_a)^{0.2}}{D_c{}^2 - D_a{}^2} \right] = 0 \; . \qquad (21)$$

Equation (21) is solved for given values of arc temperature, bulk gas temperature, mass flow rate, arc current, pressure, and constrictor diameter. The algorithm solves this equation for arc diameter using a Newton-Raphson iteration technique starting with an initial approximation for D_a. This solution is performed in subroutine ARCDIA.

The arc temperature and hence electrical power input, Equation (13), is determined by finding the arc temperature for which the power input is a minimum. This corresponds to the physical principle that processes in nature will always occur for the least possible expenditure of energy. It is from this principle that the algorithm derives the title of minimum energy addition. Figure 44 illustrates the variation of power input with arc temperature. A minimum power is clearly evident. The algorithm determines this minimum power by stepping the arc temperature in a direction that reduces the power input. When the minimum is passed, the temperature step size is reduced and proceeds in the opposite direction. The searching process continues until a small pre-set temperature step is reached. The determination of the arc temperature for which the power input is a minimum is performed in subroutine ARCTEM.

The bulk gas temperature is determined from a total gas power balance for the arc column and the bulk gas annulus. The gas temperature is iterated until the total gas power based on arc and gas annulus mass flow rates and enthalpies agree with the power based on power input less losses.

The total gas power based on input less losses is obtained from:

$$P_g \big|_{Bal} = P_1 + \dot{m} \, H_1 - (q_r \, \pi \, D_c \, L_a + q_c \, \pi \, D_c \, L_c + Q_N) , \qquad (22)$$

where $P_g \big|_{Bal}$ = total power in gas based on input less losses.

The radiative heat flux is obtained from the arc column volumetric radiation loss:

$$q_r = \frac{Y \, D_a{}^2}{\pi \, D_c} \; . \qquad (23)$$
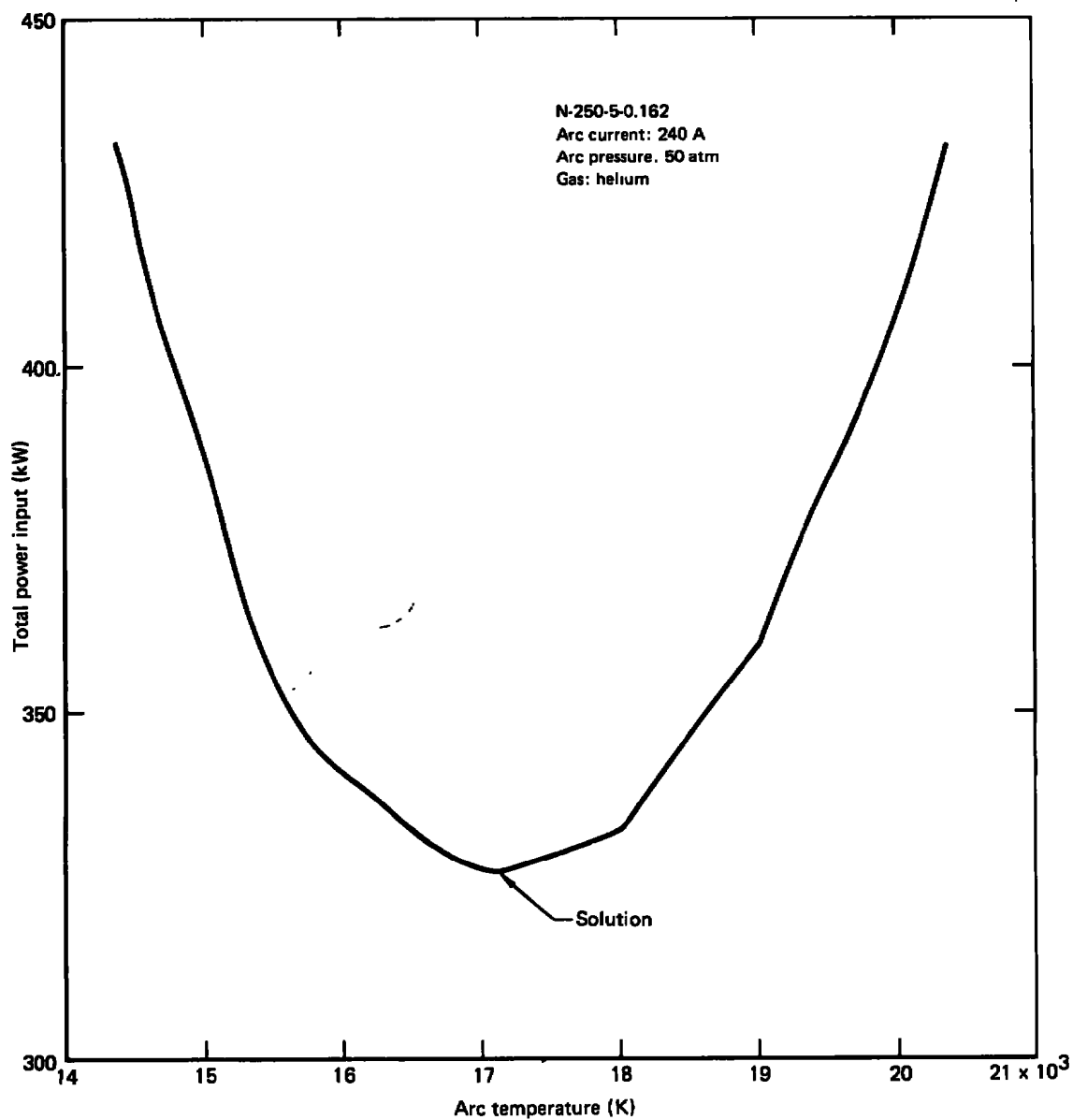
Figure 44 Minimum energy solution

The convective heat flux from the bulk gas to constrictor wall is obtained as follows:

$$q_c = h_{gw} (T_g - T_w) , \qquad (24)$$

where $T_w = 590$ K and h_{gw} is the turbulent film heat transfer coefficient:

$$h_{gw} = \frac{Nu \; \lambda}{D_c - D_a} . \qquad (25)$$

The total power in the gas, based on arc column and gas annulus flow rates and enthalpies, is obtained by assuming a uniform velocity for the arc and the gas. This assumption is in contrast to that made previously for computing the turbulent heating of the gas by the arc where the velocity was implicitly assumed to be zero. The assumption of non-zero arc column velocity is required to obtain an arc column mass flow rate which, however small, is required to obtain the power in the arc column. This is not insignificant because of the high arc column enthalpy. The velocity is obtained from:

$$v = \frac{\dot{m}}{\rho_g A_g + \rho_a A_a} . \qquad (26)$$

The flow rates for the arc column and gas annulus are hence:

$$\dot{m}_a = \rho_a A_a v , \text{ and} \qquad (27)$$

$$\dot{m}_g = \rho_g A_g v . \qquad (28)$$

The total power in the gas based on enthalpy and mass flow is:

$$P_{g|_{EN}} = H_g \dot{m}_g + H_a \dot{m}_a . \qquad (29)$$

The computation of these two expressions, Equations (22) and (29), for total gas power is performed in subroutine GASPOW. The bulk gas temperature is iterated by the method of false position until total gas power based on Equations (22) and (29) agree within a specified tolerance. The iteration process is performed in the main program.

The mass flow rate is determined by assuming the flow to be sonic at the nozzle throat:

$$\dot{m}_{SF} = A^* \ (\gamma \ \rho_o P_o)^{1/2} \left(\frac{2}{\gamma + 1}\right)^{\frac{\gamma+1}{2(\gamma-1)}} \qquad (30)$$

The mass flow rate is compared with that predicted by the above, and iterated until the two values agree within a specified tolerance. These computations are performed in the main program.

The stagnation enthalpy is the total power in the gas divided by the mass flow rate:

$$H_o = \frac{P_g}{\dot{m}} \ . \qquad (31)$$

The stagnation temperature, T_o, is the temperature that corresponds to the stagnation enthalpy, H_o, at pressure P. This determination is done in subroutine TEMP.

The voltage gradient is obtained from:

$$G = \frac{I}{\sigma_a A_a} \ . \qquad (32)$$

The arc voltage is thus:

$$V = G \ L_a \ , \qquad (33)$$

where the arc length L_a is an input parameter to the algorithm.

Efficiency is defined as the power added to the gas divided by the input electrical power:

$$\eta = \frac{P_g - \dot{m} \ H_1}{P_1} \ * \ 100 \ . \qquad (34)$$

The rear electrode heat loss is assumed to be due only to radiation, since for a Huels-type heater the reverse flow of the inlet gas at room temperature would preclude convective transfer. Hence,

$$Q_r = q_r \ \pi \ D_c \ L_r \ , \qquad (35)$$

where L_r is the length of the arc in the rear electrode.

73

The front electrode (constrictor) heat loss is due to radiation over that portion of the arc extending into this electrode, and convection from the bulk gas over the entire electrode length. Hence:

$$Q_f = q_r \, \pi \, D_c \, L_f + q_c \, \pi \, D_c \, L_c \, . \tag{36}$$

The total arc length is:

$$L_a = L_F + L_R \, . \tag{37}$$

Equations (32) through (36) are evaluated in subroutine OUTPUT.

5.1.2 Operating Gas Characterization

The minimum-energy-addition, arc heater characterization code requires information on the gas thermodynamic and transport properties as a function of temperature and pressure, nozzles losses, and front and rear electrode arc lengths. This section outlines the source of such data and describes the correlations utilized.

The helium, hydrogen, and air thermodynamic and transport data were obtained from the sources shown in Table 4 over the pressure and temperature ranges indicated. These data were incorporated into the algorithm by means of table interpolation on both temperature and pressure for helium and hydrogen with the exception of the electrical conductivity of hydrogen which was curve fit. AIRARC used curve fit routines and closed form equations. Transport properties not available above 30 atm were obtained by extrapolation using the pressure dependent relationship of the data below 30 atm.

The Prandtl number used for each gas is shown in Table 5. A single constant value was chosen because its variation over the temperature and pressure ranges of interest was not great, plus the fact that it was raised to the 0.3 power, $(Pr)^{0.3}$, which tended to further minimize any variations.

The ratio of specific heats, γ, used in the sonic flow relation is shown in Table 5. A single constant value was used for helium, and a pressure-temperature curve fit was used for hydrogen. An empirical sonic flow relation was used for air that precluded the need for γ.

The room temperature inlet enthalpy used for each gas is also shown in Table 5.

Volumetric radiation for air and hydrogen as functions of temperature and pressure were obtained from Yos.[22] For helium, radiation was determined functionally as that resulting from free-bound transitions. Kogan[27] points out that the main mechanism of radiative heat transfer for a plasma with low electron temperature (of the order of electron volts) is the process of recombination of electrons with ions as opposed to the case of high temperature plasma ($T \geq 100$ eV) where electron bremsstrahlung is the main contribution. The functional relationship for free-bound radiation,[27,28] is:

$$U = \frac{c}{\sqrt{T}} \, N_e^{\,2} \, . \tag{38}$$

TABLE 4   THERMODYNAMIC AND TRANSPORT PROPERTY SOURCES AND RANGES

Gas	Enthalpy	Density	Electron mole fraction	Thermal conductivity	Electrical conductivity	Viscosity	Volumetric radiation
Helium							
Source	Lick and Emmons[19]	Lick and Emmons[19]	Lick and Emmons[19]	Lick and Emmons[20]	Lick and Emmons[20]	Lick and Emmons[20]	
Temperature	≤ 30,000 K	≤ 30,000 K	≤ 30,000 K	≤ 30,000 K	≤ 30,000 K	≤ 30,000 K	
Pressure	1 - 1000 atm	1 - 1000 atm	1 - 1000 atm	1 - 1000 atm	1 - 1000 atm	1 - 1000 atm	
Hydrogen							
Source	Rosenbaum and Levitt[21]	Krascella[22]		Grier[23]	Yos[24]	Grier[23]	Yos[24]
Temperature	≤ 30,000 K	≤ 80,000°R		T ≤ 10,000 K	T ≤ 30,000 K	T ≤ 10,000 K	T ≤ 30,000 K
Pressure	1 - 100 atm	1 - 250 atm		1 - 100 atm	1 - 30 atm	1 - 100 atm	1 - 30 atm
Source				Yos[24]		Yos[24]	
Temperature				T ≤ 30,000 K		T ≤ 30,000 K	
Pressure				1 - 30 atm		1 - 30 atm	
Air							
Source	Swell[25]			Peng[26]	Peng[27]	Hansen[28]	Yos[24]
Temperature	3000 - 7000 K			T ≤ 16,000 K	T ≤ 16,000 K	500 - 5000 K	T ≤ 30,000 K
Pressure	1 - 200 atm			1 - 500 atm	1 - 500 atm	0.01 - 100 atm	1 - 30 atm

TABLE 5   THERMODYNAMIC CONSTANTS USED IN HYARC, HEARC AND AIRARC

Gas	Prandtl no.	Inlet enthalpy	Specific heat ratio
Helium	0.672	670 Btu/lb	1.6667
Hydrogen	0.650	1800 Btu/lb	Curve fit
Air	0.680	130 Btu/lb	Not used

The minimum-energy-addition arc heater scaling algorithm has been correlated to the experimental data of this program. The parameters (observables) were arc voltage, power input, efficiency, front and rear electrode losses, enthalpy, and front and rear electrode arc tracks. The correlation goal was to obtain as good an agreement as possible between algorithm predictions and all the above observables over the entire pressure-current test matrix. The algorithm parameters "adjusted" to obtain this correlation were: relative radiation level; the temperature used to evaluate the thermal conductivity in the expression for energy transfer between arc column and bulk gas, and likewise in the expression for energy transfer between the bulk gas and constrictor wall; and front and rear arc lengths.

The rationale for this approach was that by fitting the algorithm model to experiment, a degree of confidence for scaling to other heater designs was added. This approach also tended to remove possible discrepancies of the theoretically calculated thermodynamic and transport properties. The results of this correlation process for hydrogen and helium are described below.

Table 6 shows the observables used in adjusting each of the algorithm parameters. The scatter in the observed arc track data was generally too great to assign well defined values. Hence, arc length was made an adjustable parameter. If arc lengths had been well defined (for each pressure and current), then the correlation processes would have been easier and probably more accurate. For example, if the rear arc length were known with certainty, then the radiation level could have been directly related to rear power losses. As it was, a trade-off was required to interrelate rear length and radiation with the losses.

TABLE 6 CORRELATION PARAMETERS

Algorithm parameters	Observable correlated
Total arc length, L_T	Arc voltage (power input), arc tracks
Rear electrode arc Length, L_R	Rear electrode losses, arc tracks, $L_R = L_T - L_F$
Front electrode arc length, L_F	Front electrode losses, arc tracks $L_F = L_T - L_R$
Radiation level	Rear electrode losses, arc voltage, efficiency
Temperature for evaluating λ_{ag}	Efficiency (power in gas after arc voltage is correlated), enthalpy
Temperature for evaluating λ_{gw}	Front electrode loss

The predicted value for each observable is dependent upon more than one adjustable algorithm parameter; hence several "adjustment" iterations were required to determine the final values. These final values represent a subjective best-fit of the computed results to the experimental observables.

76

The arc length results are shown in Table 7 and in Figures 19, 29, and 35 for comparison with observed arc track data. For heaters other than scale N = 0.5, the arc lengths were scaled from L/N values equal to those obtained in this work. For example, a scale N = 1 heater front and rear arc lengths was scaled as twice those observed for this work. For fixed arc length heaters, the physical electrode gap should be input to the algorithm.

TABLE 7 ARC LENGTH CORRELATIONS: N-250-5/8-0.162

Helium	$L_F = 4.45 + 0.0106 \, (P_0 - 25) \cdot L_R$ (in.)
	$L_R = P_0/(0.288 \, P_0 + 4.22)$ (in.)
Hydrogen	$L_T = 1.3 + (4.51 + 0.086) \, (P_0 - 15) \left(\dfrac{320}{I}\right)^{0.65}$ (in.)
	$L_F = (3.2 + 0.063 \, (P_0 - 10) \left(\dfrac{400}{I}\right)^{0.22}$ (in.)
	$L_R = L_t - L_f$ (in.)
Air	$L_A = 5.0 + 0.02 \, P_0$ (in.)

The temperature at which the thermal conductivity was evaluated for computing the power transfer from the arc column to the bulk gas was determined to be:

$$T = 0.8 \, (T_a - T_g) + T_g \qquad \text{Hydrogen} \qquad (39)$$

$$T = 0.7 \, (T_a - T_g) + T_g \qquad \text{Helium} \qquad (40)$$

The temperature at which the thermal conductivity was evaluated for computing the power transfer from the bulk gas to the constrictor wall was determined to be:

$$T = 0.5 \, (T_g - T_w) + T_w \qquad \text{Hydrogen} \qquad (41)$$

$$T = T_g \qquad \text{Helium} \qquad (42)$$

The nozzle energy loss expressions used in the algorithm for use in calculating an overall gas power balance are shown in Table 8. These were correlated from the experimental data of this program, Section 4. Generally, the nozzle losses were 5-6% of the input power and were not critical for reasonable algorithm predictions. When scaling to different size heaters, the applicability of this expression should be examined.

TABLE 8 NOZZLE LOSS CORRELATIONS FOR HYARC, HEARC AND AIRARC: N-250-5/8-0.162

Helium	$Q_N = 0.04 \, (\dot{m}_{He})^{0.7} \, (h_b - 1325)$ Btu/s
Hydrogen	$Q_N = 0.0469 \, (\dot{m}_H)^{0.8} (h_b - 3600)$ Btu/s
Air	$Q_N = 0.0469 \, (\dot{m}_a)^{0.8} \, (h_b - 250)$ Btu/s

Radiation levels were correlated to the power loss of the rear electrode. Rear electrode losses were assumed to be entirely radiative because reverse flow of the inlet gas at room temperature precludes any convective transfer to the electrode walls. The resultant constant for the helium radiation, Equation (38), is $C = 4.34 \times 10^{-28}$ for radiation in W/cm^3 and electron density in cm^{-3}. For hydrogen, Yos[24] radiation levels were increased by a factor of 2.4. Yos radiation was computed according to:

$$U_{Yos} = 17.1 \times 10^{-34} \sqrt{T} \ N^2 \ , \tag{43}$$

which was an expression for free-free radiation as corrected for free-bound and modified by an empirical correction factor based on radiation data for shock heated argon. As discussed by Kogan,[27] free-bound radiation predominates for arc heater conditions. He has computed for hydrogen:

$$U_{fb} = 5.32 \times 10^{-29} \ N^2/\sqrt{T} \ . \tag{44}$$

Comparing Yos's value[22] with Kogan's[27] for hydrogen arc temperatures of 11,500 K, we obtain:

$$\frac{U_{fb}}{U_{Yos}} = \frac{3.11 \times 10^4}{T} \approx 2.71 \ , \tag{45}$$

which nearly corresponds to the factor of 2.4 found in this work.

The helium radiation is 8.1 times that for hydrogen. This can be partly explained by the higher ionization potential of helium, and possibly by non-unity Gaunt factors. In addition, the radiation constant (Equation 44) varies as the square of the effective charge on the nucleus, Z^2. A value of unity was used for hydrogen. For singly ionized helium, the effective nuclear charge is $1 \leq Z \leq 2$ since its remaining electron cannot effectively shield the inner core. Thus, up to a factor of 4 could be accounted for in this manner.

78

5.1.3 Discussion

As with any physical modeling process, trade-offs must be made between solving simpler models which include the principal physical processes (and hence more cost-effective) and solving more detailed models which may include parameters only vaguely known and/or so involved that significant phenomena such as radial pressure gradients and swirl must be ignored to obtain a solution.[29] Thus simpler approaches, particularly when correlated with data, can often be adequate for engineering estimation purposes.

The physical model upon which this algorithm is based includes the significant principal mechanisms for energy input, arc column radiation loss, turbulent convective heating of the gas, bulk gas power level determination, bulk gas wall losses, and mass flow rate determination.

This approach, however, has certain inherent limitations. The analysis is a single-point solution.[12] It evaluates a stable operating condition at a single location and projects this solution for the entire arc length. In practice, however, high pressure constricted arcs are not fully developed. The energy exchange between the arc and bulk gas annulus is based on turbulent heat transfer correlations that inadequately consider many of the details of the heating process. For that portion of the arc in the rear electrode where reverse flow occurs, the program assumes the entire flow rate for calculating the convective gas heating rate; in practice, only a fraction of the inlet gas experiences reverse flow in the rear electrode. Another undetermined parameter for the rear electrode is the effective annular cross sectional area for the flow. Since the flow is reversed, an effective diameter corresponding to the front constrictor diameter has been utilized. If in practice this diameter was smaller, it would tend to offset the reduced flow rate in the Reynolds number determination.

5.2 AIRARC COMPARISONS AND SCALING

Computations using AIRARC were made for the full range of the experimental N-250 data from this program. The initial comparisons indicated that the nozzle throat area change during test caused the sonic flow rates to be low, thus yielding high predicted gas enthalpies. The sonic flow section of the code was bypassed, and the experimental gas flow rates were input. The resultant performance predictions are shown in Figures 30 through 32 and Table 10 (see Table 9 for nomenclature).

The key predictions were the total energy losses since the experimental flow rates were used and the arc length was selected to best correlate the experimental arc voltages and arc tracks. Although the magnitudes of the energy loss predictions (Figure 32) were not significantly in error, particularly in the middle pressure range, the functional dependence on pressure appears high. The experimental losses increased as the 0.57 power of the arc pressure while AIRARC predicted an exponential dependence of approximately 0.92. This is reflected in the predicted enthalpies which exceed the measured values by as much as 30% at the 10 atm pressure level. At higher pressures, the enthalpy predictions were much better, partially because of small over-prediction of the arc voltage.

TABLE 9 AIRARC OUTPUT NOMENCLATURE

Parameter	Definition
P ATM	Arc pressure (atm)
I AMP	Arc current (A)
DIAC IN	Constrictor diam (in.)
ARCL IN	Arc length (in.)
DIAT IN	Nozzle throat diam (in.)
BGT DEGR	Bulk gas temperature (^{O}R)
V VOLT	Arc voltage (V)
PIN KW	Air power input (kW)
GASP KW	Power to gas (kW)
E V/IN	Arc potential gradient (V/in.)
RAD B/F2S	Radiant heat flux to wall in arc region (Btu/ft^{2}s)
CNV B/F2S	Convective heat flux to wall (Btu/ft^{2}s)
QE B/S	Energy loss to nozzle (Btu/s)
M LBM/S	Air flow rate (lb/s)
H B/LB	Stagnation enthalpy (Btu/lb)
EFF PERC	Thermal efficiency (%)
ARCT DEGR	Arc temperature (^{O}R)
ARCD IN	Arc diam (in.)

TABLE 10 PREDICTED N-250 PERFORMANCE BY AIRARC I

P ATM	I AMP	DIAC IN	ARCL IN	DIA T IN	BGT DEG R						
V VOLTS	PIN KW	GASP KW	E V/I	RAD B/F2S	CNV B/S	QE LB/S	M B/LB	H PERC	EFF	ARC T DEG R	ARC D IN
100	240	0.375	7.0	0.162	3500						
3137	753	460	448	2847	1292	29	0.146	3150	61	23093	0.073
100	320	0.375	7.0	0.162	9606						
2783	891	531	398	3787	1371	34	0.137	3333	60	22801	0.092
100	400	0.375	7.0	0.162	10537						
2565	1026	602	366	4673	1446	39	0.132	4470	59	22570	0.110
75	240	0.375	6.5	0.162	8639						
2360	571	350	366	2276	1015	22	0.107	3259	61	22937	0.080
75	320	0.375	6.5	0.162	9727						
2126	680	409	327	2976	1081	28	0.102	3975	60	22672	0.101
75	400	0.375	6.5	0.162	10682						
1954	782	461	301	3704	1130	32	0.097	4654	59	22455	0.121
50	240	0.375	6.0	0.162	8851						
1685	404	250	281	1614	736	18	0.071	3516	62	22790	0.091
50	320	0.375	6.0	0.162	9991						
1508	483	294	251	2140	787	22	0.063	4236	61	22520	0.114
50	400	0.375	6.0	0.162	10946						
1388	555	332	231	2700	816	25	0.065	5045	60	22345	0.136
25	240	0.375	5.5	0.162	9672						
991	238	152	180	857	451	13	0.035	4252	64	22334	0.116
25	320	0.375	5.5	0.162	10969						
875	280	176	159	1169	463	15	0.032	5347	63	22103	0.146
25	400	0.375	5.5	0.162	12023						
807	323	200	147	1508	470	18	0.030	6441	62	21991	0.172
15	240	0.375	5.3	0.162	10549						
697	167	112	132	507	319	10	0.021	5161	67	21873	0.140
15	320	0.375	5.3	0.162	11349						
619	198	129	117	740	321	12	0.019	6549	65	21811	0.173
15	400	0.375	5.3	0.162	12366						
582	233	148	110	1029	326	14	0.018	7909	64	21912	0.197

See Table 9 for nomenclature
See Table A-3 for experimental data

81

Substitution of a radiation heat transfer correlation (derived in an earlier electrode heat transfer study[7]) for the volumetric radiation of Yos, yielded much closer correlation of the electrode energy losses in the N-250 operating on air. Figure 45 and Table 11 compare the empirical version of AIRARC (AIRARC II) to the N-250 electrode energy losses. The functional dependence on pressure is closely correlated, and the magnitudes are quite accurate over the full range of the data. The arc voltage and resultant enthalpy are also correlated by the revised code with improved accuracy, as shown by comparing Tables 11 and 23.

TABLE 11 PREDICTED N-250 PERFORMANCE BY AIRARC II

P ATM	I AMP	DIAC IN	AHCL IN	DIA T IN	BGT DEG R	V VOLT	PIN KW	GASP KW	E V/IN	RAD B/F2S	CVV B/S	QE	M LBM/S	H B/LB	EFF PERC	ARC T DEG R	ARC D IN
100	240	0.37	7.0	0.162	8572.	2862	686.9	467.1	409	1764	1166	29	0.146	3194	68.0	27046	0.05
100	320	0.37	7.0	0.162	9676.	2527	808.5	535.7	361	2453	1271	34	0.137	3375	66.3	26351	0.07
100	400	0.37	7.0	0.162	10584.	2329	931.5	604.9	333	3170	1348	39	0.132	4493	64.9	26688	0.08
75	240	0.37	6.5	0.162	8774.	2237	536.8	361.4	344	1528	940	23	0.107	3362	67.3	26648	0.06
75	320	0.37	6.5	0.162	9869.	1992	637.6	418.0	307	2126	1012	29	0.102	4061	65.6	26440	0.07
75	400	0.37	6.5	0.162	10812.	1832	732.9	470.5	282	2748	1064	33	0.097	4743	64.2	26283	0.09
50	240	0.37	6.0	0.162	9000.	1647	395.4	256.8	275	1248	684	25	0.071	3605	64.9	26170	0.07
50	320	0.37	6.0	0.162	10199.	1475	471.9	306.3	246	1738	744	23	0.063	4460	64.9	25951	0.08
50	400	0.37	6.0	0.162	11172.	1359	543.5	345.7	226	2247	777	26	0.065	5245	63.6	25793	0.10
25	240	0.37	5.5	0.162	9980.	1040	249.6	163.3	189	884	428	14	0.035	4550	65.4	25192	0.09
25	320	0.37	5.5	0.162	11276.	922	295.0	188.5	168	1232	443	16	0.032	5709	63.9	25017	0.11
25	400	0.37	5.5	0.162	12376.	851	340.6	213.3	155	1597	454	19	0.030	6366	62.6	24899	0.13
15	240	0.37	5.3	0.162	10962.	772	185.2	120.5	146	686	307	11	0.021	5564	65.1	24308	0.11
15	320	0.37	5.3	0.162	12325.	689	220.6	140.8	130	958	312	14	0.019	7146	63.8	24196	0.13
15	400	0.37	5.3	0.162	13379.	647	259.0	163.2	122	1243	313	16	0.015	8716	63.0	24145	0.15

See Table 9 for nomenclature
See Table A-3 for experimental data
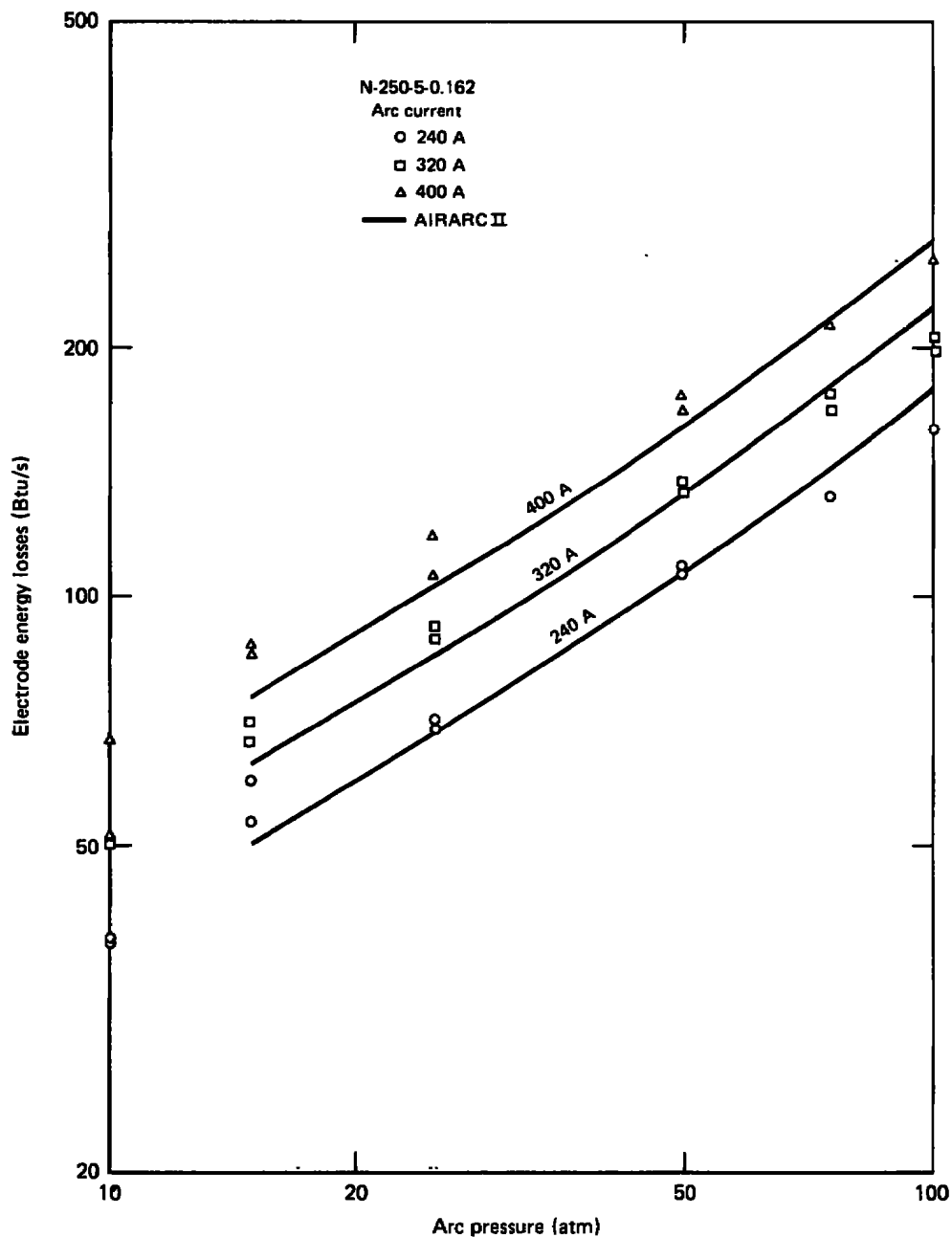
Figure 45 Comparison of AIRARC II and N-250 electrode energy losses

Further verification of the scaling accuracy of AIRARC was gained through comparisons with actual DET arc heater data. The DET heater is a scale 1.73 Huels-type unit with a 0.5625 in. diam throat. Two sets of data were available for pressures from 29 to 93 atm and arc currents from 570 to 750 A.

The first set of data was acquired using a 34 in. long cathode. The second set used 24, 27 and 30 in. long cathodes. There were significant differences in the performance of the heater. The new shorter electrodes yielded higher arc voltages and higher enthalpies from improved thermal efficiency. Table 12 compares AIRARC I to the higher performance data (shorter cathodes). The arc length selected as based on Figures 39 and 40 where, for an N = 1.73 arc heater and a scaled nozzle throat diameter of d*/N = 0.324 in., the scaled arc length (L/N = 12 in.) must be increased by 18% for a good voltage match. This yielded a 24.5 in. arc length. The resultant arc voltage, enthalpy and thermal efficiency are in good agreement over the complete test matrix.

TABLE 12 COMPARISON OF AIRARC I AND DET ARC HEATER DATA (SHORT CATHODES)

P ATM	I AMP	DIAC IN	ARCL IN	DIA T IN	BGT DEG R							
V VOLTS	PIN KW	GASP KW	E V/I	RAD B/F2S	C NV B/S	QE LB/S	H B/LB	H	EFF PERC	ARC T DEG R	ARC D IN
30 3431 (3900)	740 2539	1.300 1508	24.5 140	0.562 887	7817 336 73	0.504	2936 (3330)	59 (58)	21569	0.252
28 3253 (3650)	750 2440	1.300 1478	24.5 133	0.562 842	8026 329 73	0.474	3109 (3360)	61 (59)	21436	0.262
29 3285 (3470)	765 2513	1.300 1542	24.5	0.562 881	8120 338 76	0.484	3172 (3190)	61 (59)	21473	0.264
51 5290 (5610)	700 3703	1.300 2187	24.5 216	0.562 1344	6777 473 93	0.938	2353 (2530)	59 (60)	22087	0.192
51 5312 (5540)	715 3798	1.300 2284	24.5 217	0.562 1377	6834 495 97	0.969	2333 (2480)	60 (50)	22103	0.193
52 5239 (5210)	730 3825	1.300 2326	24.5 214	0.562 1408	7008 501 98	0.943	2473 (2510)	61 (62)	22013	0.198
64 6225 (6220)	710 4420	1.300 2630	24.5 254	0.562 1650	6622 573 108	1.211	2246 (2360)	61 (64)	22222	0.178
76 7359 (7340)	650 4784	1.300 2925	24.5 300	0.562 1603	6154 621 112	1.463	2014 (2000)	61 (61)	22227	0.158
76 7332 (7490)	675 4949	1.300 3080	24.5 299	0.562 1661	6265 648 113	1.523	2062 (2130)	62 (63)	22205	0.162
92 8704 (8480)	625 5440	1.300 3234	24.5 355	0.562 2010	5680 672 118	1.336	1813 (1870)	59 (63)	22655	0.138

See Table 9 for nomenclature

(   ) DET arc heater data[1]

84

Table 13 compares AIRARC II, the empirical version of AIRARC, with the DET arc heater data using the long (34 in.) cathode. The scaled arc length was the same as that used with AIRARC I, 24.5 in. The agreement is good over the full range of the data for arc voltage, enthalpy and thermal efficiency. Thus, both versions of AIRARC can be used with reasonable confidence for scaling air arc heaters to N = 1.73.

TABLE 13 COMPARISON OF AIRARC II AND DET ARC HEATER DATA (LONG CATHODE)

P ATM	I AMP	DIAC IN	ARCL IN	DIA T IN	BGT DEG R						
V VOLT	PIN KW	GASP KW	E V/IN	RAD B/F2S	CNV 9/S	QE LBM/S	M B/LB	H PERC	EFF DEG R	ARC T IN	ARC D
50	680	1.30	24.5	0.562	6314.						
4998	3399	2029	204	1130	406	84	0.967	2136	59.7	26677	0.13
(4770)								(1910)	(55)		
52	750	1.30	24.5	0.562	6498.						
4895	3672	2157	200	1345	422	91	0.975	2245	59.7	26688	0.14
(4870)								(2120)	(55)		
77	655	1.30	24.5	0.562	5635.						
6590	4317	2657	269	1404	512	100	1.523	1797	61.6	27329	0.10
(6660)								(1730)	(58)		
77	705	1.30	24.5	0.562	5813.						
6394	4508	2740	261	1527	525	104	1.503	1872	60.8	27284	0.11
(6500)								(1810)	(57)		
93	590	1.30	24.5	0.562	5147.						
7738	4565	2894	316	1371	544	104	1.837	1596	63.4	27675	0.09
(8150)								(1680)	(63)		
92	670	1.30	24.5	0.562	5420.						
7351	4925	3066	300	1576	572.	112	1.856	1708	62.3	27593	0.10
(7720)								(1750)	(60)		

See Table 8 for nomenclature

( ) DET arc heater data[1]

5.3 HEARC COMPARISONS AND SCALING

The results of the algorithm for helium are presented in Figures 20, 22, 32, 24, and 46 as a function of pressure with current as a parameter. For comparison, experimental results are also shown. The predicted performance is also shown in tabular form in Table 15 (see Table 14 for nomenclature). The experimental results are tabulated in Table 22.

The resulting "matched" voltages are shown in Figure 22. The predicted enthalpy and mass flow rates compared to experiment are shown in Figures 20 and 36. Note that where the calculated enthalpy deviates slightly (3%) from experiment, such as at the 100 atm 400 A point, the calculated flow rate also deviates slightly (7%). If the calculated gas power is divided by the

experimental flow rate, the resulting enthalpy is closer to the experimental value. This possibly indicates that the effective nozzle throat diameter in the experiment was slightly less than 0.162 in., the value used by the algorithm sonic flow equation for determining mass flow rates.
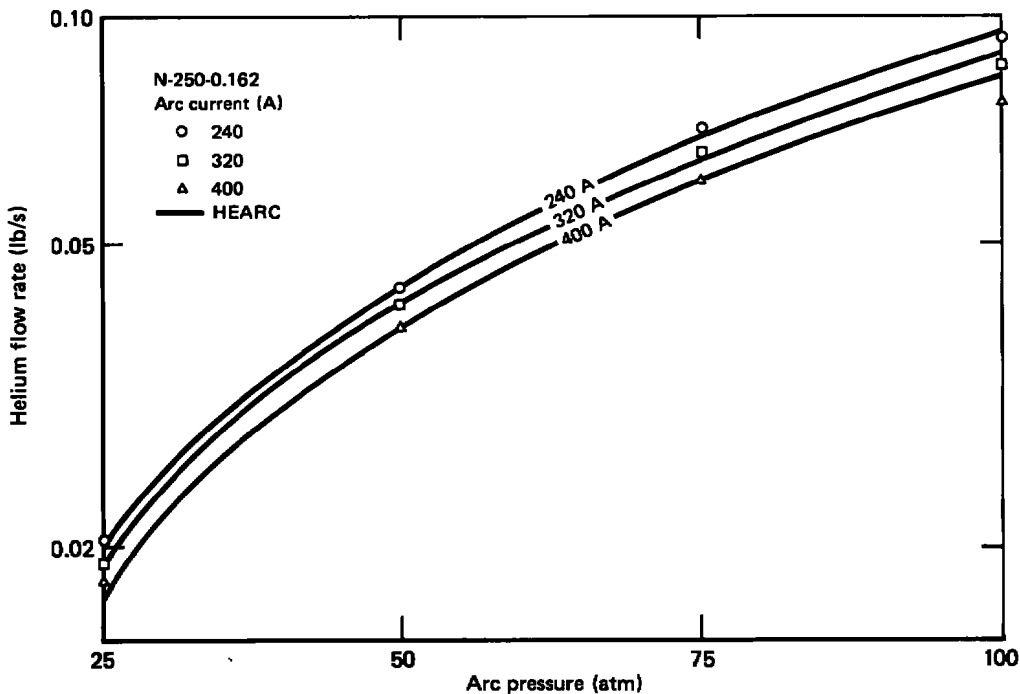
Figure 46 Comparison of measured and HEARC predicted mass flow rates

The rear electrode power loss is shown in Figure 23. These were essentially "matched" to experiment by adjusting the constant in Equation (38) and by varying the rear arc length.

The front electrode losses are shown in Figure 24. Note that the total power loss of the front plus rear electrode is in better agreement with experiment than either one separately. This indicates compensating errors in predictions for front and rear electrodes and perhaps also the difficulty in determining the fraction of the total arc length within each electrode.

The calculated efficiencies, Table 15, are in good agreement with experimental values.

The semi-empirical scaling code HEARC, having been correlated with the N-250 experimental data, has been used to predict the performance of larger scale heaters.

TABLE 14   HEARC AND HYARC OUTPUT NOMENCLATURE

Parameter	Definition
P ATM	Arc pressure (atm)
AMPS	Arc current (A)
DCONS IN	Constrictor diam (in.)
DTHRT IN	Nozzle throat diam (in.)
LCONS IN	Front constrictor length (in.)
ARCL IN	Total arc length (in.)
FRNT IN	Arc length in front electrode (in.)
REAR IN	Arc length in rear electrode (in.)
TSTAG DEGK	Stagnation temperature (K)
QREAR	Power loss to rear electrode (Btu/s)
QFRNT	Power loss to front electrode (Btu/s)
QNOZ	Power loss to nozzle (Btu/s)
VOLTS	Arc voltage (V)
PIN KW	Electrical power input to arc (kW)
GASP KW	Power added to gas (kW)
GRAD V/IN	Arc column voltage gradient (V/in.)
QRAD BTU/FT2S	Radiative heat flux to constrictor wall $(\text{Btu/ft}^2\text{s})$
QCONV	Convective heat flux to constrictor wall $(\text{Btu/ft}^2\text{s})$
WDOT LB/S	Mass flow rate (lb/s)
ENTH B/LB	Stagnation enthalpy (Btu/lb)
EFF PERC	Efficiency (%)
TARC DEGK	Arc column temperature (K)
DARC IN	Arc column diam (in.)

TABLE 15 PREDICTED N-250 PERFORMANCE BY HEARC

HELIUM ARC HEATER: SCALE N = 0.5

PRES AIM	AMPS	DCJVS IV	DFART IV	LCOVS IV	ARCL IV	FRVT IV	REAR IV	TSTAG DEG K	QREAR ----BTU/SEC------	QFRVT	QVOZ
VOLTS	PIV KW	GASP KW	GRAD V/IV	QRAD BTU/FT**2-S	QCOVV	WDOT LBM/S	ENTH B/LB	EFF PERC	TARC DEG K	DARC IV	
25	240	.375	.162	5.0	4.5	2.3	2.2	3383	13	47	18
368	232	147	217	781	309	.020	7566	63	16512	.113	
25	320	.375	.162	5.0	4.5	2.3	2.2	4029	19	53	21
846	270	165	190	1113	925	.019	8395	60	16412	.143	
25	400	.375	.162	5.0	4.5	2.3	2.2	4717	26	68	24
766	306	179	172	1453	1013	.017	10530	53	16362	.169	
50	240	.375	.162	5.0	4.7	2.0	2.7	2313	34	77	24
1695	406	262	359	1565	1259	.044	6233	64	17012	.088	
50	320	.375	.162	5.0	4.7	2.0	2.7	3279	43	97	28
1492	477	292	316	2273	1449	.042	7320	61	16925	.110	
50	400	.375	.162	5.0	4.7	2.0	2.7	3746	64	115	32
1351	540	315	286	2352	1624	.039	8362	58	16787	.133	
75	240	.375	.162	5.0	5.0	2.1	2.9	2532	51	103	30
2376	570	375	477	2152	1632	.070	5738	65	17250	.077	
75	320	.375	.162	5.0	5.0	2.1	2.9	3044	66	126	35
2059	658	417	413	2739	1938	.065	6735	63	17012	.100	
75	400	.375	.162	5.0	5.0	2.1	2.9	3417	91	153	39
1868	747	447	375	3357	2145	.061	7623	59	17012	.115	
100	240	.375	.162	5.0	5.2	2.2	3.0	2417	70	130	34
3014	723	475	574	2832	1925	.075	5395	65	17750	.065	
100	320	.375	.162	5.0	5.2	2.2	3.0	2816	92	161	40
2635	843	532	502	3745	2291	.090	6238	63	17437	.086	
100	400	.375	.162	5.0	5.2	2.2	3.0	3195	117	192	44
2371	948	574	452	4725	2600	.034	7134	60	17262	.105	

See Table 14 for nomenclature
See Table A-2 for experimental data

Results for scale N = 1 and N = 1.73 heaters corresponding to constrictor diameters of 0.75 and 1.3 in., are shown in Tables 16 and 17. Arc lengths, front and rear, were scaled from those of the N-250, (N = 0.5) heater as:

$$L = \left(\frac{N}{0.5}\right) L_{N250} \quad \cdot \tag{46}$$

The front constrictor lengths were 10 and 17.3 in. for N = 1 and 1.73 respectively. Nozzle diameters were 0.324 and 0.562 in. which were scaled as:

$$d_* = \left(\frac{N}{0.5}\right) d_{*N250} \quad . \tag{47}$$

Arc currents were scaled up approximately as:

$$I = \left(\frac{N}{0.5}\right) I_{N250} \quad . \tag{48}$$

Nozzle losses were evaluated from the expression shown in Figure 25.

TABLE 16 SCALED HELIUM ARC HEATER PERFORMANCE (N = 1.0)

HELIUM ARC HEATER: SCALE N=1

PRES ATM	AMPS	DCONS	DIHRT	LCONS	ARCL	FRNT	REAR	TSTAG	QREAR	QFRNT	QNOZ
	IN	IN	IN	IN	IN	IN	DEG K	----BTU/SEC------			
VOLTS	PIN	GASP	GRAD	QRAD	QCONV	WDOT	ENTH	EFF	TARC	DARC	
	KW	KW	V/IN	BTU/FT**2-S	LBM/S	B/LB	PERC	DEG K	IN		
25	400	.750	.324	10.0	8.9	4.5	4.4	2499	37	128	35
1767	706	499	198	528	546	.095	5530	69	16125	.166	
25	600	.750	.324	10.0	8.9	4.5	4.4	3154	61	172	44
1436	861	567	161	861	664	.054	7043	65	16000	.231	
25	800	.750	.324	10.0	8.9	4.5	4.4	3830	70	197	52
1223	978	640	137	957	761	.077	8550	65	15937	.293	
50	400	.750	.324	10.0	9.4	4.1	5.4	2103	106	213	47
3160	1264	875	335	1217	809	.206	4696	69	16712	.125	
50	600	.750	.324	10.0	9.4	4.1	5.4	2643	149	283	60
2579	1547	1026	273	1705	1037	.136	5913	66	16262	.187	
50	800	.750	.324	10.0	9.4	4.1	5.4	3213	196	340	71
2222	1778	1147	235	2117	1219	.167	7184	64	16000	.250	
75	400	.750	.324	10.0	10.0	4.2	5.3	1950	154	280	57
4423	1769	1243	444	1629	1036	.321	4354	70	17012	.105	
75	600	.750	.324	10.0	10.0	4.2	5.3	2352	265	402	70
3673	2203	1424	369	2790	1301	.295	5252	64	16537	.150	
75	800	.750	.324	10.0	10.0	4.2	5.3	2737	346	500	83
3212	2569	1557	322	3649	1546	.271	6221	61	16550	.199	
100	400	.750	.324	10.0	10.5	4.4	6.1	1305	229	364	64
5681	2272	1573	541	2308	1201	.444	4037	69	17562	.090	
100	600	.750	.324	10.0	10.5	4.4	6.1	2262	305	484	82
4624	2774	1854	440	3080	1595	.401	5049	66	17012	.133	
100	800	.750	.324	10.0	10.5	4.4	6.1	2592	460	634	94
4067	3270	2014	383	4646	1820	.373	5783	61	17012	.171	

See Table 14 for nomenclature

TABLE 17   SCALED HELIUM ARC HEATER PERFORMANCE (N = 1.73)

HELIUM ARC HEATER SCALE N=1.73

PRES ATM	AMPS	DCONS IN	DTHRT IN	LCONS IN	ARCL IN	FRNT IN	REAR IN	TSTAG DEG K	QREAR	QFRNT	QVOZ
VOLTS	PIN KW	GASP KW	GRAD V/IN	QRAD BTU/FT**2-S	QCONV	WDOT LBM/S	ENTH B/LB	EFF PERC	TARC DEG K	DARC IN	----BTU/SEC------
25	692	1.300	.562	17.3	15.4	7.3	7.6	2127	.33	296	63
2614	1309	1336	169	411	416	.310	4749	73	15975	.244	
25	1038	1.300	.562	17.3	15.4	7.3	7.6	2655	144	400	79
2121	2202	1543	137	669	513	.273	5927	70	15312	.343	
25	1364	1.300	.562	17.3	15.4	7.3	7.6	3143	207	502	93
1850	2561	1713	119	965	587	.255	7027	66	15737	.431	
50	692	1.300	.562	17.3	16.3	7.0	9.3	1309	293	520	85
4305	3325	2375	293	1113	605	.663	4035	71	16337	.191	
50	1038	1.300	.562	17.3	16.3	7.0	9.3	2302	304	625	111
3756	3899	2800	229	1154	805	.534	5139	71	15925	.293	
50	1364	1.300	.562	17.3	16.3	7.0	9.3	2637	435	785	129
3279	4539	3113	200	1650	929	.551	6022	63	15937	.370	
75	692	1.300	.562	17.3	17.3	7.2	10.1	1637	510	731	100
6839	4733	3316	396	1788	746	1.053	3654	70	16975	.152	
75	1038	1.300	.562	17.3	17.3	7.2	10.1	2039	705	993	130
5623	5637	3907	325	2471	995	.954	4553	66	16337	.236	
75	1364	1.300	.562	17.3	17.3	7.2	10.1	2417	899	1229	154
4893	6773	4374	263	3113	1210	.877	5397	64	16100	.317	
100	692	1.300	.562	17.3	18.2	7.7	10.5	1579	603	878	116
8632	5973	4267	474	2025	891	1.423	3526	71	17100	.141	
100	1038	1.300	.562	17.3	18.2	7.7	10.5	1886	1006	1297	145
7225	7500	4916	397	3379	1143	1.316	4211	65	17000	.194	
100	1364	1.300	.562	17.3	18.2	7.7	10.5	2211	1316	1641	172
6362	8805	5503	349	4420	1331	1.223	4936	62	16625	.261	

See Table 14 for nomenclature

5.4 HYARC COMPARISONS AND SCALING

The results of the algorithm for hydrogen are presented in Figures 5, 12 and 13 and in tabular form in Table 18 as a function of pressure with current as a parameter. For comparison the experimental results are shown in Table A-1.

TABLE 18   PREDICTED N-250 PERFORMANCE BY HYARC

HYDROGEN ARC HEATER: SCALE N = 0.5

PRES AIM	AMPS	DCONS IN	DIHRI IN	LCONS IN	ARCL IN	FRNT IN	REAR IN	TSTAG DEG K	QREAR	QFRNT	QVOZ
VOLTS	PIN KW	GASP KW	GRAD V/IN	QRAD BTU/FT**2-S	QCONV	WDOT LBM/S	ENTH B/LB	EFF PERC	IARC DEG K	DARC IN	----BTU/SEC------
10	240	.375	.162	5.0	6.2	3.6	2.6	3553	12	42	21
959	230	148	154	600	609	.004	35399	64	11562	.130	
10	320	.375	.162	5.0	5.4	3.4	2.0	3655	15	52	23
804	257	160	149	925	667	.004	35929	62	11675	.206	
10	400	.375	.162	5.0	4.8	3.2	1.6	3755	15	61	26
732	292	183	151	1155	760	.004	42244	62	11637	.223	
15	240	.375	.162	5.0	6.7	3.9	2.3	3472	17	58	27
1358	326	215	201	730	825	.007	31346	66	11562	.162	
15	320	.375	.162	5.0	5.8	3.7	2.1	3635	21	70	28
1053	337	209	181	1230	825	.006	36636	62	11625	.185	
15	400	.375	.162	5.0	5.2	3.5	1.7	3808	23	83	29
876	350	206	163	1713	933	.005	42431	58	11662	.224	
20	240	.375	.162	5.0	7.3	4.3	3.0	3563	24	71	30
1533	363	235	211	997	959	.007	33633	63	11475	.165	
20	320	.375	.162	5.0	6.2	4.0	2.2	3656	26	88	32
1282	410	253	205	1457	967	.007	36136	61	11562	.190	
20	400	.375	.162	5.0	5.6	3.8	1.7	3733	29	107	35
1131	452	270	203	2071	1040	.007	38437	58	11662	.203	
25	240	.375	.162	5.0	7.8	4.6	3.1	3473	29	90	37
2034	468	321	261	1158	1145	.011	30545	65	11550	.148	
25	320	.375	.162	5.0	6.7	4.4	2.3	3623	32	103	38
1574	503	314	236	1732	1147	.009	34525	62	11562	.180	
25	400	.375	.162	5.0	5.9	4.1	1.8	3741	35	130	40
1352	540	324	227	2355	1201	.009	37524	58	11625	.202	
50	240	.375	.162	8.0	10.4	6.4	4.0	3438	65	230	59
4048	971	596	390	2010	1917	.021	23971	61	11600	.127	
50	320	.375	.162	8.0	8.8	6.0	2.8	3565	65	271	63
3293	1058	631	373	2836	2021	.021	30569	58	11612	.149	
50	400	.375	.162	8.0	7.8	5.7	2.1	3599	67	321	65
2815	1126	647	360	3931	2100	.021	31313	57	11637	.166	

See Table 14 for nomenclature
See Table A-1 for experimental data

These results utilized the experimentally measured flow rates as input to the algorithm with nozzle sonic flow calculation of mass flow rate by-passed. When sonic flow is not bypassed the code over-predicts the mass flow rates. This is most likely caused by the fact that the experimental nozzle throat diameter late in the tests was not effectively 0.162 in. due to clogging. As can be seen from Figures 6 to 8, the experimental sonic flow enthalpy disagreement (with the energy balance value) increases as the running time increases, indicating a changing throat size. This was also seen in the computed results with mass flow calculations. The disagreement was greater for those experimental cases where the run time was longer, i.e., when a run consisted of the sequence 240, 320 and 400 A. The predictions for enthalpy for the 10 atm point are not in good agreement due to the short arc conditions described in Section 4.1.

The calculated efficiencies are in reasonable agreement with experiment indicating that for proper voltage (power) predictions, the power to the gas has been predicted adequately. The semi-empirical scaling code HYARC was used to predict the performance of scale $N = 1$ and $N = 1.73$ heaters. Constrictor lengths utilized were 24 and 36 in., respectively. Nozzle diameters and currents were scaled in the same manner as for helium. The nozzle loss expression was that shown in Table 8. The front and rear arc lengths were:

$$L_R = 6 \, D_c \, , \qquad\qquad\qquad (49)$$

$$L_f = 14.36 \, N^{1.2} \, P^{0.391} \, I^{-0.2} - L_R \, . \qquad\qquad (50)$$

This particular form for L_R corresponds to the rear arc terminus at a spin coil location placed six constrictor diameters behind the inlet housing. The front arc length corresponds to a total arc length correlated with data for a preliminary version of HYARC. These arc lengths scale directly. Sonic flow was used in these predictions to obtain the mass flow rate since no experimental values were available.

The scaled results are shown in Tables 19 and 20. Figures 47 and 48 show the power supply requirements for these predictions along with the characteristics of the MDRL power supply.

TABLE 19 SCALED HYDROGEN ARC HEATER PERFORMANCE (N = 1.0)

HYDROGEN ARC HEATER; SCALE N=1; D*=0.324 IN.; LCONS=24 IN.

PRES ATM	AMPS	DCONS IN	DTHRT IN	LCONS IN	ARCL IN	FRNT IN	REAR IN	TSTAG DEG K	QREAR	QFRNT	QNOZ
VOLTS	PIN KW	GASP KW	GRAD V/IN	QRAD BTU/FT**2-S	QCONV	WDOT LBM/S	ENTH B/LB	EFF PERC	TARC DEG K	DARC IN	
25	400	.750	.324	24.0	15.3	10.3	4.5	2472	71	495	79
4468	1787	1105	292	971	325	.070	16672	61	11675	.176	
25	600	.750	.324	24.0	14.1	9.6	4.5	2303	110	609	94
3523	2114	1255	250	1495	956	.066	19900	59	11537	.241	
25	800	.750	.324	24.0	13.3	9.4	4.5	3040	155	722	106
3025	2420	1381	227	2116	1064	.062	22320	57	11500	.294	
50	400	.750	.324	24.0	20.0	15.5	4.5	2539	116	970	133
8755	3502	2209	437	1583	1443	.136	17170	63	11662	.152	
50	600	.750	.324	24.0	18.4	13.9	4.5	2341	190	1242	160
6914	4148	2467	374	2583	1660	.123	20012	59	11537	.205	
50	800	.750	.324	24.0	17.4	12.9	4.5	3071	271	1494	178
5910	4728	2677	339	3634	1323	.122	22625	56	11550	.251	
75	400	.750	.324	24.0	23.4	18.9	4.5	2511	187	1572	187
13316	5326	3272	568	2541	1997	.206	16372	61	11837	.130	
75	600	.750	.324	24.0	21.6	17.1	4.5	2534	250	1967	223
10360	6216	3746	479	3393	2331	.192	20248	60	11575	.135	
75	800	.750	.324	24.0	20.4	15.9	4.5	3111	357	2266	246
8831	7064	4036	432	4855	2553	.183	22720	57	11537	.230	
100	400	.750	.324	24.0	26.2	21.7	4.5	2567	210	2020	239
17524	7009	4403	668	2853	2557	.269	17299	62	11737	.125	
100	600	.750	.324	24.0	24.2	19.7	4.5	2922	303	2504	273
13660	8208	4946	565	4193	2937	.251	20451	60	11575	.176	
100	800	.750	.324	24.0	22.3	13.3	4.5	3163	437	3033	307
11633	9306	5315	509	5943	3196	.238	22934	57	11525	.213	

See Table 14 for nomenclature

TABLE 20   SCALED HYDROGEN ARC HEATER PERFORMANCE (N = 1.73)

HYDROGEN ARC HEATER: SCALE N=1.73; D*=0.5625 IN.; LCONS=36 IN.

PRES	AMPS	DCONS	DTHR	LCONS	ARCL	FRNT	REAR	TSTAG	QREAR	QFRNT	QNOZ
ATM		IN	IN	IN	IN	IN	IN	DEG K	----BTU/SEC------		
VOLTS	PIN	GASP	GRAD	QRAD	QCONV	WDOT	ENTH	EFF	TARC	DARC	
	K*	Kb	V/IN	BIU/FT**2-S	LBM/S	B/LB	PERC	DEG K	IN		

25	692	1.300	.562	36.0	26.4	15.6	7.3	2243	166	1074	159
6582	4555	3067	248	751	663	.224	14301	67	11225	.230	
25	1033	1.300	.562	36.0	24.4	16.6	7.3	2544	276	1370	136
5180	5376	3431	212	1249	766	.210	17319	63	11162	.373	
25	1364	1.300	.562	36.0	23.0	15.2	7.3	2733	339	1632	221
4423	6122	3754	192	1761	853	.199	19725	61	11112	.465	
50	692	1.300	.562	36.0	34.7	26.3	7.3	2321	272	2145	297
13050	9031	6165	376	1232	1150	.430	15336	68	11212	.243	
50	1036	1.300	.562	36.0	32.0	24.2	7.3	2613	455	2793	343
10264	10654	6860	320	2056	1353	.406	17331	64	11150	.329	
50	1364	1.300	.562	36.0	30.2	22.4	7.3	2850	645	3342	332
8736	12093	7441	289	2917	1493	.385	20104	61	11100	.406	
75	692	1.300	.562	36.0	40.6	32.8	7.3	2369	355	3213	419
19669	13611	9337	453	1608	1634	.639	15743	69	11137	.224	
75	1036	1.300	.562	36.0	37.5	29.7	7.3	2668	593	4226	434
15504	16093	10498	413	2632	1927	.606	18215	65	11125	.303	
75	1364	1.300	.562	36.0	35.4	27.6	7.3	2833	853	5175	534
13176	18235	11312	372	3655	2114	.577	20335	62	11087	.373	
100	692	1.300	.562	36.0	45.5	37.7	7.3	2423	434	4269	533
26180	18116	12598	575	1962	2126	.832	16145	69	11175	.212	
100	1038	1.300	.562	36.0	41.9	34.1	7.3	2720	723	5675	609
20550	21330	13932	490	3290	2437	.787	18579	65	11112	.297	
100	1384	1.300	.562	36.0	39.6	31.8	7.3	2856	1033	6956	672
17445	24144	15001	440	4691	2668	.749	20775	62	11062	.355	

See Table 14 for nomenclature

94

Figure 47 HYARC predicted Huels-type arc heater characteristics 50 atm pressure
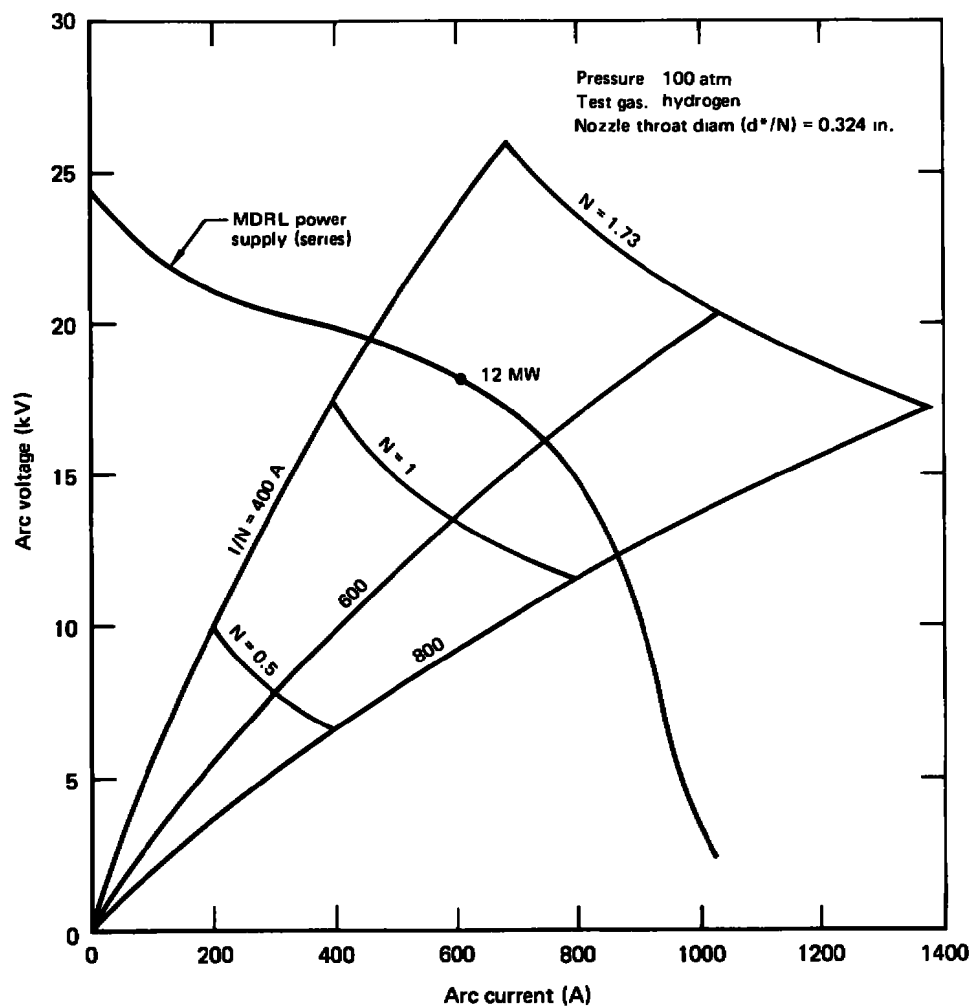
Figure 48 HYARC predicted Huels-type arc heater characteristics; 100 atm pressure

96

6. CONCLUDING REMARKS

This work has shown that significantly higher gas stagnation enthalpies can be achieved with a Huels-type arc heater operating on hydrogen and helium than are possible using air. Specifically, hydrogen enthalpies of five to seven times those on air can be achieved at pressures to 50 atm, and helium enthalpies 41% to 69% higher than air can be achieved at pressures to 100 atm. This helps verify the original hypothesis that the AEDC DET can achieve higher dust-particle velocities using these gases as accelerators.

A standard Huels-type arc heater can be operated on pure hydrogen at pressures to 50 atm and enthalpies to 40,000 Btu/lb without major redesign. Significant instrumentation and stability problems had to be solved before achieving accurate data over a wide range of arc pressures and arc currents, but no arc heater modifications are necessary other than gas injector sizing, spin coil insulation, and proper nozzle design. Hydrogen performance data are not highly repeatable. The arc-jet appears more stable on hydrogen than the arc current and voltage fluctuations indicate.

A standard Huels-type arc heater can be operated on pure helium at pressures to 100 atm and enthalpies to 9700 Btu/lb without major redesign. The arc is quite stable and the data are repeatable.

Electrode erosion and thus test stream contamination are a problem on hydrogen at low pressures where the arc is not properly stabilized in the cathode (front electrode). However, hydrogen, helium and air all exhibit less than 0.4% test stream contamination at pressures above 25 atm. Anode erosion is severe on air at pressures above 75 atm. Electrode erosion on helium is negligible in the anode and minor in the cathode over a wide test range.

A computer code based on a rod-arc model with radiation losses and convective turbulent heating of the gas can be used to characterize high pressure-high mass flow rate arc heaters. The performance of an $N = \sim 0.5$ Huels-type arc heater can be predicted for hydrogen, helium or air.

The performance of air arc heaters to scale $N = 4$ including the AEDC DET ($N = 1.73$) heater can be accurately characterized by this code thus verifying its scaling credibility and giving confidence to the scaled predictions for hydrogen and helium.

7. REFERENCES

1. R. T. Smith and J. L. Folck, Operating Characteristics of a Multi-Megawatt Arc Heater Used with the AFFDL 50 Megawatt Facility, AFFDL-TR-69-6, April 1969.

2. J. H. Painter, High Performance Arc Air Heater Studies, AIAA Paper No. 75-705 (May 1975).

3. W. A. Rinehart, J. H. Painter, R. R. Williams and R. A. Williamson, High Impact Pressure (HIP) Arc Heater Facility, 17th Annual Technical Meeting, IES, Los Angeles, Calif., 29 April 1971.

4. A. K. Repovich, Calibration of Critical Orifice Flowmeters for Air and Hydrogen, McDonnell Douglas Engineering Note EN-323, March 1962.

5. P. W. Godt, Experimental Correlation of Air, Nitrogen, Helium and Argon Flow Rates through Critical Flow Nozzles, AIP/ASME/ISA/NBS Symposium for Flow - Its Measurements and Control in Science and Industry, Pittsburgh, Pa. (May 1971).

6. B. Rosen, V. H. Dayan and R. L. Proffit, Hydrogen Leak and Fire Detection, NASA SP-5092, 1970.

7. J. H. Painter, High Pressure Arc Heater Electrode Heat Transfer Study, AIAA Paper No. 74-731 (July 1974).

8. D. R. Bartz, An Approximate Solution of Compressible Turbulent Boundary-Layer Development and Convective Heat Transfer in Convergent-Divergent Nozzles, Transactions of the ASME $\underline{11}$, 35 (1955).

9. R. C. Eschenbach, G. M. Skinner et al., Development of Stable, High Power, High Pressure Arc Air Heaters for a Hypersonic Wind Tunnel, WADD Technical Report 61-100, July 1961.

10. R. C. Eschenbach, D. A. Bryson, H. B. Sargent, R. J. Sarlitto and H. H. Trone, Characteristics of High Voltage Vortex-Stabilized Arc Heaters, IEEE Trans. on Nucl. Sci. $\underline{1}$, 41 (1964).

11. R. T. Smith and J. P. Doyle, A 50-Megawatt Arc Heater: Scaling Parameters and Performance Prediction, USAF FDL TDR 64-91, August 1964.

12. R. Richter, Ultrahigh Pressure Arc Heater Studies (Phase III), AEDC-TR-70-106, March 1970.

13. J. H. Painter, Characterization of High Pressure Constricted Arc Air Heaters, McDonnell Douglas Report (to be published).

14. Linde Arc Plasma Heaters, Linde Brochure 51-403-B (May 1965).

15. J. H. Painter and R. J. Ehmsen, Development of a High Performance Arc Heater for Ground Testing Advanced Strategic Reentry Vehicle Components, AIAA Paper No. 71-259 (March 1971).

16. J. H. Painter, Performance Characteristics of the MDC-200 Arc Air Heater Using Isolated Inter-electrode Segments, McDonnell Douglas Report MDC Q0834, July 1973.

17. W. J. Lick and H. W. Emmons, Thermodynamic Properties of Helium to 50,000°K, (Harvard University Press, Cambridge, Mass, 1962).

18. W. J. Lick and H. W. Emmons, Transport Properties of Helium from 200 to 50,000 K, (Harvard University Press, Cambridge, Mass, 1965).

19. B. M. Rosenbaum and L. Levitt, Thermodynamic Properties of Hydrogen from Room Temperature to 100,000 K, NASA TND-1107, January 1962.

20. N. L. Krascella, Tables of the Composition, Opacity, and Thermodynamic Properties of Hydrogen at High Temperatures, NASA SP-3005, 1963.

21. N. T. Grier, Calculation of Transport Properties and Heat Transfer Parameters of Dissociating Hydrogen, NASA TND-1406, October 1962.

22. J. M. Yos, Transport Properties of Nitrogen, Hydrogen and Air to 30,000 K, AVCO Corp. RAD-TM-63-7, 22 March 1963.

23. K. G. Sewell, Thermodynamic Properties of High Temperature Air, Chance Vought Report No. RE-IR-14, 28 June 1961.

24. T. C. Peng and R. J. Arave, Thermodynamic and Transport Properties of Air, Boeing Report D2-11781, 1962.

25. J. R. Viegas and T. C. Peng, Electrical Conductivity of Ionized Air in Thermodynamic Equilibrium, ARS J. 31, 654 (1961).

26. C. F. Hansen, Approximations for the Thermodynamic and Transport Properties of High-Temperature Air, NASA TR R-50, 1959.

27. V. I. Kogan, Plasma Physics and the Problem of Controlled Thermonuclear Reactions, (Pergamon Press, Ltd., 1959), Vol. III.

28. H. R. Greim, Plasma Spectroscopy, (McGraw Hill, Inc., 1964).

29. V. R. Watson and E. B. Pegot, Numerical Calculations for the Characteristics of a Gas Flowing Axially through a Constricted Arc, NASA TND-4042, June 1967.

APPENDIX A: DATA SUMMARY AND COMPUTER CODES

A-1 DATA SUMMARY

Tables A-1, A-2, and A-3 summarize the hydrogen, helium and air arc heater data from this test program. The data shown were extracted from the printed data sheet output of the RDAS. Each point represents a stable condition in near equilibrium. A complete volume of the printed data sheets was furnished to USAF-AEDC under separate cover.

The column shown in Tables A-1 through A-3 are as follows.

Symbol	Parameter	Units
I	Arc current	A
P_o	Arc pressure	atm
V	Arc voltage	V
$\dot{m}$	Gas flow rate	lb/s
Q_A	Anode energy loss	Btu/s
Q_C	Cathode-body energy loss	Btu/s
Q_N	Nozzle energy loss	Btu/s
h_b	Energy balance enthalpy	Btu/lb
h_{sf}	Sonic flow enthalpy	Btu/lb

Note that the sonic flow enthalpy is not tabulated for hydrogen since it was consistently in error because of nozzle throat-area reduction (see Section 4.1)

In addition to the data given in Tables A-1 through A-3, the printed data sheets included the arc power, thermal efficiency, flowmeter pressure, injector pressure, injector pressure ratio, differential coolant temperatures and coolant flow rates on the anode, cathode-body, and nozzle. The data reduction program assigned a value of 1°F to the differential temperatures prior to and following the test. Thus, since the specific heat of water is unity, the tabulated energy losses, pre- and post-test, were numerically the water flow rates in units of lb/s.

TABLE A-1   N-250 HYDROGEN DATA

Test	I	P_o	V	$\dot{m}$	Q_A	Q_C	Q_N	h_b
37	237	10.4	876	0.0042	11.1	54.3	14.3	29306
	296	10.0	741	0.0041	10.7	56.3	17.3	32175
	400	10.1	633	0.0043	14.7	67.6	17.2	34410
38	236	10.5	1004	0.0048	10.0	61.1	14.4	31151
	298	9.8	796	0.0044	12.0	59.9	15.7	33312
	400	10.0	549	0.0040	15.9	57.8	15.2	31706
59	240	15.5	1309	0.0068	19.7	55.1	24.3	31107
	245	15.9	1300	0.0068	18.5	55.6	25.1	31646
	314	15.2	992	0.0057	19.3	67.4	24.3	34180
	323	15.4	970	0.0057	18.8	67.6	24.4	34257
	398	15.2	757	0.0048	19.6	76.6	22.4	36052
60	241	15.1	1419	0.0065	20.1	61.8	22.3	35538
	242	15.1	1389	0.0065	19.4	62.6	23.3	34525
	311	14.5	1109	0.0052	21.8	78.3	23.0	38656
	392	15.0	939	0.0052	24.5	95.3	23.7	41574
56	240	25.0	1984	0.0106	32.1	96.2	34.3	29005
	313	24.1	1616	0.0091	32.5	116.3	33.9	34413
	395	24.9	1421	0.0086	36.0	149.2	37.7	38050
57	233	25.2	2124	0.0103	35.7	81.0	34.6	32647
	310	24.8	1727	0.0093	34.2	111.7	39.8	36206
	393	22.6	1229	0.0073	32.7	128.4	34.0	37561
64	303	49.3	3442	0.0194	74.9	266.0	54.4	32363
74	304	49.8	3578	0.0208	75.6	307.1	71.3	30008
68	302	40.1	2924	0.0179	51.2	250.3	49.0	29014

TABLE A-2   N-250 HELIUM DATA

Test	I	P_o	V	$\dot{m}$	Q_A	Q_C	Q_N	h_b	h_{sf}
95	240	25.3	968	0.0203	14.4	54.0	12.8	7508	7805
	318	24.8	871	0.0194	20.8	72.5	15.2	8593	8243
	396	25.7	807	0.0186	27.2	91.6	17.6	9669	9663
106	238	25.2	957	0.0196	13.1	64.4	14.2	7012	8332
	316	25.3	845	0.0187	19.4	82.3	16.5	7891	9234
	400	25.3	767	0,0178	25.8	99.4	17.9	8938	10204
98	237	49.8	1573	0.0442	34.8	79.4	19.7	5615	6392
	318	50.0	1473	0.0409	49.2	107.4	24.7	7106	7563
	397	50.3	1393	0.0390	62.0	133.8	29.4	8356	8395
99	237	50.3	1613	0.0449	32.9	81.3	19.4	5762	6351
	316	49.9	1518	0.0421	47.5	110.8	25.2	7118	7087
	399	50.2	1415	0.0397	61.1	137.8	29.5	8392	8088
100	242	75.3	2144	0.0721	52.4	98.8	21.1	5092	5513
	317	75.1	1997	0.0668	71.4	138.8	27.2	6105	6375
	397	74.5	1857	0.0618	92.1	167.8	34.6	7204	7335
104	236	74.9	2214	0.0696	49.8	110.5	24.3	5115	5839
	315	75.0	2059 -	0.0642	69.8	148.3	31.0	6359	6888
	398	75.2	1910	0.0580	90.3	182.1	36.0	7747	8479
103	238	96.6	2600	0.0908	61.8	120.7	25.0	4834	5706
	317	94.0	2415	0.0804	85.6	163.1	33.1	6195	6898
	399	94.6	2233	0.0737	109.9	191.0	39.5	7514	8304
105	238	100.8	2677	0.0951	66.2	129.6	27.3	4663	5665
	316	100.9	2556	0.0870	91.7	171.8	36.3	6005	6780
	396	100.8	2414	0.0786	119.3	215.1	45.8	7361	8308

TABLE A-3   N-250 AIR DATA

Test	I	P_o	V	$\dot{m}$	Q_A	Q_C	Q_N	h_b	h_{sf}
77	238	10.1	520	0.0135	7.0	34.4	8.0	5150	5300
77	315	10.3	450	0.0124	9.5	45.4	10.3	5760	6730
77	401	10.1	420	0.0145	11.4	55.5	9.8	7230	7700
79	239	9.9	570	0.0133	7.3	33.1	8.0	6140	5130
80	320	10.1	480	0.0132	8.5	41.5	7.5	6030	5510
80	400	9.9	400	0.0128	9.7	47.8	7.4	6800	5660
75	240	15.1	760	0.0201	15.6	44.9	10.0	5250	5290
75	320	14.8	660	0.0189	19.6	59.1	11.8	5910	5910
75	393	15.6	550	0.0178	17.5	67.7	13.3	6000	6000
76	237	15.2	660	0.0199	10.9	43.4	11.5	4240	5510
76	317	14.8	540	0.0171	13.0	53.4	11.2	5090	7550
76	394	15.1	480	0.0158	15.5	63.4	10.9	5850	9680
84	239	15.0	730	0.0217	9.0	34.9	7.3	5370	4310
81	320	15.0	660	0.0202	16.7	55.1	9.9	6030	5160
82	400	14.8	600	0.0196	19.3	65.6	11.2	6800	5360
78	242	25.2	1000	0.0338	15.2	54.8	18.0	4340	5160
78	322	24.9	830	0.0299	19.3	70.7	16.6	5030	6830
78	405	25.0	720	0.0279	22.1	83.0	16.2	5650	8260
84	238	24.5	1030	0.0357	15.8	55.2	13.5	4280	4220
83	320	24.7	910	0.0336	22.9	70.1	15.2	5100	5000
84	401	25.0	850	0.0326	33.3	86.7	16.6	5830	5580
92	238	49.5	1662	0.0691	27.4	77.8	18.2	3770	4680
92	317	50.4	1474	0.0660	37.8	100.2	21.0	4440	5520
92	400	50.9	1343	0.0630	48.5	124.9	23.9	5070	6340
107	236	50.5	1663	0.0721	28.5	76.7	19.7	3560	4430
107	320	51.2	1453	0.0683	36.9	100.6	22.4	4250	5260
107	400	50.9	1307	0.0652	42.1	123.6	25.0	4800	5820
93	239	75.8	2263	0.1059	38.0	92.8	25.0	3500	4700
93	320	75.2	1976	0.1007	50.9	122.2	28.7	4090	5210
93	393	75.1	1804	0.0966	62.6	149.9	32.5	4550	5780
94	317	73.8	1973	0.1017	49.6	118.8	26.7	4040	4850
108	234	100.1	3008	0.1444	47.7	111.2	32.2	3430	4330
108	319	100.8	2462	0.1355	60.1	142.2	33.7	3880	5160
108	398	100.2	2260	0.1313	72.8	179.2	40.6	4400	5510
109	314	100.1	2450	0.1311	55.4	140.7	33.1	3950	5510

A-2   HYARC AND HEARC COMPUTER CODES

The computer codes HYARC and HEARC are essentially identical with the exception of those parameters that characterize each individual gas. Thus, to avoid unnecessary duplication, only a complete description of the HEARC is given; those aspects which differ for HYARC are discussed in the following subsection.

HEARC Program

A description of the function of the main program and each subroutine is given in Table A-4. The computer variable descriptions are listed in Tables A-5 and A-6.

The FORTRAN HEARC program listing is presented in Table A-7 and the corresponding flow chart is presented in Figure A-1.

HYARC Program

A description of the function of the main program and each subroutine is given in Table A-4. The differences between HEARC and HYARC are those

TABLE A-4   HYARC-HEARC PROGRAM FUNCTIONS

Main Program	Sets up pressure and current calculational loops and initial values for TARC, TGAS, and DARC. Iterates gas temperature until gas power from enthalpy-mass flow relation agrees with energy balance value. Iterates mass flow rate until it agrees with value calculated for sonic flow at nozzle throat.
Subroutines:	
INPUT	Reads in required data in engineering units and converts to MKS system
GASPOW	Calculates gas power by: (1) energy balance on the gas and (2) enthalpy-mass flow of arc column and bulk gas annulus
ARCTEM	Calculates temperature of the arc column for minimum power input
ARCDIA	Calculates arc column diameter by solving the arc column power balance equation
OUTPUT	Computes voltage, gradient, efficiency, and electrode heat loads and presents results of solution in engineering units
GAMMAX	Finds ratio of specific heats for given temperature and pressure
TEMP	Finds temperature that corresponds to a given enthalpy and pressure
VISCX	Finds viscosity from table interpolation for a given temperature and pressure
ENTHX	Finds enthalpy from table interpolation for a given temperature and pressure
RHO	Finds gas density from table interpolation for a given temperature and pressure
SIGMAX	Helium: Finds electrical conductivity from table interpolation for a given temperature and pressure
	Hydrogen: Finds electrical conductivity by a curve fit for a given temperature and pressure
RADX	Helium: Finds volumetric radiation intensity from electron mole fraction table interpolation and electron density calculation
	Hydrogen: Obtains volumetric radiation intensity from table interpolation for a given temperature and pressure
TCONDX	Finds thermal conductivity from table interpolation for a given temperature and pressure

104

parameters that are characteristic for each gas. The thermodynamic and transport properties are from the sources shown in Table 4. The descriptions of the HYARC main program and subroutines INPUT, OUTPUT, GASPOW, ARCTEM, ARCDIA, and TEMP are shown in Table A-4. The thermophysical property determinations follow the same approach as HEARC. The front and rear arc lengths are shown in Table 7 for the N-250. The cold gas inlet enthalpy and Prandtl number are listed in Table 5. The correlation results utilized are discussed in Section 5.4.

TABLE A-5 HYARC-HEARC VARIABLE DESCRIPTIONS

Variable Name	Description
Variables common to more than one subroutine	
AMPS	Arc current, A
AMPINC	Current increment, A
ARCLEN	Total length of arc, m
CNVF01	39.3701 in./m
CNVF02	2.2046 lbm/kg
CNVF03	0.0254 m/in.
CNVF04	4.2292×10^{-4} (Btu/lbm)/(J/kg)
CNVF05	2.6839×10^{-5} (Btu/ft^3)/(J/m^3)
CNVF06	8.8056×10^{-5} (Btu/ft^{2}s)/(W/m^2)
CNVF07	0.2048 (lbm/ft^{2}s)/(kg/m^{2}s)
CNVF08	3.2808 (ft/s)/(m/s)
CONSLN	Length of front constrictor, m
DARC	Diameter of arc, m
DCONS	Diameter of constrictor, m
DTHRT	Diameter of nozzle throat, m
ENTH	Net gas exit enthalpy, J/kg
FARCLN	Arc length in front electrode, m
FNU	Nusselt number
IARCD	Arc diameter iteration counter
IARCT	Arc temperature iteration counter
IERR	Error flag indicating that a preset iteration count has been exceeded
ISONIC	Mass flow rate iteration counter
ITGAS	Bulk gas iteration counter
NAMPS	Number of current increments
NCASE	Index indicating first call to output subroutine for each input case
NPRES	Number of pressure increments
PCONV	Power convected from gas to constrictor wall, W
PGAS	Power in gas from energy balance, W
PGASEN	Power in gas from enthalpy-mass flow, W
PI	3.14159

TABLE A-5 (CONTINUED)

Variable Name	Description
PIN	Electrical power into arc, W
PINC	Pressure increment, atm
PRES	Pressure, atm
QCONV	Constrictor wall convective heat flux, W/m^2
QN	Nozzle energy loss, W
QRAD	Constrictor wall radiative heat flux, W/m^2
RARCLN	Arc length in rear electrode, m
REY	Reynolds number
SIGMA	Arc electrical conductivity, mhos/m
TARC	Arc temperature, K
TGAS	Bulk gas temperature, K
TSTAG	Stagnation temperature of exit gas, K
WDOT	Mass flow rate, kg/s
WDOTAR	Mass flow rate in arc column, kg/s
WDOTGA	Mass flow rate in bulk gas annulus, kg/s
Y	Volumetric radiation of arc x $(\pi/4)$, W/m^3

Variables used in MAIN

ASTAR	Area of nozzle throat, m^2
DELN	DELPGA value from previous iteration
DELPGA	Normalized gas power difference
DELWDT	Normalized mass flow rate difference
GAMMA	Ratio of gas specific heat, c_p/c_v
GR	$(\frac{2}{\gamma+1})$ RATIO
NEXT	Index for new case or end
RATIO	$(\gamma+1)/(2(\gamma-1))$
RHOSTG	Gas density corresponding to stagnation temperature, kg/m^3
SCALE	Scale N of heater, ratio of constriction diameter to 0.75 in.
TABS	Absolute value of difference between present and previous bulk gas temperatures, K
TGASN	Bulk gas temperature, from previous iteration, K
WDOTSF	Mass flow rate calculated from nozzle sonic flow relationship, kg/s
XP	New bulk gas temperature by method of false position, K

Variables used in subroutine GASPOW

AARC	Arc column area, m^2
AGAS	Bulk gas annulus area, m^2
ENTHAR	Arc gas enthalpy, J/kg
ENTHGA	Bulk gas enthalpy, J/kg

106

TABLE A-5 (CONTINUED)

Variable Name	Description
H	Turbulent heat transfer coefficient, W/m^2K
HIN	Cold gas inlet enthalpy, J/kg
PR	Prandtl number
REY	Reynolds number
RHOARC	Arc gas density, kg/m^3
RHOGAS	Bulk gas density, kg/m^3
TA	Dummy temperature variable, K
TCOND	Thermal conductivity, $W/m \cdot K$
TWALL	Constrictor wall temperature, K
VEL	Gas velocity in constrictor, m/s

Variables used in ARCTEM

DIRCH	Equals minus one if PIN greater than PINP, otherwise equals plus one
DT	Arc temperature increment, K
PINP	Previous calculated value of power input, W
SIGNF	Sign of arc temperature increment

Variables used in ARCDIA

ALPHA	Z/Y, used in solving energy balance
BETA	X/Y, used in solving energy balance
CORR	Term that takes into account fractional variation of DARC
DELDIA	Normalized arc diameter difference
DELD	Arc diameter iteration increment, m
DI	Previous iteration value of DARC, m
DP	Used in CORR, $D_c + D_a$
DM	Used in CORR, $D_c^2 - D_a^2$
F	Arc column energy balance function, $P_i - (P_r + P_c) = 0$
FNU	Nusselt number
FP	First derivitive of F, used for arc diameter iteration
H	Turbulent film heat transfer coefficient, W/m^2K
INN	Subroutine entry indicator flag
PR	Prandtl number
PXX	Dummy variable for power input, W
RAD	Volumetric radiation, W/m^3
TCOND	Thermal conductivity, $W/m \cdot K$
TXX	Dummy variable for arc temperature, K
TX	Dummy temperature for evaluating TCONDX, K
VISC	Viscosity of bulk gas, $N \cdot s/m^2$
X	Power input per unit length $\div D_c^2$, W/m
Z	Convective heat flux loss from arc per unit length $\div D_a$, W/m^2

TABLE A-5 (CONCLUDED)   .

Variable Name	Description
Variables used in subroutine OUTPUT	
DCONSX	Constrictor column diameter, in.
DIARCX	Arc column diameter, in.
DTHX	Nozzle throat diameter, in.
EFF	Efficiency
ENTHX	Exit gas bulk enthalpy, Btu/lbm
FRNT	Front arc length, in.
GRAD	Arc column voltage gradient, V/in.
HFRNTX	Front electrode (constrictor) power loss, Btu/s
HREARX	Rear electrode power loss, Btu/s
INN	Subroutine entry flag
IOUT	Logical device for output
LCONS	Constrictor length, in.
PGASX	Net power added to gas, kW
PINX	Power input, kW
QCONVX	Constrictor wall convective heat flux, Btu/ft^{2}s
QNX	Nozzle heat load, Btu/s
QRADX	Constrictor wall radiative heat flux, Btu/ft^{2}s
REAR	Rear arc length, in.
VOLTS	Arc column voltage drop, V
WDOTX	Total mass flow rate, lbm/s
Variables used in subroutine TEMP	
CONV	Normalized temperature convergence parameter
DT	Temperature increment, K
ERR	Convergence error
H	Enthalpy, J/kg
HTN	Enthalpy corresponding to temperature TN, J/kg
HTNP	Enthalpy corresponding to temperature TN + DT, J/kg
K	Iteration index
P	Pressure, atm
T	Temperature, K
TI	Initial starting temperature, K
TN	Previous iteration temperature value, K
TNP1	Temperature calculated for this iteration, K

TABLE A-6 HEARC GAS PROPERTY VARIABLE DESCRIPTIONS

Variable Name	Description
Variables used in subroutine VISCX	
ATM1	Data temperature array for 1 atmosphere
ATMI0	Data temperature array for 10 array for 10 atmospheres
ATMI00	Data temperature array for 100 atmospheres
ATMI000	Data temperature array for 1000 atmospheres
DT	Temperature difference between table value J and T
I	Pressure index for table values
J	Temperature index for last table value before T
P	Pressure, atm
PR	Pressure values in table array, atm
PP	Logarithmic pressure increment
T	Temperature, K
TC	Viscosity table array, dyne $- s/cm^2$
TC1	Viscosity interpolated to temperature T at pressure PR (I)
TC2	Viscosity interpolated to temperature T at pressure PR (I + 1)
TVISC	Viscosity, Nt s/m^2
Variables used in subroutine ENTH	
ATM1	Data temperature array for 1 atmosphere
ATMI0	Data temperature array for 10 atmospheres
ATMI00	Data temperature array for 100 atmospheres
ATMI000	Data temperature array for 1000 atmospheres
DT	Temperature difference between table value J and T
I	Pressure index for table values
J	Temperature index for last table value before T
P	Pressure, atm
PR	Pressure values in table array TC, atm
PP	Logarithmic pressure increment
RHE	Helium gas constant, J/kg K
TENTH	Enthalpy corresponding to T, P, J/kg
T	Temperature, K
TC	Enthalpy table array, normalized to $R_{He}T_o$
TC1	Enthalpy interpolated to temperature T at pressure PR (I)
TC2	Enthalpy interpolated to temperature T at pressure PR (I + 1)
TO	Standard temperature, 273.16 K

TABLE A-6 (CONTINUED)

Variable Name	Description
Variables used in subroutine RHO	
ATM1	Data temperature array for 1 atmosphere
ATMl0	Data temperature array for 10 atmospheres
ATMl00	Data temperature array for 100 atmospheres
ATMl000	Data temperature array for 1000 atmospheres
DT	Temperature difference between table value J and T
I	Pressure index for table values
J	Temperature index for last table value before T
P	Pressure, atm
PP	Logarithmic pressure increment
PR	Pressure values in table array TD, atm
RHO0	0.17859, density normalization, kg/m^3
T	Temperature, K
TD	Density table array normalized to RHO0
TDENS	Density corresponding to T and P, kg/m^3
TD1	Density interpolated to temperature T at pressure PR (I)
TD2	Density interpolated to temperature T at pressure PR (I+ 1)
T0	Standard temperature, 273.16 K
Variables used in subroutine SIGMAX	
ATM1	Data temperature array for 1 atmosphere
ATMl0	Data temperature array for 10 atmospheres
ATMl00	Data temperature array for 100 atmospheres
ATMl000	Data temperature array for 1000 atmospheres
DT	Temperature difference between table value J and T
I	Pressure index for table values
J	Temperature index for last table value before T
JSHIFT	Temperature index shift parameter
P	Pressure, atm
PR	Pressure values in table array TS, atm
PP	Logarithmic pressure increment
T	Temperature, K
TS	Electrical conductivity array, (log_{10} to 13,000 K) mho/cm
TSIG	Electrical conductivity corresponding to T and P, mho/m
TS1	Electrical conductivity interpolated to temperature T at pressure PR (I)
TS2	Electrical conductivity interpolated to temperature T at pressure PR (I + 1)

TABLE A-6 (CONCLUDED)

Variable Name	Description
Variables used in subroutine RADX	
ATM1	Data temperature array for 1 atmosphere
ATMI0	Data temperature array for 10 atmospheres
ATMI00	Data temperature array for 100 atmospheres
ATMI000	Data temperature array for 1000 atmospheres
DT	Temperature difference between table value J and T
I	Pressure index for table values
J	Temperature index for last table value before T
JSHIFT	Temperature index shift parameter
KP	Helium equilibrium constant
KPP	Square root of KP ÷ Pressure
NE	Electron number density, #/cm^3
NT	Total particle number density, #/cm^3
P	Pressure, atm
PP	Logarithmic pressure increment
PR	Pressure values in table array TR, atm
T	Temperature, K
TR	Electron mole fraction array $(\log_{10}$ to 16,000 K)
TR1	Mole fraction interpolated to temperature T at pressure PR (I)
TR2	Mole fraction interpolated to temperature T at pressure PR (I + 1)
TRAD	Volumetric radiation intensity at T and P, W/m^3
XE	Electron mole fraction
Variables used in subroutine TCONDX	
ATM1	Data temperature array for 1 atmosphere
ATMI0	Data temperature array for 10 atmospheres
ATMI00	Data temperature array for 100 atmospheres
ATMI000	Data temperature array for 1000 atmospheres
DT	Temperature difference between table value J and T
I	Pressure index for table values
J	Temperature index for last table value before T
P	Pressure, atm
PP	Logarithmic pressure increment
PR	Pressure values in the table array TC, atm
T	Temperature, K
TC	Thermal conductivity array, erg/cm s K
TC1	Thermal conductivity interpolated to temperature T at pressure PR (I)
TC2	Thermal conductivity interpolated to temperature T at pressure PR (I + 1)
TCOND	Thermal conductivity for T and P, W/m K

TABLE A-7 HEARC LISTING

```
CARD NO        ****                              CONTENTS                                    ****

     1        C     MININUM ENERGY ADDITION ARC HEATER CHARACTERIZATION ALGORITHM
     2        C           FOR HELIUM
     3        C     MCDONNELL DOUGLAS RESEARCH LABORATORIES, ST.LOUIS, MO.
     4        C     PROGRAMED BY J.F.SHAEFFER
     5
     6              BLOCK DATA
     7              COMMON/ CONVF /
     8             +CNVFO1,  CNVFO2,  CNVFO3,  CNVFO4,
     9             +CNVFO5,  CNVFO6,  CNVFO7,  CNVFO8,  PI
    10        C
    11              DATA CNVFO1,CNVFO2,CNVFO3,CNVFO4,CNVFO5,CNVFO6,CNVFO7,CNVFO8,PI
    12             +/39.3701, 2.2046, .0254, 4.2992E-4,  2.6839E-5,  8.8056E-5,
    13             +0.2048,  3.2808,  3.14159 /
    14              END
    15
    16        C     CNVFO1= M * 39.3701 = INCHES
    17        C     CNVFO2= KG/SEC * 2.2046 = LBM/SEC
    18        C     CNVFO3= VOLTS/M * 2.54E-2 = VOLTS/INCH
    19        C     CNVFO4= JOULES/KG * 4.2992E-4 = BTU/LBM
    20        C     CNVFO5= JOULES/M  3 * 2.6839E-5 = BTU/FT  3
    21        C     CNVFO6= WATTS/M  2 * 8.8056E-5 = BTU/FT  2-SEC
    22        C     CNVFO7= KG/M  2-SEC * 0.2048 = LBM/FT  2-SEC
    23        C     CNVFO8= M/SEC * 3.2808 = FT/SEC
    24              COMMON / CONVF /
    25             +CNVFO1,  CNVFO2,  CNVFO3,  CNVFO4,
    26             +CNVFO5,  CNVFO6,  CNVFO7,  CNVFO8,  PI
    27              COMMON/ BLK1 / AMPS,ARCLEN,DARC,DCONS,DTHRT,ENTH,PCONV,PGAS,
    28             +PGASEN,  PIN,PRAD,PRES,QCONV,QRAD,SIGMA,TARC,TGAS,WDOT,Y
    29              COMMON/ BLK2 / QN, TSTAG
    30              COMMON/ ERROR / IARCD,IARCT,IERR,ISONIC,ITGAS
    31              COMMON/ LOOPS / AMPINC,NAMPS,PINC,NPRES
    32              COMMON/ LENGTH / CONSLN,FARCLN,RARCLN
    33              COMMON/ NCASE / NCASE
    34              COMMON/ REY / REY,WDOTAR,WDOTGA,FNU
    35              IN=5
    36              TARC=18000.
    37              TGAS=2900.0
    38        100 CALL INPUT
    39              WDOTGA=WDOT
    40              SCALE=(DCONS/(0.75*0.0254))
    41              NCASE=0
    42              AMPST=AMPS
    43              PREST=PRES
    44              DARC=0.9*DCONS
    45              DO  160 IP=1,NPRES
    46              DO  160 IA=1,NAMPS
    47              AMPS=AMPST + AMPINC*(IA-1)
    48              PRES=PREST + PINC*(IP-1)
    49        C     ARC LENGTH CORRELATION FOR HELIUM N-250 HEATER
    50              RARCLN=(PRES/(0.288*PRES + 4.22))*CNVFO3
    51              FARCLN=(4.45 + 0.0106*(PRES-25.)-RARCLN/CNVFO3)*CNVFO3
    52              FARCLN=(SCALE/0.5)*FARCLN
    53              RARCLN=(SCALE/0.5)*RARCLN
    54              ARCLEN=FARCLN + RARCLN
    55              IERR=0
    56              ISONIC=0
    57        110 ITGAS=0
    58        120 CONTINUE
    59        C     CALCULATE ARC TEMPERATURE AND DIAMETER
    60              CALL  ARCTEM
    61              IF(IERR.EQ.1)GO TO 150
    62              CALL GASPOW
    63              ITGAS=ITGAS+1
    64              IF(ITGAS.GT.100) IERR=1
    65              IF(IERR.EQ.1) GO TO 150
    66              DELPGA =(PGAS-PGASEN)/PGAS
    67              IF(ITGAS.NE.1) GO TO 130
    68              DELN=DELPGA
    69              TGASN=TGAS
    70              TGAS=TGAS - 100.0
    71              GO TO 120
    72        130 XP=(TGASN*DELPGA - TGAS*DELN)/(DELPGA-DELN)
    73              TABS=ABS(XP - TGAS)
    74              IF(TABS.GT.300.) XP=TGAS + (XP - TGAS)/TABS*100.
    75              TGASN=TGAS
    76              DELN=DELPGA
    77              IF(ABS(DELPGA).LE..01) GO TO 140
    78              TGAS=XP
    79              GO TO 120
    80        140 CONTINUE
    81        C
    82        C     CALCULATE MASS FLOW TO SATISFY SONIC FLOW RELATION
    83              ENTH=PGAS/WDOT
    84              CALL TEMP(ENTH,PRES,TSTAG)
    85              CALL GAMMAX(TSTAG,PRES,GAMMA)
    86              CALL RHO(TSTAG,PRES,RHOSTG)
    87              RATIO=(GAMMA+1.0)/(2.0*(GAMMA-1.0))
    88              GR=(2.0/(GAMMA+1.0))**RATIO
    89              ASTAR=PI*DTHRT*DTHRT/4.0
    90              WDOTSF=ASTAR*SQRT(GAMMA*RHOSTG*PRES*1.013E5)*GR
    91              ISONIC=ISONIC+1
    92              IF(ISONIC.GT.100) IERR=1
    93              IF(IERR.EQ.1) GO TO 150
    94              DELWDT=(WDOTSF - WDOT) / WDOTSF
    95              IF(ABS(DELWDT).LT.0.01) GO TO 150
    96              WDOT=WDOTSF
    97              GO TO 110
    98        150 CONTINUE
    99              CALL OUTPUT
   100        160 CONTINUE.
   101              READ(IN,175) NEXT
   102        175 FORMAT(9X,I1)
   103              GO TO ( 100,170),NEXT
   104        170 CONTINUE
   105              END
   106        C
   107        C
   108              SUBROUTINE INPUT
```

112

TABLE A-7 (CONTINUED)

CARD NO	****	CONTENTS	****

```
109      C    READS REQUIRES DATA IN ENGINEERING UNITS AND CONVERTS TO
110      C    MKS SYSTEM FOR THE COMPUTATIONS
111           COMMON/ CONVF /
112          +CNVF01,CNVF02,CNVF03,CNVF04,CNVF05,CNVF06,CNVF07,CNVF08,PI
113           COMMON/ BLK1 / AMPS,ARCLEN,DARC,DCONS,DTHRT,ENTH,PCONV,PGAS,
114          +PGASEN, PIN,PRAD,PRES,QCONV,QRAD,SIGMA,TARC,TGAS,WDOT,Y
115           COMMON/ LOOPS / AMPINC,NAMPS,PINC,NPRES
116           COMMON/ TITLE / TITLE(18),DAT(4)
117           COMMON/ LENGTH /CONSLN, FARCLN, RARCLN
118           IN=5
119           READ(IN,100)(TITLE(J),J=1,18)
120      100  FORMAT(18A4)
121           READ(IN,110)AMPS,AMPINC,NAMPS
122      110  FORMAT(2E10.1,8X,I2)
123           READ(IN,110)PRES,PINC,NPRES
124           READ(IN,120)CONSLN,FARCLN,RARCLN
125      120  FORMAT(3E10.2)
126           READ(IN,120)WDOT,DCONS,DTHRT
127           CONSLN=CONSLN*CNVF03
128           FARCLN=FARCLN*CNVF03
129           RARCLN=RARCLN*CNVF03
130           ARCLEN=FARCLN + RARCLN
131           DREAR=DREAR*CNVF03
132           WDOT=WDOT/CNVF02
133           DCONS=DCONS*CNVF03
134           DTHRT=DTHRT*CNVF03
135           CALL DATIME(DAT)
136           RETURN
137           END
138      C
139      C
140           SUBROUTINE GASPOW
141      C
142      C    COMPUTES POWER IN GAS BY CALCULATING CONVECTIVE LOSS TO CONSTRICTOR
143      C
144
145           COMMON/ BLK1 / AMPS,ARCLEN,DARC,DCONS,DTHRT,ENTH,PCONV,PGAS,
146          +PGASEN, PIN,PRAD,PRES,QCONV,QRAD,SIGMA,TARC,TGAS,WDOT,Y
147           COMMON/ BLK2 /QN,TSTAG
148           COMMON/ ERROR / IARCD,IARCT,IERR,ISCNIC,ITGAS
149           COMMON/ LENGTH /CONSLN, FARCLN, RARCLN
150           COMMON/ REY / REY,WDOTAR,WDOTGA,FNU
151           PI=3.14159
152           TWALL=590.
153      C    CALCULATE CONVECTION LOSS TO CONSTRICTOR WALL
154           TA=1.00*(TGAS - TWALL) + TWALL
155           CALL TCONDX( TA,PRES,TCOND)
156           H=FNU*TCOND/ (DCONS-DARC)
157           QCONV=H*(TGAS-TWALL)
158      C    RADIATED HEAT FLUX OUT FROM ARC
159           QRAD=Y*(DARC*DARC)/(PI*DCONS)
160      C    POWER IN GAS FROM ARC (BY CONVECTION) IS Z*DARC*ARCLEN
161      C    HIN=COLD GAS ENTHALPY (JOULES/KG)
162           HIN=670.0/4.2992E-4
163      C    LOSSES  RADIATION OVER ARCLENGTH, CCNV, OVER FRONT CONSTRICTOR
164           PGAS=PIN - QRAD*PI*DCONS*ARCLEN - QCONV*PI*DCONS*CONSLN
165          ++ WDOT*HIN
166      C    NOZZLE LOSS CORRELATION FOR HELIUM,QN IS LOSS IN WATTS
167           ENTH=(PGAS/WDOT)*4.3E-4
168           QN=0.04*((WDOT*2.2046)**0.7)*(ENTH-1325.)*1054.
169           PGAS=PGAS - QN
170      C
171      C    CALCULATE POWER IN GAS,ARC FROM ENTHALPY-MASS FLOW RELATION
172      C    ASSUME UNIFORM VELOCITY
173           CALL RHO(TGAS,PRES,RHOGAS)
174           CALL RHO(TARC,PRES,RHOARC)
175           AGAS=PI*(DCONS**2-DARC**2)/4.0
176           AARC=PI*DARC*DARC/4.0
177           VEL=WDOT/(RHOGAS*AGAS + RHOARC*AARC)
178           WDOTAR=RHOARC*VEL*AARC
179           WDOTGA=RHOGAS*VEL*AGAS
180           CALL ENTHX(TGAS,PRES,ENTHGA)
181           CALL ENTHX(TARC,PRES,ENTHAR)
182           PGASEN=ENTHGA*WDOTGA + ENTHAR*WDOTAR
183           RETURN
184           END
185      C
186      C
187           SUBROUTINE ARCTEM
188      C
189      C    CALCULATES ARC TEMPERATURE FOR POWER INPUT TO BE A MININUM
190      C
191           COMMON/ BLK1 / AMPS,ARCLEN,DARC,DCONS,DTHRT,ENTH,PCONV,PGAS,
192          +PGASEN,PIN,PRAD,PRES,QCONV,QRAD,SIGMA,TARC,TGAS,WDOT,Y
193           COMMON/ ERROR / IARCD,IARCT,IERR,ISONIC,ITGAS
194           SIGNF=1.0
195           IARCT=0
196           DT=200.0
197      100  IARCT=IARCT+1
198           CALL ARCDIA(TARC    ,PIN )
199           IF(IERR.EQ.1)RETURN
200           IF(IARCT.NE.1)GO TO 50
201           TARC=TARC + DT
202           PINP=PIN
203           GO TO 100
204      50   DIRCH=SIGN(1.0,(PINP-PIN))
205           SIGNF=DIRCH*SIGNF
206           DT=DT/(1.+(1.-DIRCH)/2.)
207           IF(ABS(DT    ).LT.10.0) RETURN
208           TARC=TARC + SIGNF*DT
209           PINP=PIN
210           IF(IARCT.GT.100) GO TO 110
211           GU TO 100
212      110  IERR=1
213      120  RETURN
214           END
215      C
216      C
217           SUBROUTINE ARCDIA(TXX,PXX)
218      C
219      C    CALCULATE APC DIAMETER FOR ENERGY BALANCE
```

TABLE A-7 (CONTINUED)

| CARD NO | **** | CONTENTS | **** |

```
220        C
221              COMMON / BLK1 / AMPS,ARCLEN,DARC,DCONS,DTHRT,ENTH,PCONV,PGAS,
222             +PGASEN,  PIN,PRAD,PRES,QCONV,QRAD,SIGMA,TARC,TGAS,WDOT,Y
223              COMMON/ ERROR / IARCD,IARCT,IERR,ISONIC,ITGAS
224              COMMON / REY / REY,WDOTAR,WDOTGA,FNU
225              DATA INN /0/
226              IF( INN.NE.0) GO TO 100
227              PI=3.14159
228              DI=DARC
229        100 INN=1
230              IARCD=0
231        C    POWER IN   = X(TARC)/DARC**2 PER UNIT LENGTH
232              CALL SIGMAX(TXX ,PRES,SIGMA)
233              X=4.0*AMPS*AMPS/(PI*SIGMA)
234              CALL RADX(TXX ,PRES,RAD)
235        C    POWER RADIATED = Y(TARC)*DARC**2 PER UNIT LENGTH
236              Y=PI*RAD/4.0
237              TX=0.70*(TARC - TGAS) + TGAS
238              CALL VISCX(TGAS,PRES,VISC)
239              CALL TCONDX(TX,PRES,TCOND)
240        110 CONTINUE
241              IARCD=IARCD+1
242              PXX=(X/DARC**2)*ARCLEN
243        C    POWER OUT OF ARC COLUMN CONVECTED = Z(TARC)*DARC PER UNIT LENGTH
244              REY=(4.0*WDOTGA)/(PI*VISC*(DARC+DCONS))
245        C    PRANDTL NO FOR HE IS 0.672
246              PR=0.672
247              FNU=0.0265*(REY**0.8)*PR**0.3
248              H=FNU*TCOND/(DCONS-DARC)
249              Z=PI*H*(TXX -TGAS)
250              ALPHA=-Z/Y
251              BETA=-1.*X/Y
252              F=(DI**4) + ALPHA*(DI**3) + BETA
253              DP=DCONS + DI
254              DM=DCONS*DCONS - DI*DI
255              CORR=1.0 + 0.2*DI/3.0/DP + 2.0*DI*DI/3.0/DM
256              FP=4.0*(DI**3) + 3.0*ALPHA*DI*DI*CORR
257              DELD=-1.*F/FP
258              DARC=DI + DELD
259              DELDIA=(DARC-DI)/DARC
260              IF(IARCD.GT.100) GO TO 120
261              IF(ABS(DELDIA).LE.1.E-5) GO TO 130
262              DI=DARC
263              GO TO 110
264        120 IERR=1
265              RETURN
266        130 CONTINUE
267        C
268              RETURN
269              END
270        C
271        C
272              SUBROUTINE OUTPUT
273        C
274        C    CALCULATE REMAINING ARC PARAMETERS
275        C    CONVERT MKS TO ENGINEERING UNITS AND PRINT OUT RESULTS
276        C
277              REAL LENX,LCONS
278              COMMON/ BLK1 / AMPS,ARCLEN,DARC,DCONS,DTHRT,ENTH,PCCNV,PGAS,
279             +PGASEN, PIN,PRAD,PRES,QCONV,QRAD,SIGMA,TARC,TGAS,WDOT,Y
280              COMMON/ BLK2 / QN,TSTAG
281              COMMON/ ERROR / IARCD,IARCT,IERR,ISONIC,ITGAS
282              COMMON/ TITLE / TITLE(18),DAT(4)
283              COMMON/ CONVF /
284             +CNVF01,   CNVF02,  CNVF03,  CNVF04,
285             +CNVF05,   CNVF06,  CNVF07,  CNVF08,  PI
286              COMMON/ RAD / KNUP,KNU
287              COMMON/ LENGTH /CONSLN,FARCLN,RARCLN
288              COMMON/ NCASE / NCASE
289              COMMON/ REY / REY,WDOTAR,WDOTGA,FNU
290              IOUT=6
291              GRAD=(AMPS/(SIGMA*DARC*DARC*PI/4.0))*CNVF03
292              LCONS=CONSLN*CNVF01
293              FRNT=FARCLN*CNVF01
294              REAR=RARCLN*CNVF01
295              LENX=ARCLEN*CNVF01
296              VOLTS=GRAD*LENX
297        C    HELIUM ROOM TEMP ENTHALPY = 670 BTU/LB
298              HIN=(670./CNVF04)*WDOT
299              EFF=((PGAS - HIN)/PIN)*100.
300              WDOTX=WDOT*CNVF02
301              QRADX=QRAD*CNVF06
302              QCONVX=QCONV*CNVF06
303              QNX=QN*0.948E-3
304              ENTHX=ENTH*CNVF04
305              DIARCX=DARC*CNVF01
306              DCONSX=DCONS*CNVF01
307              DTHX=DTHRT*CNVF01
308              PINX=PIN*0.001
309              PGASX=(PGAS - HIN)*0.001
310              HREARX=QRAD*PI*(DCONS)        *RARCLN*0.948E-3
311              HFRNTX=(QRAD*PI*DCONS*FARCLN + QCONV*PI*DCONS*CONSLN)*.948E-3
312              IF(NCASE.NE.0) GO TO 100
313              WRITE(IOUT,105)
314        105 FORMAT(1H1,//,1X
315             +61HHEARC  HELIUM MINIMUM ENERGY ARC HEATER CHARACTERIZATION CODE)
316              WRITE(IOUT,110)DAT,TITLE
317        100 NCASE=1
318        110 FORMAT(   1X, 4A4,//,1X18A4, //,6H  PRES ,6H  AMPS,6H DCONS,
319             +6H DTHRT,6H LCONS,6H  ARCL,6H  FRNT,6H  REAR,6H TSTAG,
320             +6H QREAR,6H QFRNT,6H  QNOZ,
321             +/, 6H  ATM,6X,6(4X2HIN),6H DEG K,18H ----BTU/SEC------  ,//,
322             +6H VOLTS,6H   PIN,6H  GASP,6H  GRAD,6H  QRAD,6H QCONV,
323             +6H  WDOT,6H  ENTH,6H   EFF,6H  TARC,6H  DARC,/,6X,6H    KW,
324             +6H    KW,6H  V/IN,12H BTU/FT**2-S ,   6H LBM/S,
325             +6H B/LB,6H  PERC,6H DEG K,6H   IN,/)
326              IF(IERR.EQ.1)WRITE(IOUT,120)ISONIC,ITGAS,IARCD,IARCT
327        120 FORMAT(//, 7HERROR   ISONIC=,I4,  7H ITGAS=,I4,  7H IARCD=,I4
328             +7H IARCT=,I4 )
329              WRITE(IOUT,130)PRES,AMPS,DCONSX,DTHX, LCONS,LENX,FRNT,REAR,
330             +               TSTAG,HREARX,HFRNTX,QNX
```

114

TABLE A-7 (CONTINUED)

CARD NO	****	CONTENTS	****

```
331        130 FORMAT(/,2I6,2F6.3,4F6.1,4I6)
332            WRITE(IOUT,140)VOLTS,PINX,PGASX,GRAD,QRADX,QCONVX,
333           +WDOTX,ENTHX,EFF,TARC,DIARCX
334        140 FORMAT(6I6,  F6.3,3I6,F6.3)
335            RETURN
336            END
337        C
338        C
339            SUBROUTINE GAMMAX(TEMP,PRES,GAMMA )
340            GAMMA=1.6667
341            RETURN
342            END
343        C
344        C
345        C
346        C
347
348            SUBROUTINE TEMP(H,P,T)
349        C GIVEN H,P FIND T USING ITERATION SCHEME
350        C T IN DEG K
351        C P IN ATM
352        C H IN JOULES/KG
353        C TI INITIAL TEMPERATURE GUESS
354            TI=5000.
355            TN=TI
356        100 CONTINUE
357            ERR=.00001
358            K=0
359        110 CONTINUE
360            K=K+1
361            CALL     ENTHX(TN,P,HTN)
362            DT=.01*TN
363            CALL     ENTHX(TN+DT,P,HTNP)
364            TNP1=TN+(H-HTN)/((HTNP-HTN)/DT)
365            IF (K.GT.1000.) GO TO 120
366            CONV=(TNP1-TN)/TN
367            CONV=ABS(CONV)
368            TN=TNP1
369            IF (CONV.GT.ERR) GO TO 110
370            T=TNP1
371            RETURN
372        120 CONTINUE
373            END
374        C
375            SUBROUTINE VISCX(T,P,TVISC)
376        C   HELIUM VISCOSITY   1-1000 ATM.   TO 30,000DEG K
377            DIMENSION TC(4,31),PR(4),ATM1(30),ATM10(30),ATM100(30),AT1000(30)
378            DATA PR/1.0,10.0,100.0,1000.0/
379            DATA IN/0/
380            DATA ATM1
381           +/.4409E-03,.6957E-03,.9414E-03,.1212E-02,.1474E-02,
382           +.1729E-02,.1980E-02,.2226E-02,.2468E-02,.2705E-02,
383           +.2933E-02,.3137E-02,.3290E-02,.3342E-02,.3230E-02,
384           +.2923E-02,.2452E-02,.1914E-02,.1409E-02,.9943E-03,
385           +.6874E-03,.4717E-03,.3288E-03,.2388E-03,.1849E-03,
386           +.1544E-03,.1386E-03,.1318E-03,.1307E-03,.1330E-03  /
387            DATA ATM10/.4409E-03,
388           +.6957E-03,.9414E-03,.1212E-02,.1474E-02,
389           +.1729E-02,.1980E-02,.2226E-02,.2468E-02,.2707E-02,
390           +.2940E-02,.3164E-02,.3369E-02,.3537E-02,.3636E-02,
391           +.3628E-02,.3477E-02,.3184E-02,.2768E-02,.2304E-02,
392           +.1844E-02,.1432E-02,.1099E-02,.8356E-03,.6380E-03,
393           +.4946E-03,.3933E-03,.3251E-03,.2802E-03,.2522E-03  /
394            DATA ATM100/.4409E-03,
395           +.6957E-03,.9414E-03,.1212E-02,.1474E-02,
396           +.1729E-02,.1980E-02,.2226E-02,.2468E-02,.2707E-02,
397           +.2942E-02,.3173E-02,.3395E-02,.3604E-02,.3786E-02,
398           +.3926E-02,.3937E-02,.3982E-02,.3856E-02,.3619E-02,
399           +.3288E-02,.2890E-02,.2485E-02,.2089E-02,.1731E-02,
400           +.1423E-02,.1168E-02,.9630E-03,.9021E-03,.6778E-03  /
401            DATA AT1000/.4409E-03,
402           +.6957E-03,.9414E-03,.1212E-02,.1474E-02,
403           +.1729E-02,.1980E-02,.2226E-02,.2468E-02,.2707E-02,
404           +.2943E-02,.3176E-02,.3404E-02,.3626E-02,.3838E-02,
405           +.4032E-02,.4201E-02,.4330E-02,.4403E-02,.4406E-02,
406           +.4227E-02,.4162E-02,.3917E-02,.3609E-02,.3265E-02,
407           +.2904E-02,.2551E-02,.2213E-02,.1924E-02,.1665E-02  /
408            IF(IN.NE.0)  GO TO 120
409            DO 100 J=1,30
410            TC(1,J+1)=ATM1(J)
411            TC(2,J+1)=ATM10(J)
412            TC(3,J+1)=ATM100(J)
413            TC(4,J+1)=AT1000(J)
414        100 CONTINUE
415            DO 110 I=1,4
416            TC(I,1)=0.0
417        110 CONTINUE
418            IN=1
419        120 CONTINUE
420            IF(P.GT.PR(3))  I=3
421            IF(P.LE.PR(3))  I=2
422            IF(P.LE.PR(2))  I=1
423            J=AINT(T/1000.)+1
424            DT=T-(J-1)*1000.
425            DT=DT/1000.
426            PP=ALOG10(P/PR(I))
427            TC1=TC(I,J)+(TC(I,J+1)-TC(I,J))*DT
428            TC2=TC(I+1,J)+(TC(I+1,J+1)-TC(I+1,J))*DT
429            TVISC=TC1+(TC2-TC1)*PP
430            TVISC=TVISC*0.10
431            RETURN
432            END
433            SUBROUTINE ENTHX(T,P,TENTH)
434        C   HELIUM ENTHALPY    1-1000 ATM    TO 30,000 DEG K
435        C
436            DIMENSION ATM1(21),ATM10(21),ATM100(21),AT1000(21)
437            DIMENSION TC(4,21),PR(4)
438            DATA PR/1.0,10.0,100.0,1000.0/
439            DATA IN/0/
440            DATA RHE/2077.02/
441            DATA T0/273.16/
```

115

TABLE A-7 (CONTINUED)

CARD NO	****	CONTENTS	****

```
442          DATA ATM1 /
443        +.9160E 02,.1010E 03,.1110E 03,.1223E 03,.1361E 03,
444        +.1547E 03,.1811E 03,.2196E 03,.2755E 03,.3547E 03,
445        +.4628E 03,.6002E 03,.7622E 03,.9331E 03,.1093E 04,
446        +.1226E 04,.1330E 04,.1407E 04,.1464E 04,.1508E 04,
447        +.1543E 04,         /
448          DATA ATM10 /
449        +         .9155E 02,.1008E 03,.1102E 03,.1200E 03,
450        +.1307E 03,.1429E 03,.1577E 03,.1765E 03,.2011E 03,
451        +.2340E 03,.2773E 03,.3344E 03,.4080E 03,.4988E 03,
452        +.6080E 03,.7322E 03,.8652E 03,.9989E 03,.1123E 04,
453        +.1234E 04,.1327E 04 /
454          DATA ATM100 /
455        +         .9153E 02,.1007E 03,.1099E 03,
456        +.1193E 03,.1290E 03,.1391E 03,.1501E 03,.1625E 03,
457        +.1768E 03,.1939E 03,.2148E 03,.2405E 03,.2725E 03,
458        +.3113E 03,.3591E 03,.4165E 03,.4843E 03,.5626E 03,
459        +.6500E 03,.7465E 03,.8492E 03  /
460          DATA AT1000 /
461        +.9152E 02,.1007E 03,
462        +.1099E 03,.1191E 03,.1284E 03,.1379E 03,.1477E 03,
463        +.1579E 03,.1689E 03,.1808E 03,.1941E 03,.2091E 03,
464        +.2265E 03,.2466E 03,.2697E 03,.2970E 03,.3287E 03,
465        +.3655E 03,.4083E 03,.4556E 03,.5093E 03 /
466          IF(IN.NE.0) GO TO 110
467          DO 100 K=1,21
468          TC(1,K)=ATM1(K)
469          TC(2,K)=ATM10(K)
470          TC(3,K)=ATM100(K)
471      100 TC(4,K)=AT1000(K)
472          IN=1
473      110 CONTINUE
474          IF(T.LT.10000.)  GO TO 120
475          IF(P.GT.PR(3))  I=3
476          IF(P.LE.PR(3))  I=2
477          IF(P.LE.PR(2))  I=1
478          J=AINT(T/1000.)-9
479          DT=T-(J+9)*1000.
480          DT=DT/1000.
481          PP=ALOG10(P/PR(I))
482          TC1=TC(I,J)+(TC(I,J+1)-TC(I,J))*DT
483          TC2=TC(I+1,J)+(TC(I+1,J+1)-TC(I+1,J))*DT
484          TENTH=TC1+(TC2-TC1)*PP
485          TENTH=TENTH*RHE*TO
486          RETURN
487      120 TENTH=2.5*T*RHE
488          RETURN
489          END
490          SUBROUTINE RHO(T,P,TDENS)
491   C      HELIUM DENSITY  1-1000 ATM.   TO 30,000 DEG K
492   C
493          DIMENSION ATM1(21),ATM10(21),ATM100(21),AT1000(21)
494          DIMENSION TD(4,21),PR(4)
495          DATA PR/1.0,10.0,100.0,1000.0/
496          DATA IN/0/
497          DATA TO,RHOO/273.16,0.17859/
498          DATA ATM1  /
499        +.2731E-01,.2483E-01,.2274E-01,.2095E-01,.1938E-01,
500        +.1795E-01,.1659E-01,.1525E-01,.1389E-01,.1251E-01,
501        +.1110E-01,.9758E-02,.8536E-02,.7509E-02,.6703E-02,
502        +.6097E-02,.5647E-02,.5304E-02,.5033E-02,.4810E-02,
503        +.4619E-02  /
504          DATA ATM10 /
505        +         .2732E 00,.2483E 00,.2276E 00,.2099E 00,
506        +.1947E 00,.1812E 00,.1691E 00,.1579E 00,.1473E 00,
507        +.1369E 00,.1267E 00,.1165E 00,.1063E 00,.9628E-01,
508        +.8671E-01,.7790E-01,.7011E-01,.6348E-01,.5806E-01,
509        +.5369E-01,.5018E-01  /
510          DATA ATM100 /
511        +         .2732E 01,.2483E 01,.2276E 01,
512        +.2101E 01,.1950E 01,.1818E 01,.1702E 01,.1597E 01,
513        +.1502E 01,.1414E 01,.1331E 01,.1251E 01,.1173E 01,
514        +.1097E 01,.1022E 01,.9488E 00,.8770E 00,.8080E 00,
515        +.7428E 00,.6825E 00,.6276E 00  /
516          DATA AT1000  /
517        +.2732E 02,.2483E 02,
518        +.2276E 02,.2101E 02,.1951E 02,.1820E 02,.1705E 02,
519        +.1604E 02,.1512E 02,.1429E 02,.1353E 02,.1283E 02,
520        +.1216E 02,.1153E 02,.1093E 02,.1035E 02,.9780E 01,
521        +.9226E 01,.8682E 01,.8163E 01,.7656E 01  /
522          IF(IN.NE.0)  GO TO 110
523          DO 100 K=1,21
524          TD(1,K)=ATM1(K)
525          TD(2,K)=ATM10(K)
526          TD(3,K)=ATM100(K)
527      100 TD(4,K)=AT1000(K)
528          IN=1
529      110 CONTINUE
530          IF(T.LT.10000.)  GO TO 120
531          IF(P.GT.PR(3))  I=3
532          IF(P.LE.PR(3))  I=2
533          IF(P.LE.PR(2))  I=1
534          J=AINT(T/1000.)-9
535          DT=T-(J+9)*1000.
536          DT=DT/1000.
537          PP=ALOG10(P/PR(I))
538          TD1=TD(I,J)+(TD(I,J+1)-TD(I,J))*DT
539          TD2=TD(I+1,J)+(TD(I+1,J+1)-TD(I+1,J))*DT
540          TDENS=TD1+(TD2-TD1)*PP
541          TDENS=TDENS*RHOO
542          RETURN
543      120 TDENS=P*(TO/T)*RHOO
544          RETURN
545          END
546          SUBROUTINE SIGMAX(T,P,TSIG)
547   C      HELIUM ELECTRICAL CONDUCTIVITY   1-1000ATM.    TO 30,000 DEG K
548   C
549          DIMENSION ATM1(25),ATM10(25),ATM100(25),AT1000(25)
550          DIMENSION TS(4,26),PR(4)
551          DATA PR/1.0,10.0,100.0,1000.0/
552          DATA IN/0/
```

116

TABLE A-7 (CONTINUED)

CARD NO	****	CCNTENTS	****

```
553           DATA ATM1     /
554      +.2234E-04,.7520E-03,.1070E-01,.8643E-01,.4793E 00,
555      +.2071E 01,.7102E 01,.1775E 02,.3148E 02,.4434E 02,
556      +.5555E 02,.6574E 02,.7544E 02,.8482E 02,.9395E 02,
557      +.1027E 03,.1109E 03,.1186E 03,.1258E 03,.1325E 03,
558      +.1389E 03,.1452E 03,.1513E 03,.1573E 03,.1633E 03       /
559           DATA ATM10    /
560      +.7065E-05,.2380E-03,.3385E-02,.2717E-01,.1474E 00,
561      +.6072E 00,.2065E 01,.5986E 01,.1445E 02,.2821E 02,
562      +.4484E 02,.6149E 02,.7679E 02,.9114E 02,.1046E 03,
563      +.1176E 03,.1303E 03,.1424E 03,.1540E 03,.1650E 03,
564      +.1753E 03,.1850E 03,.1941E 03,.2026E 03,.2108E 03       /
565           DATA ATM100   /
566      +.2235E-05,.7534E-04,.1073E-02,.8633E-02,.4650E-01,
567      +.1882E 00,.6162E 00,.1747E 01,.4380E 01,.9853E 01,
568      +.1963E 02,.3485E 02,.5409E 02,.7583E 02,.9799E 02,
569      +.1197E 03,.1407E 03,.1605E 03,.1798E 03,.1983E 03,
570      +.2161E 03,.2332E 03,.2495E 03,.2648E 03,.2792E 03       /
571           DATA AT1000   /
572      +.7500E-06,.2387E-04,.3407E-03,.2752E-02,.1486E-01,
573      +.6011E-01,.1960E 00,.5397E 00,.1320E 01,.2959E 01,
574      +.6064E 01,.1149E 02,.2055E 02,.3428E 02,.5334E 02,
575      +.7755E 02,.1061E 03,.1376E 03,.1705E 03,.2039E 03,
576      +.2373E 03,.2701E 03,.3027E 03,.3329E 03,.3624E 03       /
577           IF(IN.NE.0) GO TO 150
578           DO 100 N=1,25
579           TS(1,N)=ATM1(N)
580           TS(2,N)=ATM10(N)
581           TS(3,N)=ATM100(N)
582      100  TS(4,N)=AT1000(N)
583      110  DO 140 K=1,4
584           DO 120 L=1,18
585           M=26-L
586      120  TS(K,M+1)=TS(K,M)
587           DO 130 L=1,8
588      130  TS(K,L)=ALOG10(TS(K,L))
589      140  CONTINUE
590           IN=1
591      150  CONTINUE
592           IF(T.LT.6000.)  GO TO 180
593           IF(P.GT.PR(3))  I=3
594           IF(P.LE.PR(3))  I=2
595           IF(P.LE.PR(2))  I=1
596           JSHIFT=5
597           IF(T.GE.13000.) JSHIFT=4
598           J=AINT(T/1000.)-JSHIFT
599           DT=T-(J+JSHIFT)*1000.
600           DT=DT/1000.
601      160  PP=ALOG10(P/PR(I))
602           TS1=TS(I,J)+(TS(I,J+1)-TS(I,J))*DT
603           TS2=TS(I+1,J)+(TS(I+1,J+1)-TS(I+1,J))*DT
604           TSIG=TS1+(TS2-TS1)*PP
605           IF(T.LT.13000.) GO TO 170
606           TSIG=TSIG*100.0
607           RETURN
608      170  TSIG=10**TSIG
609           TSIG=TSIG*100.0
610           RETURN
611      180  TSIG=0.0
612           RETURN
613           END
614           SUBROUTINE RADX(T,P,TRAD)
615      C
616      CCC
617      C
618           REAL NE,NT
619           DIMENSION ATM1(21),ATM10(21),ATM100(21),AT1000(21)
620           DIMENSION TR(4,22),PR(4)
621           CATA PR/1.0,10.0,100.0,1000.0/
622           DATA IN/0/
623           DATA ATM1      /
624      +.7310E-04,.3073E-03,.1016E-02,.2817E-02,.6778E-02,
625      +.1457E-01,.2842E-01,.5092E-01,.8443E-01,.1301E 00,
626      +.1870E 00,.2498E 00,.3126E 00,.3678E 00,.4112E 00,
627      +.4420E 00,.4626E 00,.4758E 00,.4841E 00,.4894E 00,
628      +.4928E 00       /
629           DATA ATM10     /
630      +       .2368E-04,.9809E-04,.3256E-03,.9074E-03,
631      +.2195E-02,.4762E-02,.9419E-02,.1729E-01,.2943E-01,
632      +.4751E-01,.7213E-01,.1044E 00,.1442E 00,.1893E 00,
633      +.2382E 00,.2871E 00,.3327E 00,.3726E 00,.4049E 00,
634      +.4301E 00,.4490E 00       /
635           DATA ATM100    /
636      +       .7556E-05,.3146E-04,.1045E-03,
637      +.2942E-03,.7187E-03,.1572E-02,.3120E-02,.5804E-02,
638      +.1001E-01,.1641E-01,.2561E-01,.3827E-01,.5519E-01,
639      +.76C7E-01,.1017E 00,.1317E 00,.1652E 00,.2014E 00,
640      +.2386E 00,.2755E 00,.3108E 00  /
641           DATA AT1000    /
642      +.2429E-05,.1016E-04,
643      +.3413E-04,.9581E-04,.2360E-03,.5252E-03,.1059E-02,
644      +.1965E-02,.3451E-02,.5738E-02,.9101E-02,.1383E-01,
645      +.2029E-01,.2880E-01,.3965E-01,.5302E-01,.6915E-01,
646      +.8804E-01,.1100E 00,.1334E 00,.1592E 00  /
647           IF(IN.NE.0)  GO TO 130
648           DO 100 N=1,21
649           TR(1,N)=ATM1(N)
650           TR(2,N)=ATM10(N)
651           TR(3,N)=ATM100(N)
652      100  TR(4,N)=AT1000(N)
653           DO 120 K=1,4
654           DO 110 L=1,15
655           M=22-L
656      110  TR(K,M+1)=TR(K,M)
657           DO 120 L=1,7
658           TR(K,L)=ALOG10(TR(K,L))
659      120  CONTINUE
660           IN=1
661      130  CONTINUE
662           IF(T.LT.10000.)  GO TO 160
663           IF(P.GT.PR(3))  I=3
```

117

TABLE A-7 (CONCLUDED)

```
CARD NO        ****                        CONTENTS                          ****

  664               IF(P.LE.PR(3))  I=2
  665               IF(P.LE.PP(2))  I=1
  666               JSHIFT=9
  667               IF(T.GE.16000.) JSHIFT=8
  668               J=AINT(T/1000.)-JSHIFT
  669               DT=T-(J+JSHIFT)*1000.
  670               DT=DT/1000.
  671         140   PP=ALOG10(P/PR(I))
  672               TR1=TR(I,J)+(TR(I,J+1)-TR(I,J))*DT
  673               TR2=TR(I+1,J)+(TR(I+1,J+1)-TR(I+1,J))*DT
  674               XE =TR1+(TR2-TR1)*PP
  675               IF(T.GE.16000.)  GO TO 150
  676               XE=10**XE
  677         150   NT=(P*1.0132E 5/(1.38E-23*T))*1.E-6
  678               NE=XE*NT
  679               TRAD=(4.34E-28)*NE**2/SQRT(T)
  680               TRAD=TRAD*1.0E+6
  681               RETURN
  682         160   KP=0.1352*T**(5/2)*EXP(-285500./T)
  683               KPP=SQRT(KP/(1.0132E 5*P))
  684               XE=KPP/(1.0+KPP)
  685               GO TO 150
  686               END
  687               SUBROUTINE  TCONDX(T,P,TCOND)
  688         C       HELIUM THERMAL CONDUCTIVITY   1-1000 ATM.   TO 30,000EG K
  689               DIMENSION  TC(4,31),PR(4)
  690               DIMENSION  ATM1(30),ATM10(30),ATM100(30),AT1000(30)
  691               DATA PR/1.0,10.0,100.0,1000.0/
  692               DATA IN/0/
  693               DATA ATM1        /
  694              +.3408E 05,.5378E 05,.7277E 05,.9366E 05,.1139E 06,
  695              +.1337E 06,.1530E 06,.1721E 06,.1910E 06,.2104E 06,
  696              +.2321E 06,.2600E 06,.2985E 06,.3459E 06,.3990E 06,
  697              +.4611E 06,.5428E 06,.6556E 06,.8011E 06,.9618E 06,
  698              +.1098E 07,.1165E 07,.1136E 07,.1030E 07,.8982E 06,
  699              +.7858E 06,.7105E 06,.6710E 06,.6593E 06,.6670E 06   /
  700               DATA ATM10       /
  701              +.3408E 05,.5378E 05,.7277E 05,.9366E 05,.1139F 06,
  702              +.1337E 06,.1530E 06,.1721E 06,.1909E 06,.2096E 06,
  703              +.2289E 06,.2503E 06,.2764E 06,.3109E 06,.3557E 06,
  704              +.4079E 06,.4645E 06,.5263E 06,.5988E 06,.6877E 06,
  705              +.7957E 06,.9186E 06,.1046E 07,.1161E 07,.1245E 07,
  706              +.1284E 07,.1278E 07,.1241E 07,.1190E 07,.1143E 07   /
  707               DATA ATM100      /
  708              +.3408E 05,.5378E 05,.7277E 05,.9366E 05,.1139E 06,
  709              +.1337E 06,.1530E 06,.1721E 06,.1908E 06,.2094E 06,
  710              +.2280E 06,.2471E 06,.2676E 06,.2913E 06,.3210E 06,
  711              +.3593E 06,.4084E 06,.4667E 06,.5320E 06,.6035E 06,
  712              +.6820E 06,.7671E 06,.8645E 06,.9739E 06,.1093E 07,
  713              +.1217E 07,.1341E 07,.1457E 07,.1558E 07,.1639E 07   /
  714               DATA AT1000      /
  715              +.3408E 05,.5378E 05,.7277E 05,.9366E 05,.1139E 06,
  716              +.1337E 06,.1530E 06,.1721E 06,.1908E 06,.2093E 06,
  717              +.2277E 06,.2460E 06,.2648E 06,.2845E 06,.3062E 06,
  718              +.3314E 06,.3622E 06,.4014E 06,.4513E 06,.5141E 06,
  719              +.5902E 06,.6799E 06,.7824E 06,.8882E 06,.1011E 07,
  720              +.1145E 07,.1291E 07,.1448E 07,.1608E 07,.1774E 07   /
  721               IF(IN.NE.0)  GO TO 120
  722               DO 100 N=1,30
  723               TC(1,N+1)=ATM1(N)
  724               TC(2,N+1)=ATM10(N)
  725               TC(3,N+1)=ATM100(N)
  726         100   TC(4,N+1)=AT1000(N)
  727               DO 110 I=1,4
  728               TC(I,1)=0.0
  729         110   CONTINUE
  730               IN=1
  731         120   CONTINUE
  732               IF(P.GT.PR(3))  I=3
  733               IF(P.LE.PR(3))  I=2
  734               IF(P.LE.PR(2))  I=1
  735               J=AINT(T/1000.)+1
  736               DT=T-(J-1)*1000.
  737               DT=DT/1000.
  738               PP=ALOG10(P/PR(I))
  739               TC1=TC(I,J)+(TC(I,J+1)-TC(I,J))*DT
  740               TC2=TC(I+1,J)+(TC(I+1,J+1)-TC(I+1,J))*DT
  741               TCOND=TC1+(TC2-TC1)*PP
  742               TCOND=TCOND*1.0E-5
  743               RETURN
  744               END
```

Figure A-1   HEARC flow chart

119

Figure A-1 HEARC flow chart (Continued)

Figure A-1   HEARC flow chart (Continued)

CHART TITLE - SUBROUTINE INPUT

```
                              / --------- /
                              /  INPUT   /
                              / --------- /

                              06.02---1*
                              ---------------------
                              READS REQUIRES DATA
                              IN ENGINEERING UNITS
                              AND CONVERTS TO
                              MKS SYSTEM FOR THE
                              COMPUTATIONS
                                   *
                                   I           01
                              *----------------*
                              I     IN = 5     I
                              *----------------*

                                   I           02
                              / ------------- /
                              / READ FROM DEV /
                              /      IN       /
                              /  VIA FORMAT   /
                              /     100       /
                              / INTO THE LIST /

                                   I    NOTE  03
                              * * * * * * * * * *
                              *     LIST =      *
                              *   (TITLE(J),J =  *
                              *     1,18)       *
                              * * * * * * * * * *

                                   I           04
                              / ------------- /
                              / READ FROM DEV /
                              /      IN       /
                              /  VIA FORMAT   /
                              /     110       /
                              / INTO THE LIST /

                                   I    NOTE  05
                              * * * * * * * * * *
                              *  LIST = AMPS,   *
                              *  AMPINC, NAMPS  *
                              * * * * * * * * * *

                                   I           06      +-------------------->)*
            / ------------- /                          I              NOTE  11
            / READ FROM DEV /                          * * * * * * * * * *
            /      IN       /                          *  LIST = WDOT,   *
            /  VIA FORMAT   /                          *  DCONS, DTHRT   *
            /     110       /                          * * * * * * * * * *
            / INTO THE LIST /                               I
                                                            I           12
                 I    NOTE  07                         *----------------*
            * * * * * * * * * *                        I    CONSLN =     I
            *  LIST = PRES,   *                        I  CONSLN*CNVF03  I
            *  PINC, NPRES    *                        I                I
            * * * * * * * * * *                        I    FARCLN =     I
                                                       I  FARCLN*CNVF03  I
                 I           08                        I                I
            / ------------- /                          I    RARCLN =     I
            / READ FROM DEV /                          I  RARCLN*CNVF03  I
            /      IN       /                          I                I
            /  VIA FORMAT   /                          I ARCLEN = FARCLN + I
            /     120       /                          I    PARCLN       I
            / INTO THE LIST /                          *----------------*

                 I    NOTE  09                              I           13
            * * * * * * * * * *                        *----------------*
            *  LIST = CONSLN, *                        I    DREAR =      I
            *  FARCLN, RARCLN *                        I  DREAR*CNVF03   I
            * * * * * * * * * *                        I                I
                                                       I    WDUT =       I
                 I           10                        I  WDOT/CNVF02    I
            / ------------- /                          I                I
            / READ FROM DEV /                          I    DCONS =      I
            /      IN       /                          I  DCONS*CNVF03   I
            /  VIA FORMAT   /                          I                I
            /     120       /                          I    DTHRT =      I
            / INTO THE LIST /                          I  DTHRT*CNVF03   I
                 I                                     *----------------*
                 +--------------------+                     I           14
                                                       *----------------H
                                                       I  I              H
                                                       I  I   DATIME     H
                                                       I  I   (DAT)      H
                                                       I  I              H
                                                       I                H

                                                            I           15
                                                       *--------------*
                                                       *    EXIT       *
                                                       *--------------*
```

Figure A-1   HEARC flow chart (Continued)

CHART TITLE - SUBROUTINE GASPOW

```
                    /  GASPOW  /
                    ----------------
   07.19---)*                        +--------------------)*
COMPUTES POWER IN GAS              NOZZLE LOSS
BY CALCULATING                     CORRELATION FOR
CONVECTIVE LOSS TO                 HELIUM,QN IS LOSS IN
CONSTRICTOR                        WATTS
         *          01                                  08
   I PI = 3.14159    I               I     ENTH =        I
   I                 I               I   (PGAS/WDOT)      I
   I TWALL = 590.    I               I    *4.3E-4         I
   -------------------               I                    I
CALCULATE CONVECTION               I      QN =            I
LOSS TO CONSTRICTOR                I  0.04*((WDOT*2.      I
WALL                               I   2046)**0.7)        I
                    02             I   *(ENTH -           I
   I TA = 1.00*(TGAS - I           I    1325.)*1054.      I
   I  TWALL) + TWALL   I           I  PGAS = PGAS - QN    I
   ---------------------           ----------------------
                    03             CALCULATE POWER IN
   I4 I             H              GAS,ARC FROM
   I3 I   TCONDX    H              ENTHALPY-MASS FLOW
   IO I (TA,PRES,   H              RELATION
   I1 I   TCOND)    H              ASSUME UNIFORM
   -------------------             VELOCITY
                    04                                  09
   I      H =        I              I5 I             H
   I FNU*TCOND/(DCONS I              I5 I    RHO      H
   I  - DARC)        I              I. I (TGAS,PRES, H
   I                 I              IO I   RHOGAS)    H
   I QCONV = H*(TGAS - I             I1 I             H
   I  TWALL)         I              -------------------
   -------------------                             10
RADIATED HEAT FLUX                  I3 I             H
OUT FROM ARC                        I5 I    RHO      H
                    05             I. I (TARC,PRES, H
   I     QRAD =      I              IO I   RHOARC)    H
   I Y*(DARC*DARC)   I              I1 I             H
   I /(PI*DCONS)     I              -------------------
   -------------------                             11
POWER IN GAS FROM ARC               I     AGAS =        I
(BY CONVECTION) IS                  I PI*(DCONS**2 -     I
Z=DARC*ARCLEN                       I  DARC**2)/4.0      I
HIN=COLD GAS ENTHALPY               I                    I
(JOULES/KG)                         I     AARC =         I
                    06             I PI*DARC*DARC/4.0    I
   I                 I              I                    I
   I 670.0/4.2992E-4 I              I     VEL =          I
   -------------------              I WDOT/(RHOGAS*      I
LOSSES RADIATION                    I  AGAS +           I
OVER ARCLENGTH, CONV.               I  RHOARC*AARC)      I
OVER FRONT                          -------------------
CONSTRICTOR                                       12
                    07             I    WDOTAR =        I
   I PGAS = PIN -     I             I RHOARC*VEL*AARC    I
   I QRAD*PI*DCONS*   I             I                    I
   I  ARCLEN -        I             I    WDOTGA =        I
   I DCONV*PI*DCONS*  I             I RHOGAS*VEL*AGAS    I
   I CONSLN + WDOT*HIN I            -------------------
   -------------------                            13                      )*
                                    I3 I             H                             15
                                    I3 I   ENTHX     H        I3 I             H
                                    I. I (TGAS,PRES, H        I2 I    ENTHX     H
                                    IO I   ENTHGA)    H        I. I (TARC,PRES, H
                                    I1 I             H        IO I   ENTHAP)    H
                                    -------------------       I1 I             H
                                                              -------------------
                                                                             16
                                                              I    PGASEN =      I
                                                              I FNTHGA*WDOTGA +  I
                                                              I FNTHAP*WDOTAP    I
                                                              -------------------
                                                                     I 17
                                                                  *  EXIT  *
```

Figure A-1 HEARC flow chart (Continued)

CHART TITLE - SUBROUTINE ARCTEM

```
           / ARCTEM /

07.17---)*
CALCULATES ARC
TEMPERATURE FOR POWER
INPUT TO BE A MINIMUM
         *          01
  I---------------I
  I  SIGNF = 1.0  I
  I  IARCT = 0    I
  I  DT = 200.0   I

17.07*--)I(---------------------------------------+
100     I        02                                I
  I IARCT = IARCT + 1 I                            I
                                                   I
         I          03                             I
  I2I--------------I H                             I
  I2I              I H                             I
  I1I   ARCDIA     I H                             I
  I0I  (TARC,PIN)  I H                             I
  I1I              I H                             I
  I---------------I H                             I
                                                   I
         *  04                                      I
      *  IERR .EQ. 1  *   FALSE                     I
      *               *---------------+             I
         *           *                I             I
            * TRUE                     I            )I(
              I                        I        06   I
              I                    *  IARCT .NE. 1 *  TRUE                    )I*
         I  05                     *               *---------------------------I
      *  EXIT  *                      *           *                       50  I          08
                                         * FALSE                   I--------------------I
                                           I                       I     DIRCH =        I
                                           I                       I SIGN(1.0,(PINP -   I
                                           I                       I    PIN))           I
                                           I          07           I     SIGNF =        I
                                     I--------------I              I  DIRCH*SIGNF       I
                                     I TARC = TARC + DT I          I  DT = DT/(1. +     I
                                     I  PINP = PIN    I            I  (1. - DIRCH)/2.)  I
                                     I--------------I
                                           I                               I
              +----------------------------+                       *  09
                                                                *  ABS(DT) .LT. *   FALSE                    )I*
                                                                *    10.0       *---------------------------I
                                                                   *           *                        11  I
                                                                      * TRUE                   I--------------------I
                                                                        I                      I  TARC = TARC +     I
                                                                        I                      I   SIGNF*DT         I
                                                                   I  10                       I  PINP = PIN        I
                                                                *  EXIT  *                     I--------------------I
                                                                                                     I
                                                                                                *  12
                                                                                             *  IARCT .GT. *   TRUE
                                                                                             *    100      *----+
                                                                                                *       *       I
                                                                                                   * FALSE  .18.
                                                                                                     I      . 01 .
                                                                                                     I      .110.
                                                                                                     I
                                                                                                   ...
                                                                                                 .17.02.
                                                                                                 . ... 100
```

CHART TITLE - SUBROUTINE ARCTEM

```
                    / 110 /

         17.12---)I
                 I          01
         I-------------------I
         I    IERR = 1       I
         I-------------------I

         120     I   02
              *  EXIT  *
```

Figure A-1   HEARC flow chart (Continued)

07/11/75   AUTOFLOW CHART SET -   PAGE 21

CHART TITLE - SUBROUTINE ARCDIA(TXX,PXX)

```
/ ARCDIA /

17.03---)*
CALCULATE ARC
DIAMETER FOR ENERGY
BALANCE
          *  01
TRUE *  *  *  *
*--* INN .NE. 0 *
     *  *  *  *
       IFALSE

02
| PI = 3.14159 |
| DI = DARC    |

100           03
| INN = 1     |
| IARCD = 0   |

POWER IN =
X(TARC)/DARC**2 PER
UNIT LENGTH

04
|13|   SIGMAX   H
|7 | (TXX,PRES, H
|10|   SIGMA)   H
|11|            H

05
|    X =         |
| 4.0*AMPS*AMPS/ |
| (PI*SIGMA)     |

06
|14|   RADX     H
|10| (TXX,PRES,RAD) H
|10|            H
|11|            H

POWER RADIATED =
Y(TARC)*DARC**2 PER
UNIT LENGTH

07
| Y = PI*RAD/4.0       |
| TX = 0.70*(TARC -    |
| TGAS) + TGAS         |
```

```
--)*         08
|13|   VISCX   H
|10| (TGAS,PRES, H
|11|   VISC)   H

09
|14|   TCONDX   H
|13| (TX,PRES,  H
|11|   TCOND)   H

110      NOTE 10
* CONTINUE *

11
| IARCD = IARCD + 1 |

| PXX =           |
| (X/DARC**2)     |
| *ARCLEN         |

POWER OUT OF ARC
COLUMN CONVECTED =
Z(TARC)*DARC PER UNIT
LENGTH

12
| REY =              |
| (4.0*MDOTGA)       |
| /(PI*VISC*(DARC +  |
| DCONS))            |

PRANDTL NO FOR HE IS
0.672

13
| PR = 0.672         |
| FNU =              |
| 0.0265*(REY**0.8)  |
| *PR**0.3           |
| H =                |
| FNU*TCOND/(DCONS   |
| - DARC)            |
| Z = PI*H*(TXX -    |
| TGAS)              |

14
| ALPHA = Z/Y        |
| BETA = - 1.*X/Y    |
| F = (DI**4) +      |
| ALPHA*(DI**3) +    |
| BETA               |
| DP = DCONS + DI    |
```

```
--)*          15
| DM =                |
| DCONS*DCONS -       |
| DI*DI               |
| CORR = 1.0 +        |
| 0.2*DI/3.0/DP +     |
| 2.0*DI*DI/3.0/DM    |
| FP =                |
| 4.0*(DI**3) +       |
| 3.0*ALPHA*DI*DI*    |
| CORR                |

16
| DELD = - 1.*F/FP    |
| DARC = DI + DELD    |
| DELDIA = (DARC -    |
| DI)/DARC            |

           17
*  *  *  *       TRUE
* IARCD .GT. *------)*
*    100     *        120      20
*  *  *  *        | IFPP = 1 |
    IFALSE
                      21
                   *  EXIT  *

           18
*  *  *  *       TRUE
* ABS(DELDIA)*------*
* .LE. 1.E-5 *
*  *  *  *        130    NOTE 22
    IFALSE       * CONTINUE *
                      23
19                 *  EXIT  *
| DI = DARC |
```

Figure A-1 HEARC flow chart (Continued)

125

CHART TITLE - SUBROUTINE OUTPUT

```
                    / OUTPUT /
                    ----------
         07.22---)*                        ----------------)| I
         -------------------                                          06
         CALCULATE REMAINING               **************************
         ARC PARAMETERS                    I    HREARX =            I
         CONVERT MKS TO                     I  QRAD*PI*(DCONS)       I
         ENGINEERING UNITS AND              I *RARCLN)*0.948E-3      I
         PRINT OUT RESULTS                  I                       I
                    *                       I    HFRNTX =            I
         -------------------  01            I (QRAD*PI*DCONS*        I
         I    IOUT = 6       I              I   FARCLN +            I
         I                   I              I QCONV*PI*DCONS*        I
         I     GRAD =        I              I CCNSLN)*.948E-3        I
         I  (AMPS/(SIGMA*    I              **************************
         I DARC*DARC*PI/4.0) I
         I )*CNVFO3          I                          I
         I                   I                          *    07
         I    LCONS =        I              TRUE    *  *  *  *
         I  CONSLN*CNVFO1    I              ----- * NCASE .NE. 0 *
         I                   I                  I    *  *  *  *
         I    FRNT =         I                  I
         I  FARCLN*CNVFO1    I                  I       I FALSE
         -------------------                   I       I
                    I                          I       I
         -------------------  02               I       I
         I    REAR =         I                 I       ----------------)
         I  RARCLN*CNVFO1    I                 I       -----------------  08
         I                   I                 I       /               /
         I    LENX =         I                 I       /  WRITE TO DEV  /
         I  ARCLEN*CNVFO1    I                 I       /     IOUT       /
         I                   I                 I       /  VIA FORMAT    /
         I  VOLTS = GRAD*LENX I                I       /     105        /
         -------------------                   I       -----------------
                    I                          I               I
         HELIUM ROOM TEMP                      I       -----------------  09
         ENTHALPY = 670 BTU/LB                 I       /  WRITE TO DEV  /
                    I                          I       /     IOUT       /
         -------------------  03               I       /  VIA FORMAT    /
         I    HIN =          I                 I       /     110        /
         I  (670./CNVFO4)    I                 I       / FROM THE LIST  /
         I  *WDOT            I                 I       -----------------
         I                   I                 I               I
         I  EFF = ((PGAS -   I                 I       ***************  NOTE 10        **************  NOTE 14
         I HIN)/PIN)*100.    I                 I       * LIST = DAT, TITLE *           * LIST = ISONIC, *
         I                   I                 I       ***************                 *   ETGAS, IARCD,  *
         I  WDOTX =          I                 I       100--)|                         *     IARCT        *
         I WDOT*CNVFO2       I                 I       -----------------  11           **************
         I                   I                 I       I   NCASE = 1    I<---------------         I
         I  QRADX =          I                 -----) | -----------------                ------------------  15
         I QRAD*CNVFO6       I                                I                         /  WRITE TO DEV  /
         -------------------                                  I                         /     IOUT       /
                    I                                         *   12                    /  VIA FORMAT    /
         -------------------  04                   *  *  *  *  *  FALSE I               /     130        /
         I    QCONVX =       I                   *  IERR .EQ. 1  * ---------            / FROM THE LIST  /
         I QCONV*CNVFO6      I                     *  *  *  *  *         I              ------------------
         I                   I                          *               I                      I
         I  QNX = QN*0.948E-3 I                          I TRUE          I              **************  NOTE 16
         I                   I                          I               I              * LIST = PRES,   *
         I    ENTHX =        I                          I               I              * AMPS, DCONSX,  *
         I ENTH*CNVFO4       I                          I               I              *  DTHX, LCONS,  *
         I                   I                 ----------------- 13     I              * LENX, FRNT, FPEAR,*
         I    DIARCX =       I                 /  WRITE TO DEV  /        I              *  TSTAG, HREAPX,  *
         I DARC*CNVFO1       I                 /     IOUT       /        I              *  HFRNTX, QNX,   *
         -------------------                   /  VIA FORMAT    /        I              **************
                    I                          /     120        /       I                      I
         -------------------  05               / FROM THE LIST  /        I              ------------------  17
         I    DCONSX =       I                 -----------------         I              /  WRITE TO DEV  /
         I DCONS*CNVFO1      I                          I                I              /     IOUT       /
         I                   I                          ----------------)|              /  VIA FORMAT    /
         I    DTHX =         I                                                          /     140        /
         I DTHRT*CNVFO1      I                                                          / FROM THE LIST  /
         I                   I                                                          ------------------
         I  PINX = PIN*0.001 I                                                                   I
         I                   I                                                          **************  NOTE 18
         I  PGASX = (PGAS -  I                                                          * LIST = VOLTS,  *
         I HIN)*0.001        I                                                          *  PINX, PGASX,  *
         -------------------                                                            *  GRAD, QRADX,  *
                    I                                                                   *  QCONVX, WDOTX, *
                    ----------------)|                                                  *  ENTHX, EFF, TAPF,*
                                                                                        *   DIARCX,       *
                                                                                        **************
                                                                                                 I
                                                                                                 *  19
                                                                                              ----------
                                                                                              *  EXIT  *
                                                                                              ----------
```

CHART TITLE - SUBROUTINE GAMMAX(TEMP,PRES,GAMMA)

```
                    / GAMMAX /
                    -----------
         08.04---)|
                          01
         -------------------
         I  GAMMA = 1.6667  I
         -------------------
                    I
                    I  02
              ----------
              *  EXIT  *
              ----------
```

Figure A-1   HEARC flow chart (Continued)

```
                              /----------/
                             /    TEMP   /
                             /----------/

                          08.03---)*
                          GIVEN H,P FIND T
                          USING ITERATION
                          SCHEME
                          T  IN DEG K
                          P  IN ATM
                          H  IN JOULES/KG
                          TI INITIAL
                          TEMPERATURE GUESS
                                 I
                                 I               01
                          *------------------*
                          I     TI = 5000.    I
                          I     TN = TI        I
                          *------------------*
                                 I
                           100   I        NOTE 02
                          *****************
                          *   CONTINUE     *
                          *****************
                                 I
                                 I               03
                          *------------------*
                          I    ERR = .00001   I
                          I    K = 0          I
                          *------------------*
                       29.13---)
                           110   I        NOTE 04
                          *****************
                          *   CONTINUE     *
                          *****************
                                 I
                                 I               05
                          *------------------*
                          I    K = K + 1      I
                          *------------------*
                                 I
                                 I               06
                          *------------------*          *------------------------*
                          I13I     ENTHX      H          120---)  I      NOTE 11
                          I3 I  (TN,P,HTN)    H          *********************
                          I0 I                H          *    CONTINUE        *
                          I1 I                H          *********************
                          *------------------*
                                 I
                                 I               07
                          *------------------*
                          I    DT = .01*TN    I
                          *------------------*
                                 I
                                 I               08
                          *------------------*          *------------------------*
                          I13I     ENTHX      H          )*              12
                          I3 I   (TN +        H          *------------------------*
                          I0 I  DT,P,HTNP)    H          I  CONV = (TNP1 -        I
                          I1 I                H          I       TN)/TN           I
                          *------------------*          I  CCNV = ABS(CONV)       I
                                 I                       I  TN = TNP1             I
                                 I               09      *------------------------*
                          *------------------*                     I
                          I TNP1 = TN + (H -  I                     I         13
                          I HTN)/((HTNP -     I            *  *  *  *  *
                          I HTN)/DT)          I          *  CONV .GT. ERR *----TRUE
                          *------------------*            *  *  *  *  *  *----+
                                 I                                  I
                                 I        10                    IFALSE  .30.
                            *  *  *  *  *                              .04.
                          *  K .GT. 1000. *----TRUE----+            .110.
                            *  *  *  *  *                    I               14
                                 I                     *------------------------*
                              IFALSE                    I     T = TNP1           I
                                 I                      *------------------------*
                                 +----------------------+         I
                                                                  I       15
                                                               *  EXIT  *
```

Figure A-1   HEARC flow chart (Continued)

CHART TITLE - SUBROUTINE VISCX(T,P,TVISC)

```
                    / VISCX /

   21.08---)*                         ----)I          08
   HELIUM VISCOSITY                   I   IN = 1      I
   1-1000 ATM.  TO
   30,000DEG K                        ----)I   NOTE 09
                                120    CONTINUE
        *      01
     IN .NE. 0   TRUE                          10
                                        P .GT. PR(3)   FALSE
      IFALSE
                                            ITRUE
                NOTE 02
     BEGIN DO LOOP                            11
     100 J = 1, 30                   I   I = 3      I

                     03
     I TC(1,J + 1) =                           12
       ATM1(J)                        P .LF. PR(3)   FALSE
     TC(2,J + 1) =
       ATM10(J)                           ITRUE
     TC(3,J + 1) =
       ATM100(J)                             13
     TC(4,J + 1) =                   I   I = 2      I
       AT1000(J)

     100      04                              14
     END OF DO                       P .LE. PR(2)   FALSE
   NO   LOOP
                                         ITRUE
      IYES
                                            15
                NOTE 05             I   I = 1      I
     BEGIN DO LOOP
     110 I = 1, 4                        J =          16
                                    AINT(T/1000.) + 1
                     06
     I TC(I,1) = 0.0 I               DT = T - (J -
                                      1)*1000.
     110      07
     END OF DO                       DT = DT/1000.
   NO   LOOP
                                    PP =
      IYES                          ALOG10(P/PR(I))

                                                       --)*        17
                                                  I   TC1 = TC(I,J) +
                                                      (TC(I,J + 1) -
                                                       TC(I,J))*DT
                                                    TC2 = TC(I +
                                                    1,J) + (TC(I +
                                                    1,J + 1) - TC(I +
                                                    1,J))*DT

                                                    TVISC = TC1 +      18
                                                    (TC2 - TC1)*PP
                                                    TVISC =
                                                    TVISC*0.10

                                                         19
                                                    *  EXIT  *
```

Figure A-1　HEARC flow chart (Continued)

CHART TITLE - SUBROUTINE ENTHX(T,P,TENTH)

Figure A-1 HEARC flow chart (Continued)

CHART TITLE - SUBROUTINE RHO(T,P,TDENS)

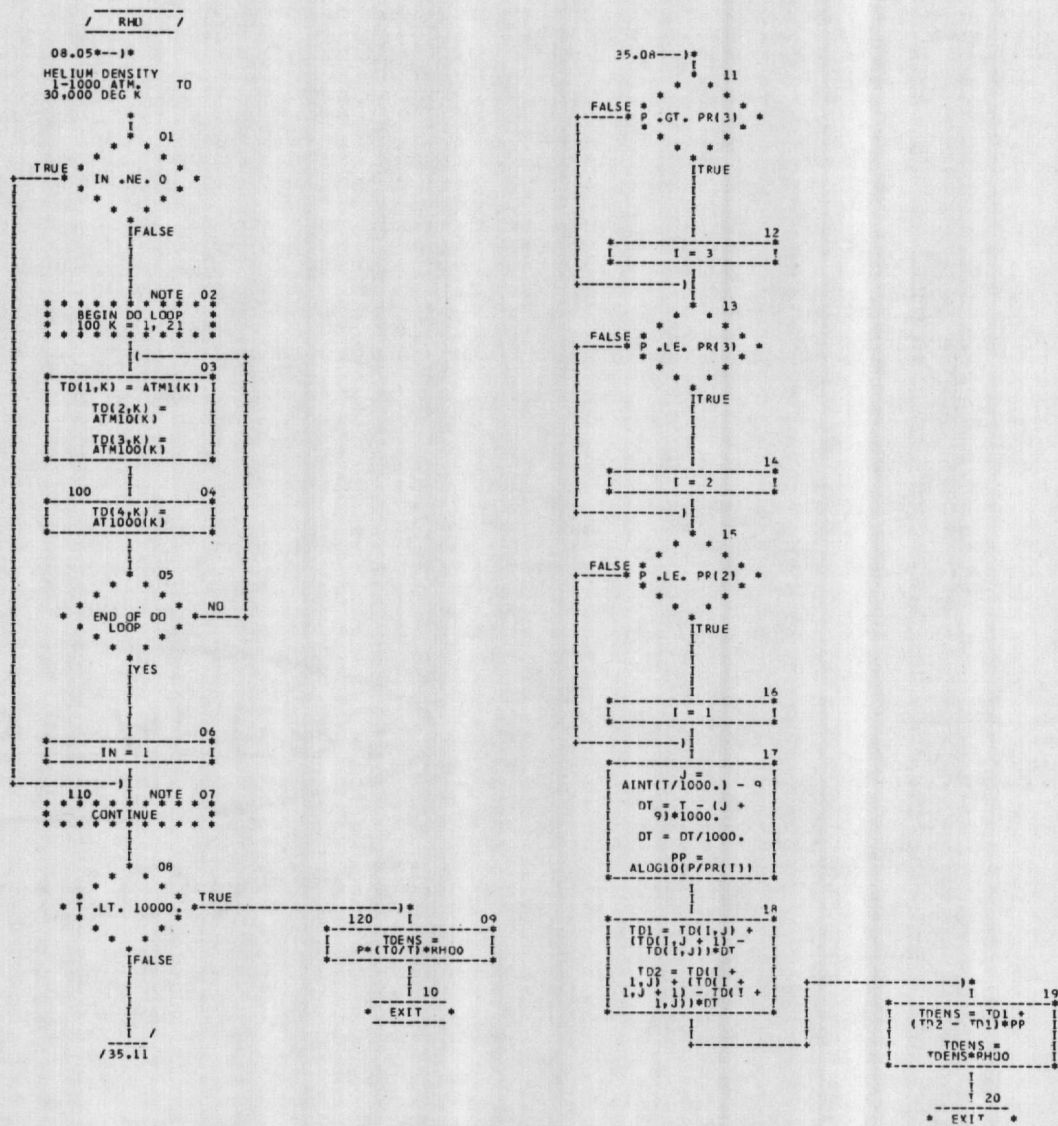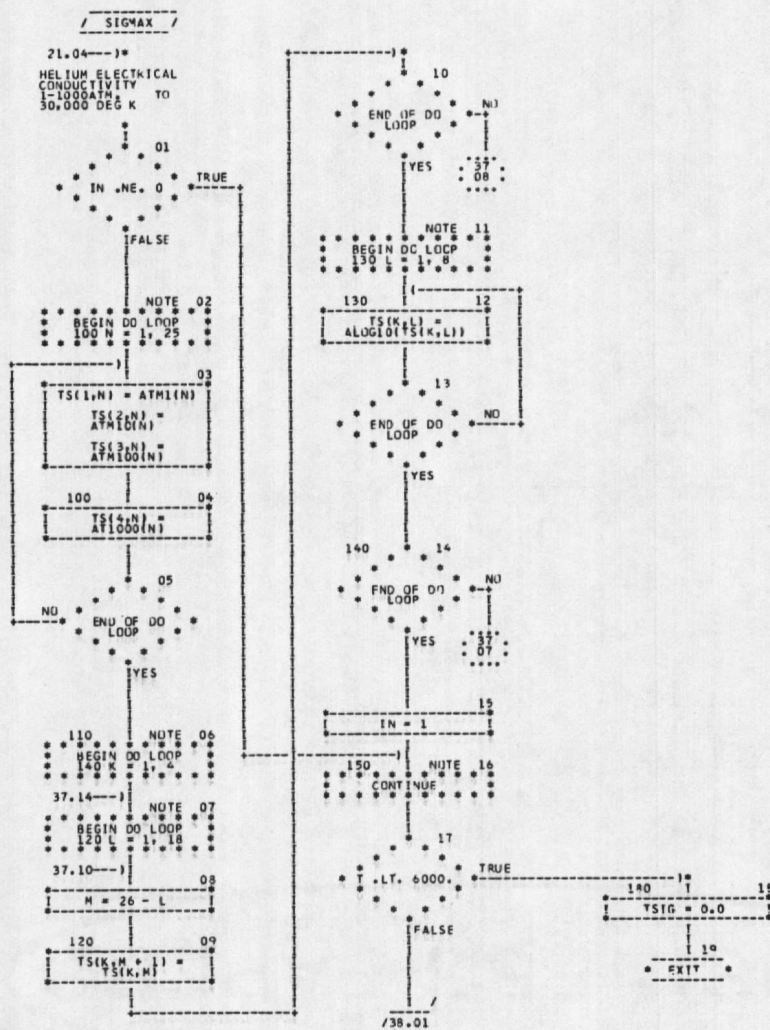Figure A-1   HEARC flow chart (Continued)

130

CHART TITLE - SUBROUTINE SIGMAX(T,P,TSIG)

Figure A-1   HEARC flow chart (Continued)

131

CHART TITLE - SUBROUTINE SIGMAX(T,P,TSIG)

Figure A-1   HEARC flow chart (Continued)
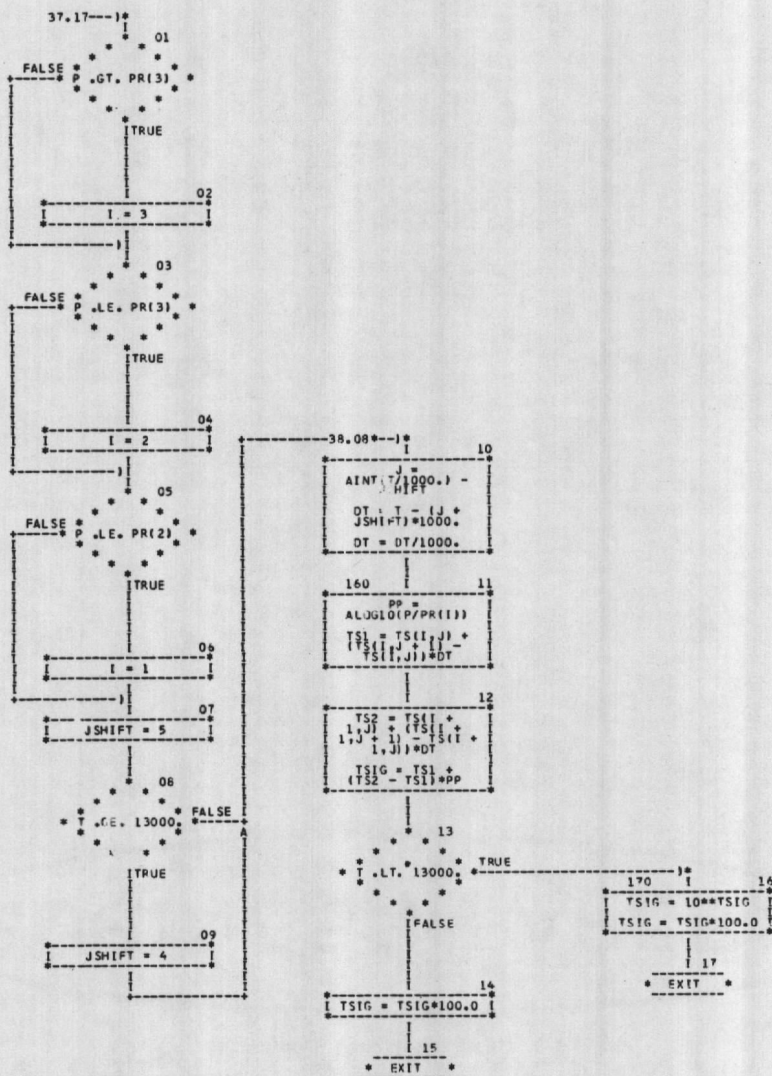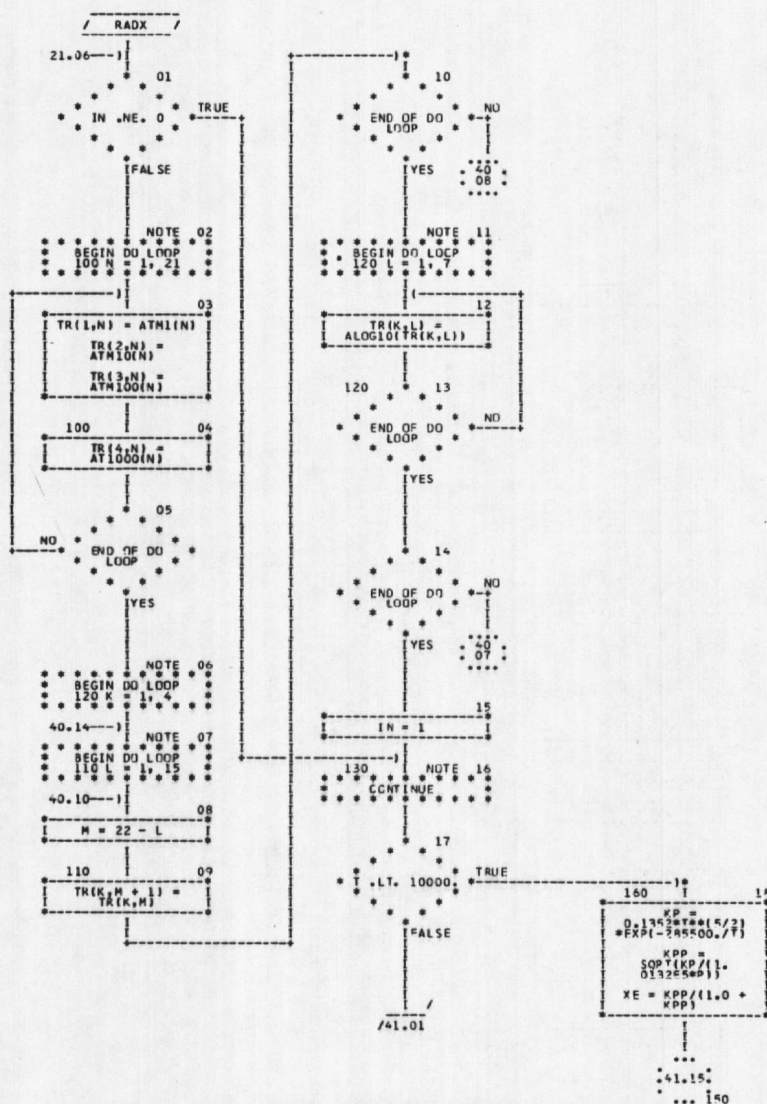
CHART TITLE - SUBROUTINE RADX(T,P,TRAD)

Figure A-1   HEARC flow chart (Continued)
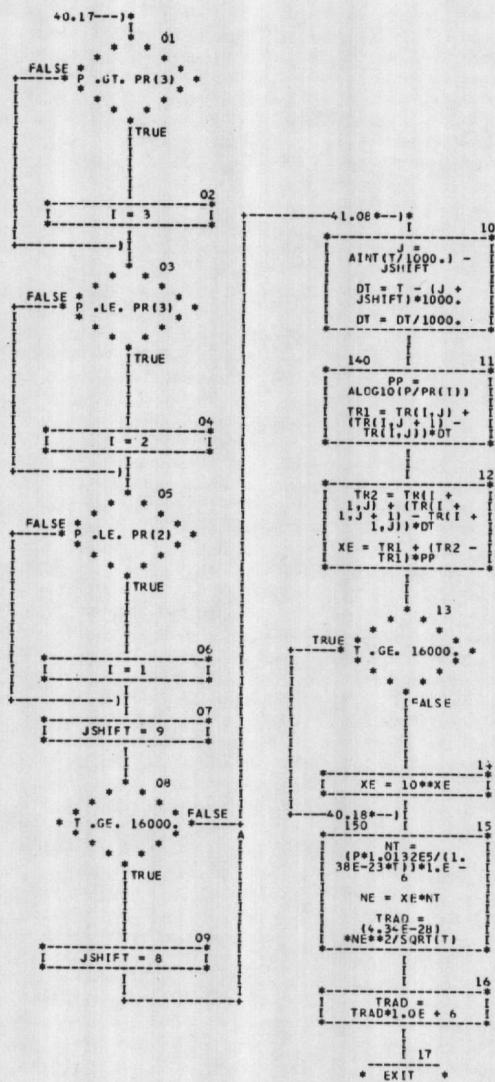
CHART TITLE - SUBROUTINE RADXIT(T,P,TRAD)

Figure A-1   HEARC flow chart (Continued)

CHART TITLE — SUBROUTINE TCONDX(T,P,TCOND)

Figure A-1   HEARC flow chart (Concluded)

NOMENCLATURE

A	Cross sectional area
C	Radiation constant, mass flow constant
D	Diameter
g	Gravity constant
G	Electrical voltage gradient
H	Enthalpy (computer codes)
h	Turbulent heat transfer coefficient
h	Enthalpy
I	Arc current
L	Arc length
$\dot{m}$	Mass flow rate
N	Arc heater scale
Ne	Electron density in arc column
Nu	Nusselt number
P	Pressure
P	Power
Pr	Prandtl number
R	Gas constant
Re	Reynolds number
Q	Heat loss
q	Heat flux
T	Temperature
U	Arc column volumetric radiation
V	Arc voltage
v	Gas velocity in constrictor
w	Water flow rate
X	Input power parameter
Y	Radiation parameter
Z	Convection parameter
γ	Ratio of specific heats
λ	Thermal conductivity

136

NOMENCLATURE

η	Efficiency
μ	Viscosity
ρ	Density
σ	Electrical conductivity
Δ	Differential

Subscripts

a	Arc column
a	Air (mass flow rate)
A	Anode
b	Bulk gas at nozzle
c	Constrictor or convection
C	Cathode
F	Front electrode
g	Bulk gas around arc column
H	Hydrogen
He	Helium
i	Input injector or value
N	Nozzle
N-250	N-250 arc heater
o	Stagnation condition
r	Radiation
R	Rear electrode
sf	Sonic flow value
w	Wall value
x	Weighted conductivity - temperature

Superscript

| * | Nozzle throat value |